

Mannath, Jayan (2013) Endoscopic multimodal imaging in Barrett's oesophagus. DM thesis, University of Nottingham.

Access from the University of Nottingham repository:

<http://eprints.nottingham.ac.uk/28688/1/606343.pdf>

Copyright and reuse:

The Nottingham ePrints service makes this work by researchers of the University of Nottingham available open access under the following conditions.

- Copyright and all moral rights to the version of the paper presented here belong to the individual author(s) and/or other copyright owners.
- To the extent reasonable and practicable the material made available in Nottingham ePrints has been checked for eligibility before being made available.
- Copies of full items can be used for personal research or study, educational, or not-for-profit purposes without prior permission or charge provided that the authors, title and full bibliographic details are credited, a hyperlink and/or URL is given for the original metadata page and the content is not changed in any way.
- Quotations or similar reproductions must be sufficiently acknowledged.

Please see our full end user licence at:

http://eprints.nottingham.ac.uk/end_user_agreement.pdf

A note on versions:

The version presented here may differ from the published version or from the version of record. If you wish to cite this item you are advised to consult the publisher's version. Please see the repository url above for details on accessing the published version and note that access may require a subscription.

For more information, please contact eprints@nottingham.ac.uk

ENDOSCOPIC MULTIMODAL IMAGING
IN BARRETT'S OESOPHAGUS

Jayan Mannath MD, MRCP

Thesis submitted to The University of Nottingham

for the degree of Doctor of Medicine

MEDICAL LIBRARY
QUEENS MEDICAL CENTRE

April 2013

Abstract

The incidence of oesophageal adenocarcinoma (OA) has increased exponentially in the western world over the past few decades. Barrett's oesophagus (BO) is a well known precursor of OA with a risk approximately 20 times more than that of background population. Regular endoscopic surveillance in patients with BO is recommended by most of the national gastroenterological societies. The advantage of Barrett's surveillance is to identify early subtle lesions which could then be managed early to avoid symptomatic and advanced cancers. The detection of such early lesions are challenging as they could be flat and inconspicuous on routine endoscopic examination. In the absence of any lesions, four quadrant biopsies every 1-2 cm of the whole length of Barrett's oesophagus is advised. This technique would map only 5-10% of the surface area of Barrett's segment and hence it is associated with significant sampling error. The improvement in electronics over the past decade has led to the production of endoscopes with better charged coupled devices and image enhancement techniques by altering the spectrum of light.

This thesis examines the role of multimodal imaging in Barrett's oesophagus with a focus on detecting dysplasia and early cancer (EC). Firstly, the role of high definition (HD) imaging in routine clinical setting was studied using data from patients who have undergone Barrett's surveillance. The yield of dysplasia by HD endoscopy was compared to standard definition (SD) endoscopy in this study. The role of narrow band imaging (NBI) with magnification in characterising abnormal lesions detected during BO surveillance was evaluated by performing a meta-

analysis of clinical studies. The role of autofluorescence imaging (AFI) in Barrett's oesophagus was examined in detail with a view to understand the biological basis of autofluorescence and to improve the specificity of this technique as it is associated with significant false positive results in clinical studies. A meta-analysis was performed to identify whether AFI has a clinical advantage over white light endoscopy in detecting Barrett's dysplasia and the inter-observer reliability of this technology was studied using AFI expert and AFI non-expert endoscopists. An objective method of measuring the autofluorescence intensity was proposed as a ratio of the red to the green colour tone (AF ratio) of the area of interest. When the AF ratio of the lesion was divided by the AF ratio of the background mucosa, an AF index is obtained. A pilot study was performed to identify a cut-off value of AF index to differentiate high grade dysplasia (HGD) and EC from non-dysplastic BO. Finally, the biological basis of AF intensity was examined using APC^{min} mouse colonic models. This study looked into the AF ratio of the colonic mucosal lesions and correlated it with the amount of collagen and elastin in the submucosal tissue. Collagen and elastin are known to be the strongest fluorophores of the gastrointestinal tract and the question addressed is whether the low AF intensity associated with dysplastic lesions is due to the thickening of mucosa or to a reduction of collagen and elastin.

Publications and presentations related to the work in this thesis

Publications

1. Mannath J, Subramanian V, Telakis E, Lau K, Ramappa V, Wireko M, Kaye PV, Raguath K. An inter-observer agreement study of autofluorescence endoscopy in Barrett's esophagus among expert and non-expert endoscopists. *Dig Dis Sci*. 2013 Feb; 58(2):465-70
2. Mannath J, Subramanian V, Hawkey CJ, Raguath K. Narrow band imaging for characterization of high grade dysplasia and specialized intestinal metaplasia in Barrett's esophagus: a meta-analysis. *Endoscopy*. 2010 May; 42(5):351-9
3. Mannath J, Raguath K. Era of Barrett's surveillance: does equipment matter? *World J Gastroenterol*. 2010 Oct 7; 16(37):4640-5
4. Mannath J, Raguath K. Reflux and Barrett's disease. *Endoscopy*. 2010 Jan; 42(1):34-7
5. Mannath J, Raguath K. Management of Barrett's Oesophagus. *F1000 Med Rep*. 2009 Jan 21; 1.

Book chapters

1. Mannath J, Ragunath K. Barrett's esophagus and esophageal adenocarcinoma-Wide field imaging techniques. *Gastrointestinal Cancers Endoscopic Imaging and Treatment*. Editors: P Sharma, N Reddy. ISBN-13: 978-9350258934
2. Mannath J, Ragunath K. Upper Gastrointestinal Endoscopy and Mucosal Biopsy. *Textbook of Clinical Gastroenterology and Hepatology*. Second Edition. Editors: CJ Hawkey, J Bosch, JE Richter, G Garcia-Tsao, FKL Chan. ISBN-13: 978-1405191821

Oral presentations

1. Mannath J, Subramanian V, Telakis E, Lau K, Ramappa V, Wireko M, Kaye PV, Ragunath K. An inter-observer agreement study of autofluorescence endoscopy in Barrett's esophagus among expert and non-expert endoscopists. Presented at UEGW 2011 at Stockholm
2. Mannath J, Subramanian V, Thomas T, Ragunath K. Multimodal imaging assisted endoscopic mucosal resection of Barrett's dysplasia and cancer. Presented at BSG annual meeting. *GUT*. 2010 Apr; 59(S1): A11-A12

Posters

1. Mannath J, Subramanian V, Rangunath K. Meta analysis: Utility of Narrow Band imaging in detecting high grade dysplasia in patients with Barrett's oesophagus. *Gut* 2009 Apr; 58(S2): A134
2. Mannath J, Subramanian V, Telakis E, Rangunath K. Accuracy of autofluorescence imaging video endoscopy in detecting high grade dysplasia and early cancer in Barrett's oesophagus: A meta-analysis. *UEGW*, 2011.

Acknowledgements

I am grateful to the following for their valuable help and support without which this thesis would not have been possible.

First and foremost I thank all the patients who participated directly or indirectly in the studies and I have learned a lot from them.

Appropriate ethical approval was obtained wherever necessary. The clinical study in chapter 3 was conducted as a service evaluation audit at Nottingham University Hospitals NHS Trust. The meta-analyses in chapters 4 & 5 were performed using published studies and no patient data was used. Clinical studies in Chapters 6 & 7 were performed using endoscopic images from a central database. These images were collected from 3 different studies [Endoscopic trimodal imaging studies (ETMI feasibility, ETMI RCT) and EURO II trial] which were approved by the Nottinghamshire Research Ethics Committees (ETMI-06/Q2403/29, ETMI RCT-07/H0407/65, EURO II-08/H0408/38). The mice colonic study in chapter 8 utilised formalinised mice colons obtained from the placebo arm of a study on chemo preventive agents on colonic cancer formation which was approved by the Nottingham Research Ethics Committee.

My primary supervisor Prof Krish Rangunath for giving me the opportunity to conduct research at Nottingham and providing help and support throughout the period.

My supervisor Dr Venkataraman Subramanian, Consultant Gastroenterologist, St James University Hospital, Leeds for providing me invaluable help in design of the studies, statistical analysis and correcting the thesis.

Dr Emmanouil Telakis and Dr Sarmed Sami, Research Fellows, Nottingham for helping me through some of the studies and in data collection.

Dr Philip Kaye, Consultant Histopathologist, Nottingham University Hospitals, for providing valuable support in the histopathological aspects of all the studies

Dr Anthony Shonde, Consultant Gastroenterologist, Kings Mill Hospital, Mansfield, for helping me with the mice colonic study.

My colleagues at Nottingham University Hospitals and University of Nottingham, Dr Steve Morgan, Prof Robin Spiller, Prof Chris Hawkey, Prof John Atherton, Dr Kar Lau, Dr Vidyasagar Ramappa and Dr Matthew Wireko for their support, guidance and inspiration. I also thank all the nursing and supporting staff at Nottingham for their valuable support.

Last but not least; I thank my wife Reji and my daughter Neelima for supporting me throughout the research period.

My outlook towards endoscopy has been completely transformed by the clinical exposure I have received throughout the research period and this has definitely made me a better clinician

Table of contents

Abstract	2
Publications and presentations	4
Acknowledgements	7
Chapter 1: Introduction	21
1.1 Introduction to endoscopic techniques	22
1.1.1 History of endoscopy	22
1.1.2 Endoscopy system	24
1.1.3 New modalities of image enhanced endoscopy	25
1.1.4 High resolution and magnification endoscopy	25
1.1.5 Chromoendoscopy	29
1.1.5.1 Methylene blue chromoendoscopy	30
1.1.5.2 Chromoendoscopy with other dyes	32
1.1.6 Fuji intelligent chromoendoscopy and I-scan	34
1.1.7 Confocal laser endomicroscopy	36
1.1.8 Infra red endoscopy	37
1.1.9 Narrow band imaging	38
1.1.10 Autofluorescence endoscopy	42
1.2 Barrett's oesophagus	47
1.2.1 Epidemiology of Barrett's oesophagus and oesophageal adenocarcinoma	47
1.2.2 Aetiology and pathogenesis of Barrett's oesophagus	49
1.2.3 Development of neoplasia in Barrett's oesophagus	52

1.2.4	Preventive strategies for developing Barrett's Oesophagus	53
1.2.5	Surveillance strategies in Barrett's oesophagus	55
1.2.6	Endoscopic imaging techniques used in Barrett's surveillance	56
1.2.7	Molecular markers in Barrett's oesophagus	57
1.2.8	Management of Barrett's oesophagus	59
1.2.8.1	Medical management of Barrett's oesophagus	59
1.2.8.2	Endoscopic resection of Barrett's neoplasia	60
1.2.8.3	Endoscopic ablative therapies	62
1.2.8.4	Surgical management of Barrett's neoplasia	65
1.2.9	How to improve outcome in patients with Barrett's oesophagus	65
	Chapter 2: Aims	67
	Chapter 3: High definition versus standard definition white light endoscopy for detecting early neoplasia in Barrett's oesophagus surveillance	69
3.1	Abstract	70
3.2	Introduction	72
3.3	Material and Methods	73
3.3.1	Data collection	63
3.3.2	Statistical analysis	74
3.4	Results	75

3.4.1 Dysplasia detection on target biopsies	75
3.4.2 Dysplasia detection on random and target biopsies	79
3.5 Discussion	83
3.5.1 Conclusions	86
Chapter 4: Narrow band imaging for characterisation of high grade dysplasia and specialised intestinal metaplasia in Barrett’s oesophagus; a meta-analysis	87
4.1 Abstract	88
4.2 Background	90
4.3 Methods	92
4.3.1 Selection of studies	92
4.3.2 Search Strategy	92
4.3.3 Data extraction and assessment of study quality	94
4.3.4 Data synthesis	96
4.4 Results	98
4.4.1 Description of studies	98
4.4.2 Diagnostic accuracy of NBI in HGD	99
4.4.3 Diagnostic accuracy of NBI in SIM	104
4.4.4 Heterogeneity of studies	109
4.5 Discussion	111
4.5.1 Principal findings	111
4.5.2 Clinical implications	111
4.5.3 Study limitations	112
4.5.4 Conclusions	114

Chapter 5: Role of video autofluorescence endoscopy in detection of dysplasia in Barrett’s oesophagus; a meta-analysis	116
5.1 Abstract	117
5.2 Introduction	119
5.3 Methods	120
5.3.1 Search Strategy	120
5.3.2 Selection of studies	120
5.3.3 Meta-analysis	121
5.3.4 Heterogeneity analysis	121
5.4 Results	121
5.4.1 Detection of high grade dysplasia/cancer	122
5.4.2 Detection of all dysplasia	124
5.4.3 False positive rates	124
5.4.4 Miss rates of high grade dysplasia and all dysplasia	128
5.5 Discussion	128
5.5.1 Limitations of the study	130
5.5.2 Conclusions	130
Chapter 6: An inter-observer agreement study of Autofluorescence endoscopy in Barrett’s oesophagus among expert and non-expert endoscopists	131
6.1 Abstract	132
6.2 Introduction	134
6.3 Methods	135
6.3.1 Patients	135
6.3.2 Endoscopic equipment	135

6.3.3 Endoscopic procedure	136
6.3.4 Selection of images for the study	136
6.3.5 Image evaluation	137
6.3.6 Histological assessment	138
6.3.7 Statistical analysis	138
6.4 Results	139
6.4.1 Number of AF positive lesions	139
6.4.2 Site of AF positive lesions	141
6.4.3 Inter-observer agreement for dysplasia	141
6.4.4 Accuracy of dysplasia detection	145
6.4.5 Quality of AFI images	145
6.5 Discussion	145
6.5.1 Limitations of the study	148
6.5.2 Conclusions	149
Chapter 7: Utility of an autofluorescence index to detect early neoplasia in Barrett's oesophagus; a pilot study	150
7.1 Abstract	151
7.2 Background	153
7.3 Methods	154
7.3.1 Images	154
7.3.2 Endoscopy system	154
7.3.3 Image analysis	155
7.3.4 Statistical analysis	155
7.4 Results	156
7.5 Discussion	160

**Chapter 8: Correlation of quantitative measures of autofluorescence
from video autofluorescence endoscopy with collagen and elastin
and changes over with time in a mouse model of colon cancer**

(APC^{min} mice)	162
8.1 Introduction	163
8.2 Materials and methods	165
8.2.1 Endoscopic equipment	165
8.2.2 Mouse colon cancer model (APC ^{min} mouse)	165
8.2.3 Mice colonic imaging	166
8.2.4 Image analysis using soft ware	167
8.2.5 Staining mice colons for elastin and collagen	167
8.2.6 Quantifying the amount of collagen and elastin with ImageJ	168
8.2.7 Statistical analysis	175
8.3 Results	175
8.3.1 Quantifying Autofluorescence in normal colon of APCmin mice sacrificed at different time points	175
8.3.2 Autofluorescence in mice colonic lesions from different ages	178
8.3.3 Elastin and collagen staining	178
8.4 Discussion	179
8.4.1 Limitations of the study	182
8.4.2 Conclusions	182

Chapter 9: Conclusions and clinical implications	183
9.1 The role of multimodal imaging in Barrett's oesophagus	184
Chapter 10: References	189

List of Tables

Chapter 1

Table 1: Diagnostic accuracy of magnification endoscopy to differentiate adenomatous from non-adenomatous colonic polyps 28

Table 2: Lesion characterisation in colon using narrow band imaging 39

Chapter 3

Table 1: Demographic and clinico-pathological details of endoscopy procedures 77

Table 2: Logistic regression for all dysplasia detected on targeted biopsies 78

Table 3: Logistic regression for all dysplasia detected on random and targeted biopsies 80

Table 4: Logistic regression for HGD/cancer for random and targeted biopsies 81

Table 5: Logistic regression for all dysplasia on random biopsies only 82

Chapter 4

Table 1: 'Quality Assessment of Diagnostic Accuracy Studies' 95

Table 2: Characteristics of the studies included in the meta-analysis 115

Table 3: Meta-regression analysis to identify sources of heterogeneity 110

Chapter 6

Table 1: Interobserver agreement κ (95% CI) for the number of AF positive lesions 140

Table 2: Interobserver agreement κ (95% CI) for the site of AF positive lesions	142
Table 3: Interobserver agreement κ (95% CI) for dysplasia	143
Table 4: Sensitivity, specificity and accuracy (95% CI) of dysplasia with histology as gold standard	144

Chapter 7

Table 1: Coordinates of the receiver operating characteristic curve showing the sensitivity and 1-specificity for various autofluorescence index ratios of one set of recordings.	158
---	-----

Chapter 8

Table 1: Autofluorescence ratio (red/green tone) of background mice colonic mucosa and mice colonic lesions of different ages	176
Table 2: Area fraction of collagen and elastin in background mice colonic mucosa and colonic lesions of different age groups	177

List of figures

Chapter 1

- Figure 1: Narrow band imaging with magnification showing regular pit patterns and regular micro-vascular patterns in non-dysplastic Barrett's 41
- Figure 2: Narrow band imaging with magnification showing distorted pits and irregular vascular patterns in dysplastic Barrett's 41
- Figure 3: High definition white light endoscopy showing a Barrett's cancer highlighted in purple on autofluorescence imaging 46
- Figure 4: Barrett's high grade dysplasia seen as a subtle lesion on white light endoscopy highlighted in purple colour on autofluorescence imaging 46

Chapter 3

- Figure 1: Flow chart of study procedures 76

Chapter 4

- Figure 1: Flow chart of study selection for meta-analysis 93
- Figure 2: Pooled sensitivity and specificity of NBI in diagnosing HGD on per-lesion analysis 100
- Figure 3: SROC curve of NBI in diagnosing HGD on per-lesion analysis 101
- Figure 4: Pooled sensitivity and specificity of NBI in diagnosing HGD on per-patient analysis 102
- Figure 5: SROC curve of diagnostic accuracy of NBI in characterising HGD on per-patient analysis 103
- Figure 6: Pooled sensitivity and specificity of NBI diagnosis of SIM

on per-lesion analysis	105
Figure 7: SROC curve of NBI diagnosis of SIM on per-lesion analysis	106
Figure 8: Pooled sensitivity and specificity of NBI diagnosis of SIM on per-patient analysis	107
Figure 9: SROC curve of NBI accuracy in diagnosing SIM on per-patient analysis	108
Chapter 5	
Figure 1: Pooled incremental yield of AFI compared to WLE in detecting HGD/cancer	123
Figure 2: Funnel plot for publication bias for detection of HGD/cancer comparing AFI and WLE	123
Figure 3: Pooled incremental yield of AFI compared to WLE in detecting all dysplasia	125
Figure 4: Pooled false positive rates for autofluorescence imaging detected lesions	125
Figure 5: Pooled false positive rates for white light endoscopy detected lesions	126
Figure 6: Pooled Odd's ratio of miss rates of high grade dysplasia or cancer compared between AFI and WLE	126
Figure 7: Pooled Odd's ratio of miss rates of all dysplasia compared between AFI and WLE	127

Chapter 7

Figure 1: ROC of two different sets of autofluorescence index ratios 157

Chapter 8

Figure 1: Image of mice colonic lesions stained with EVG, showing collagen stained in red (black arrow) and elastin in blue-black 169

Figure 2: Image of mice colonic lesions stained with EVG, showing collagen stained in red (black arrow) and elastin in blue-black 170

Figure 3: Background colonic mucosa stained with EVG stain with collagen in red and elastin in blue-black 171

Figure 4: Background colonic mucosa stained with EVG stain with collagen stained in red and elastin in blue-black 172

Figure 5: ImageJ software with RGB image converted to a 8-bit image before measuring the area fraction of collagen and elastin 173

Figure 6: The 8 bit image is analysed with 'threshold colour' marking the areas of interest in red and analysing the area fraction 174

CHAPTER 1

INTRODUCTION

1.1 Introduction to endoscopic techniques

1.1.1 History of endoscopy

The evolution of endoscopic technology over the past century has been closely related to the developments in the field of electronics and fibre optics. The credit of first gastroscopy goes to Kussmaul in 1868, which was lacking in illumination. Even after the invention of the first commercially available incandescent light by Thomas Edison in 1878, it took more than a quarter of a century to incorporate them into the endoscope. It was Hoffman, who first made an endoscope in 1911, which could tackle the tortuosity of the gut using multiple lenses and prisms. A semi flexible gastroscope using the same concept was materialised after another two decades by the efforts of Wolf and Schindler ¹.

A flexible fibre optical imaging device was first built in 1954 but the first use of flexible fibre optic endoscope materialised in 1958 by the efforts of Larry Curtis, a graduate in physics and Basil Hirschowitz, a trainee in gastroenterology ². This marked a new era in the history of endoscopy to tackle the tortuous and dark lumen of gastrointestinal tract, which was not examined using a flexible instrument before. The fibre scope was based on optical viewing bundles transmitting light focused onto the face of each fibre by repeated internal reflections. The image reconstructed at the top of the bundle is transmitted to the eye via a focusing lens. The fibres are closely packed, however there is always some space between the fibres resulting in a 'packing fraction' that is responsible for the fine mesh like effect frequently apparent in the transmitted images. Disadvantage of these scopes were the frequent breakage of the fibre optics due to

continued flexing of the endoscope, leading to loss of pixels and image quality. The technology evolved over the next 3 decades until the invention of charge coupled devices (CCD) in 1969. In the late 70's, CCDs were incorporated into the endoscopes and this started a new era for endoscopy. The CCDs produced electronic images that could be viewed on a television and this improved the audience experience and facilitated teaching. Essentially a CCD 'chip' is an array of several thousand individual photo cells known as picture elements (pixels) that receive photons reflected back from the mucosal surface and producing electrons in proportion to light received. The variable levels of charge are sent electronically to a video processor, which transposes this analog information into digital data, which in turn is processed to produce an image on a television monitor. The pixel density of CCDs have evolved since then to the current standards of high resolution endoscopy containing more than 850,000 pixels in the CCD³. This has improved the clarity of images thus facilitating early diagnosis of subtle lesions that could be tackled before progressing into an advanced disease.

Over the past decade, tremendous improvements occurred in the field of electronics and endoscopy. This is true in cases of imaging techniques and therapeutic capabilities. The introduction of capsule endoscopy and echo endoscope was some of the recent innovations that has revolutionised the practice of endoscopy.

1.1.2 Endoscopy system

The current standard video endoscopy system comprises of flexible endoscope, electronic processor, light source, and a television monitor. The endoscope has a control head and a flexible shaft with a manoeuvrable tip. The head contains a small and a larger wheel, which assists in the right and left as well as up and down movements of the tip respectively. It also has up to four buttons that help in freezing the image, printing and so on. The head is connected to a light source via an umbilical cord, through which pass other tubes transmitting air, water and suction. The vinyl covered shaft contains to and fro wiring and supporting electronics to the CCD 'chip' mounted at the distal end. This shaft also houses the light guide for providing illumination at the distal tip, control wires for manoeuvring the distal tip, a channel for suction that also accepts a variety of accessory devices and a channel for insufflations of air and water. The distal end unit has the CCD, lens system, opening for the accessory channel, and the light guide for providing illumination.

The umbilicus of the endoscope is connected directly to the light source. This box contains a xenon lamp that emits white light, which is passed through a red-green-blue (RGB) filter in the commonly used Olympus systems. The umbilicus is also connected to a video processor that receives the RGB images from the CCD, integrates them into a single image that is transmitted to the television monitor. Current television monitors offer high definition clarity.

1.1.3 New modalities of image enhanced endoscopy

Advanced techniques are developed to enhance the endoscopic image by increasing the resolution of the CCD and using high definition television to view the processed images. Currently, endoscopes with integrated zoom lenses and microscopes are available and with these technologies, intestinal tissues can be imaged at cellular and nuclear levels which provide in-vivo optical histology. Image enhancement using dye (chromoendoscopy) or optical methods (Narrow Band Imaging (NBI), Fuji Intelligent Chromo Endoscopy (FICE) and I-Scan) could allow improved visualisation and characterisation of lesions.

1.1.4 High resolution and magnification endoscopy

Conventional video endoscopes were equipped with CCDs of 100 000 to 300 000 pixels, so that each image is built up from those numbers of individual pixels. This is referred to as pixel density, which is important because it relates to the image resolution and indicates the ability to discriminate two closely approximated points. The higher the pixel density, better the image resolution and this in turn will help in identifying subtle lesions. The pixel density of CCDs has improved over the years and currently CCDs of 850 000 pixel density are available in the market ³. They are called high resolution scopes. Some of the endoscopes are equipped with optical zoom facility, by using a movable lens in the tip of the scope. The focal distance of these lenses can be controlled by a lever at the head of the endoscope. This allows visualisation of mucosa very closely and the micro-vascular and micro-structural details can be assessed ⁴⁻⁷. Endoscopes with

magnification up to 115 times are available commercially. The optical magnification is closely related to the high resolution abilities of endoscopes. Using the same level of optical magnification, high resolution chips will offer much more mucosal details. Image manipulation with electronic zooming is also feasible. However the level of magnification is limited and the quality of image will be lost after a particular level of magnification, which does not happen with optical zoom scopes with high resolution CCDs.

High resolution endoscopy (HRE) with magnification had been widely studied in upper gastrointestinal disorders. Gastric atrophy and *H.Pylori* gastritis could be reliably identified by magnified endoscopic assessment of gastric antrum and corpus^{8,9}. The normal gastric mucosa was seen as honeycomb like sub-epithelial capillary network pattern (SECN) with collecting venules (CV). The SECN and CV were lost and enlarged white pits were seen in *H.Pylori* gastritis. Gastric atrophy manifested with loss of normal pit patterns and irregular collecting venules. The sensitivity and specificity of these findings were more than 90%^{10, 11}. Other investigators have also reported good sensitivity and specificity for magnification endoscopy to identify *H.Pylori* gastritis⁹. Magnification endoscopy (ME) is also useful in identifying intestinal villi, which will be useful in patients with suspected celiac disease. This could be used to assess the degree of villous atrophy and was found to be well correlated with histology^{12, 13}.

Patients with reflux symptoms and no macroscopic evidence of oesophagitis are labelled as non-erosive reflux disease (NERD). Role of magnifying endoscopy was studied in this context to identify subtle changes at the gastro-oesophageal

junction. No particular feature was sensitive enough to identify NERD, but changes like triangular indentations, apical mucosal breaks, and pinpoint blood vessels at the squamo-columnar junction were identified more frequently in the patients with reflux disease ^{14, 15}.

In Barrett's oesophagus (BO), role of magnification endoscopy had been studied mostly in conjunction with chromoendoscopy. Kara *et al* found that HRE alone could detect most of the dysplastic lesions; the yield of which was improved by indigocarmine dye and narrow band imaging ¹⁶. ME has also been proposed to improve yield of specialised intestinal metaplasia in BO. Indigocarmine and methylene blue were used with ME to identify intestinal metaplasia using ridged or villous pit patterns. This has shown significant correlation with histology in these studies ^{17, 18}. Improved yield of specialised intestinal metaplasia and dysplasia was found with acetic acid chromoscopy and magnification as well ^{19, 20}. HRE was compared with acetic acid chromoscopy, indigocarmine chromoscopy and NBI in an inter-observer study of Barrett's oesophagus by Curvers *et.al* ²¹. Interestingly, the addition of chromoscopy or NBI did not improve the inter-observer agreement or yield of dysplasia. The yield for identifying early neoplasia with white light images was 86% for all observers, 90% for experts, and 84% for non-experts.

Table 1: Diagnostic accuracy of magnification endoscopy to differentiate adenomatous from non-adenomatous colonic polyps.

Author	Year	Type of study	Patients	Lesions	Sensitivity %	Specificity %	Accuracy %
Rogart <i>et al.</i> ²²	2008	Prospective	131	265	69	86	77
Zanoni <i>et al.</i> ²³	2007	Prospective	161	213	91	67	84
Pohl <i>et al.</i> ²⁴	2008	Prospective	63	150	84	64	76

Magnification endoscopy was used to differentiate adenomatous from non-adenomatous colonic polyps using pit patterns. Kudo classification of various pit patterns in colonic polyps are useful in differentiating non-adenomatous polyps (Hyperplastic polyp, inflammatory polyp etc.) from adenomatous polyps and colon cancer²⁵. These include 6 patterns. Patterns I and II were considered non-neoplastic polyps, IIIS, IIIL and IV were considered to depict adenomatous polyps. Pattern V, which describes irregular pit patterns, were noted to represent cancer. Magnification endoscopy alone was found to have a modest accuracy to differentiate these. Diagnostic accuracy of studies which used magnification endoscopy is summarised in table 1. However when magnification endoscopy is combined with chromoendoscopy, the diagnostic accuracy was significantly better. Most reported studies had accuracy more than 90%^{26,27}.

1.1.5 Chromoendoscopy

The use of special stains in combination with magnification endoscopy enhances the mucosal details seen at endoscopy with characteristic mucosal appearances such as pit patterns in various parts of the gastrointestinal tract^{28,29}. This will help in targeting biopsies from suspicious areas and thus improve the yield of dysplasia in precancerous conditions like Barrett's oesophagus. Vital stains like Lugol's solution and methylene blue are absorbed into the cells and thus highlight the surface pit patterns. Contrast stains like indigo carmine are not absorbed into the cells but accumulate in pits between cells highlighting mucosal details. Reactive stains like Congo red and phenol red react to changing conditions of acid secretion and carry a potential with regard to the early detection of gastric cancer. It is

important that a special spraying catheter is used permitting optimal dispersion of the dye onto the mucosal surface. Even though chromoendoscopy is cheap and effective it is underused in the western world compared to the Far East. Also, there have been concerns raised as photosensitisation of methylene blue with white light can induce formation of reactive oxygen species, causing single strand breaks and generation of oxidative alterations within the DNA^{30,31}. However, this is not the case with contrast stains, which are used preferentially, and yields comparative results.

1.1.5.1 Methylene blue chromoendoscopy

Methylene blue (MB) is an absorptive dye which is probably the most widely studied in Barrett's oesophagus. It is taken up by actively absorbing intestinal epithelial cells and dysplastic mucosa, but not by normal oesophageal and gastric mucosa. During MB chromoendoscopy, specialised intestinal metaplasia (SIM) typically stains blue, where as a lighter intensity and increased heterogeneity in the staining pattern predict high grade dysplasia (HGD) and/or adenocarcinoma.

One of the earlier studies by Canto *et al* investigated the MB staining patterns and the yield of SIM and dysplasia in Barrett's. The accuracy of SIM detection was 90% and they found that light to absent staining and moderate to marked heterogeneity were significantly associated with high grade dysplasia or cancer³². Further to this various studies compared the yield of MB directed target biopsies to random biopsies in detection of dysplasia and SIM. Some of the studies demonstrated significantly higher yield of SIM using MB chromoendoscopy with

sensitivities ranging from 80 to 98%^{33,34}, while others showed much lower sensitivities³⁵⁻³⁷. Difference in concentration of MB, the volume used and the time of contact could all be the reasons for this variability in results. The results for detecting dysplasia are even more inconsistent. A recent meta-analysis included 9 studies comparing MB directed biopsies to random biopsies. They found that there was no significant incremental yield of SIM and dysplasia with MB chromoendoscopy³⁸. The yield of SIM with MB was 75% versus 70% for random biopsies, and that for dysplasia was 43% and 32% respectively for MB targeted biopsies and random biopsies. Sub analysis showed a modest 7% incremental yield for detecting HGD and cancer³⁸. Even among experts there is a controversy regarding the ideal ways to target the biopsies. The staining patterns for SIM and dysplasia are also controversial, which had made this technique less frequently used in the present era. The advent of electronic chromoendoscopy techniques which could also provide details on the vascular patterns has superseded chromoendoscopy to some extent.

Colonic MB chromoendoscopy had shown to improve dysplasia detection in inflammatory bowel disease³⁹. There is a paucity of data on MB chromo colonoscopy, probably due to the concerns raised about the potential DNA damage and the larger volume of MB necessary compared to upper gastrointestinal examination⁴⁰.

1.1.5.2 Chromoendoscopy with other dyes

Lugol's iodine is a compound iodine solution which is absorbed by the glycogen containing squamous epithelium and stains it dark brown. This is particularly useful in identifying oesophageal squamous dysplasia which will appear lighter in colour compared to the normal squamous epithelium⁴¹⁻⁴³. It is also possible to differentiate the columnar lining and gastric mucosa effectively. In a screening study for high risk patients, Lugol's iodine increased the sensitivity of oesophageal squamous dysplasia detection significantly⁴⁴. In BO, the specialised intestinal metaplasia does not stain after Lugol's iodine application. This can be used to demarcate the columnar lined oesophagus from the normal squamous mucosa⁴⁵.

Crystal violet is another absorptive stain which was used in colonoscopic assessment of polyps^{46,47}, as it is taken up by crypts of Lieberkuhn⁴⁸. Its role in Barrett's oesophagus is not clearly understood as there is a paucity of literature.

Indigocarmine (IC) is much more widely used in clinical practice now. This dye is not absorbed by the epithelial cells, but augments the mucosal details thus enabling to identify mucosal irregularities. The use of IC in Barrett's oesophagus and colonic lesion detection had been widely studied. Sharma *et al* found that magnification endoscopy with indigocarmine spray is useful in identifying intestinal metaplasia and dysplasia in BO. All patients with HGD had irregular/distorted pit patterns on inspection. Ridged/villous pattern were suggestive of intestinal metaplasia. However LGD patients also had ridged pattern and could not be differentiated from intestinal metaplasia alone⁴⁹. However

compared to high resolution endoscopy, IC chromoendoscopy (ICC) could detect only a limited number of additional dysplastic lesions and did not alter the sensitivity of detecting dysplasia ¹⁶. Similar results were obtained by Curvers *et al*, who did not find any improvement in inter-observer variability and yield of dysplasia when magnification ICC is compared with magnified high resolution images ²¹. The high resolution endoscopy with the high definition systems and magnification are able to provide much more mucosal details compared to the previous generation of endoscopes, which could explain these results.

ICC is much more widely used in colonic lesions for differentiating polyps and detecting dysplasia. The adenoma detection rates of ICC were superior to standard white light endoscopy in various comparative studies. This was particularly sensitive in detecting small and flat adenomas ⁵⁰⁻⁵². Contrary to these findings, one of the studies did not find any difference in detecting adenomas using HRE and chromoscopy compared to standard endoscopy. However the total number of flat lesions detected was better with chromoscopy as with hyperplastic polyps ⁵³.

ICC seems to be beneficial in characterisation of polyps and differentiating adenomatous from non-adenomatous polyps using Kudo pit patterns. The sensitivities of ICC vary from 82% to 100% and specificities vary between 82% and 95%. The Japanese endoscopists are more experienced than the western endoscopists in differentiating the polyp pit patterns and this could explain the variations in the diagnostic accuracy ⁵⁴⁻⁵⁶.

Various studies have evaluated the role of ICC in detecting dysplasia during ulcerative colitis surveillance. Pan colonic dye spray and targeted biopsies are found to have better yield in detecting dysplasia. Rutter *et al* compared the yield of dysplasia in random biopsies and targeted biopsies after ICC. Out of the 2904 non-targeted biopsies, none of them showed dysplasia in 100 patients. The same patients required only 157 targeted biopsies after ICC, and detected 9 dysplastic lesions⁵⁷. Similarly, magnification ICC was found to improve the yield of dysplasia and also helped in characterising detected lesions⁵⁸.

The chromoendoscopy had been in use for more than two decades but has its own limitations. The spraying of dye can increase the procedure time and is sometimes messy. Also there is a lack of standardisation of the technique, producing variable results in the clinical trials. Lack of evidence from well controlled studies to assess the clinical utility, cost effectiveness and patient acceptability are some of the reasons for its under use, especially so in the western world.

1.1.6 Fuji Intelligent Chromo Endoscopy (FICE) and I-Scan

These techniques are based on a new computed spectral estimation technology. FICE (Fujinon endoscopy®) and I-Scan (Pentax Medical®) transforms an ordinary endoscopic image taken from the video processor and arithmetically processes the reflected photons to reconstitute virtual images by increasing the relative intensity of narrowed blue light to a maximum and by decreasing narrowed red and green light to a minimum. This leads to better delineation of microvasculature and mucosal pit patterns due to the differential absorption of

light by haemoglobin in the mucosa. FICE has been compared with standard endoscopy and indigocarmine chromoendoscopy in colonic polyps to differentiate neoplastic polyps from non-adenomatous polyps. The diagnostic accuracy of FICE with and without magnification was 83% and 90%. This was significantly better than standard endoscopy with and without magnification and was comparable to chromoendoscopy²⁴. A randomised study looked at the adenoma detection rates of FICE without magnification and chromoendoscopy. The detection rates were similar; however these results are valuable in that, chromoendoscopy could be replaced by FICE which is a dye less technique⁵⁹. There is a paucity of data on the use of FICE in upper gastrointestinal tract⁶⁰. A recent study has found that Barrett's oesophagus can be easily diagnosed with FICE compared to standard endoscopy, with a clear demarcation between the Barrett's segment and gastric mucosa⁶¹. More studies are necessary in Barrett's oesophagus comparing to other modalities to assess the utility of this new technique.

I-Scan is the latest addition to the field of electronic chromoendoscopy based on a similar mechanism as in FICE. It was found to improve detection of small colonic polyps in the left colon compared to high definition colonoscopy. However there was no difference in neoplasia pick up rates among I-scan, high definition colonoscopy and chromoendoscopy⁶². I-scan was found to improve the yield of minimal change reflux oesophagitis compared to white light endoscopy in a randomised trial. This study also showed improvement in the inter-observer reliability of Los Angeles classification of reflux oesophagitis⁶³.

1.1.7 Confocal laser endomicroscopy

The concept of 'optical biopsy' has been achieved in its true sense by the confocal laser endomicroscopy. Two systems are commercially available, which includes an endoscope with integrated confocal microscope at the tip (Pentax Medical®), and a probe based confocal microscope which can be passed through the working channel of an ordinary endoscope (Mauna Kea). To create confocal images, blue laser light is focused on the desired tissue via the distal end of confocal endoscope. Applied fluorescent materials (usually intravenously) are excited by laser lights, which is detected by the confocal optical unit in an exactly defined horizontal level. Extreme magnification (up to 1000 times) is obtained with this technology acquiring images at the cellular/nuclear level mimicking histopathology sections, thereby allowing targeted biopsy and reducing the number of random biopsies.

One of the earliest reports on confocal laser endomicroscopy (CLE) was published in 2005, detecting *H.Pylori* colonisation of stomach in a 70 years old gentleman ⁶⁴. CLE was used in Barrett's oesophagus to study the mucosal morphology and predict dysplasia. The sensitivity in predicting intestinal metaplasia and dysplasia compared to targeted histology was 98% and 93% with a specificity of 94% and 98% ⁶⁵. CLE with optical biopsies or targeted biopsies have shown to improve the yield of endoscopically inapparent BO dysplasia in a randomised trial, compared to non-targeted biopsies ⁶⁶. In colon, CLE was found to be highly accurate in predicting intra-epithelial neoplasia and differentiating dysplasia associated mass lesions and adenomas in ulcerative colitis ^{67, 68}.

The endocytoscopy is a relatively new addition to the endoscopic magnification technology and these are ultra-magnification (450-1125 times) catheter based endoscopes that can be passed through the working channel of a standard endoscope. In combination with chromo agents, they can provide in vivo histological images. Unlike confocal endoscopy, endocytoscopes produce colour images but does not scan deeper cellular levels.

1.1.8 Infra red endoscopy

This recently developed technology uses near-infrared light, which has limited scattering characteristics and low absorption by water and haemoglobin that in turn allows deeper penetration into the tissue compared to white light. This endoscopy system uses a high performance CCD which is sensitive to infrared and white light along with two ranges of infrared light emitted by the light source. Intravenously administered indocyanine green dye enables to clearly visualise mucosal and submucosal vessels with the infrared light and is found to be useful in identifying the depth of gastric cancers. Indocyanine is excited by rays at a wavelength of 768 nm to emit fluorescence at a wavelength of 807 nm in the infrared (IR) range. Thirty patients with gastric tumours were examined using infra red endoscopy. Fluorescence was positive in 8 of 10 gastric cancers with sub mucosal invasion and 1 of 20 adenomas or intra-mucosal gastric cancers. IR endoscopy could be a useful tool to estimate the depth of invasion of gastric lesions ^{69, 70}. Further studies are necessary to assess its utility in other parts of gastro intestinal tract.

1.1.9 Narrow band imaging

Narrow band imaging (NBI) is a relatively new technology of image enhanced endoscopy. It offers advantages of chromoscopy without the use of dye spray. This was first described in 2004 by a Gono *et al* ⁷¹ and is patented by Olympus corporation, Tokyo, Japan. Standard white light endoscopy uses full visible wavelength range of 400 to 700 nm, to produce a red-green-blue image. White light from a xenon lamp is passed through a red-green-blue filter (RGB filter) and the mucosa is sequentially illuminated with these three colours. The red, green, and blue reflected light is detected by a monochromatic charged coupled device (CCD) integrated at the tip of the endoscope, and the three images are merged into a single colour image by the video processor. In endoscopic systems with NBI, an additional filter is activated by pressing a button on the hand control of the endoscope. This filter narrows the band widths of the emitted blue (440-460 nm) and green light (540-560 nm) and the relative contribution of blue light has been increased. The penetration of light into the tissue depends on the wavelength; the longer the wavelength, the deeper the penetration. Blue light penetrates only the superficial layers; whereas the red light penetrates deeply. By narrowing the bandwidths of blue and green light, the superficial mucosal details are better visualised. Also, the blue light is absorbed by haemoglobin, enabling visualisation of superficial vasculature. The RGB based system and NBI are used mainly in Japan and United Kingdom, whereas in other parts of world, a white light illumination system with a colour CCD is used.

NBI is often called as ‘electronic chromoendoscopy’ and offers a few advantages over traditional chromoendoscopy. NBI is user friendly and does not need any additional dyes to be used. It allows uniform visualisation of the endoscopic field, whereas the use of dye might not distribute equally over the mucosa. In addition to these practical advantages, NBI also allows visualisation of micro vasculature with high contrast, which is not possible with chromoscopy. Examining the mucosal pit patterns and vascularity using NBI could help in identifying subtle abnormalities harbouring dysplasia. This had been widely studied in upper and lower gastrointestinal tract. The details of lesion characterisation in colon are outlined below (Table 2).

Table 2: Lesion characterisation in colon using narrow band imaging

Author	Year	No of patients	No of lesions	Sensitivity %	Specificity %
Machida <i>et al.</i> ⁷²	2004	34	43	91	100
Su <i>et al.</i> ⁷³	2006	78	110	96	88
Chiu <i>et al.</i> ⁵⁵	2006	133	180	95	72
East <i>et al.</i> ²⁶	2007	20	33	86	80
Hirata <i>et al.</i> ⁷⁴	2007	99	148	99	94

NBI could be useful in detecting Barrett's dysplasia compared to standard resolution white light endoscopy (WLE). In a prospective tandem endoscopy study of 65 patients, higher grades of dysplasia were detected by NBI compared to WLE. NBI directed target biopsies yielded more dysplasia than WLE directed biopsies and the number of biopsies taken by WLE were significantly more than that of NBI ⁷⁵. An earlier study by Kara *et al* compared the dysplasia detection rates of HRE, indigocarmine chromoscopy and NBI with magnification. Targeted biopsies with HRE alone had a sensitivity of 79% in detecting HGD. The addition of chromoscopy and NBI did not improve the yield significantly. The first study described above, used standard resolution endoscopy, while the latter study used HRE. This could explain the variability in the results. More studies are necessary to comment on the ability of NBI in detecting dysplastic lesions ¹⁶.

Narrowband imaging with magnification however could help in assessing the micro-structural and vascular patterns of any suspicious areas detected in the Barrett's segment (Figure 1-2). Irregular vascular patterns and irregular micro-structural patterns indicate possibility of dysplasia, while inflammation and scarring could be excluded. There are various studies which identified different mucosal pit patterns and vascular patterns in dysplastic and non-dysplastic Barrett's. Singh *et al* described four different mucosal pit patterns and two vascular patterns (regular or irregular) on NBI with magnification. Type A was round pits with regular micro-vasculature. Type B was villous/ridged patterns with regular micro-vasculature. Type C patterns showed absent pit patterns with regular vascular patterns and type D was irregular pits with irregular micro-vasculature ⁷⁶.

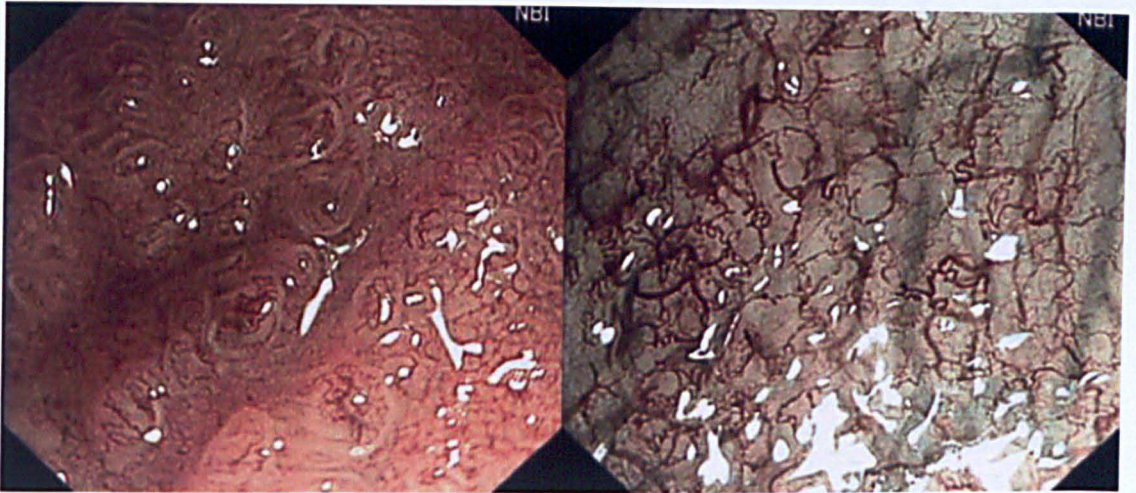


Figure 1: Narrow band imaging with magnification showing regular pit patterns and regular micro-vascular patterns in non-dysplastic Barrett's

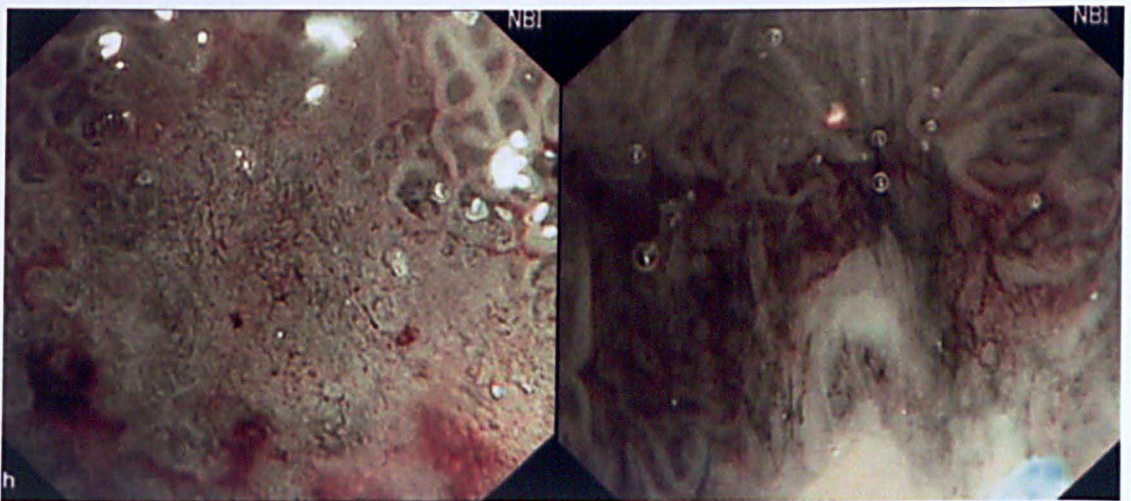


Figure 2: Narrow band imaging with magnification showing distorted pits and irregular vascular patterns in dysplastic Barrett's

Type A pattern was associated with columnar epithelium and the positive and negative predictive values were 100% and 89% respectively. Similarly patterns B and C were thought to represent intestinal metaplasia and the positive and negative predictive values were 90% and 96%. Type D pattern represents HGD or early cancer with positive and negative predictive values of 79% and 100%. Reports from other studies were variable and some of the investigators used different classification systems of the mucosal pit patterns.

NBI is widely available for clinical use and magnification endoscopes are commercially available. In this setting it is important to clarify whether NBI with magnification is truly worthwhile on routine surveillance of Barrett's patients. The role of NBI in detecting dysplastic lesions remains controversial, but most of the studies used NBI to characterise the detected lesions. If NBI offers good accuracy in characterising lesions, this would help in reducing the number of random of biopsies and help in targeting lesions. This also has implications in endotherapy where NBI could be used to delineate the lesions based on the pit patterns and vascular patterns.

1.1.10 Autofluorescence endoscopy

The endoscopic techniques are evolving constantly and we are moving beyond white light endoscopy to the newer modalities using the light tissue interaction. The phenomenon of autofluorescence occurs when a light of shorter wavelength interacts with a tissue containing endogenous fluorophores, which in turn emits light of longer wavelength. A number of biological substances in the gastrointestinal tract such as collagen, elastin, nicotinamide, and flavins can act as

endogenous fluorophores⁷⁷. Earlier autofluorescence imaging systems used fibre optic endoscopes which failed to produce sufficient image quality for clinical utility. However the emergence of high resolution video endoscopy with a second CCD for autofluorescence imaging has made it possible to obtain pseudo colour images with significant improvement in quality. AFI offers an easy way to distinguish between normal and tumorous tissue by combining an autofluorescence image on irradiating with a blue light of wavelength of 390-470 nm. The image of green reflected light depicts the absorbed light by haemoglobin, so that normal tissue appears pale green and tumour tissue appears magenta.

There are various studies which examined the role of AFI in Barrett's oesophagus. One of the earliest studies used a fibre based laser induced fluorescence system, which could be passed through the accessory channel of the endoscopes.

Panjehpour *et al* studied this system in 36 patients with BO. The probe was kept in close contact with the site of interest and using a foot pedal the measurement was taken. Analysis was done using a mathematical model. They found that 96% of non-dysplastic Barrett's was classified as benign and 90% HGD as pre-malignant⁷⁸. 5-aminolevulinic acid-induced protoporphyrin IX fluorescence was found to identify areas of HGD with a modest sensitivity of 70% in a later study⁷⁹. In vitro studies on surgical specimens showed that the highest fluorescence ratio was obtained in areas of adenocarcinoma, compared to dysplastic Barrett's and non-dysplastic Barrett's⁸⁰. The next generation of light induced autofluorescence endoscopes (LIFE) was investigated in the turn of this century. Utility of autofluorescence endoscopy to detect the presence and extent of occult malignant

and premalignant oesophageal and gastric lesions were demonstrated by the Amsterdam group in 2001⁸¹. In a randomised crossover trial Kara *et al* investigated the role of AFI in detection of dysplasia in BO compared to WLE. The sensitivity of WLE targeted biopsies was better than that of AFI in this study (85% vs. 69%)⁸². Thus, AFI did not improve dysplasia detection rates using this system. This resulted in introduction of a video autofluorescence endoscope which was studied in 2005 again by the Amsterdam group. This was a prototype system from Olympus Corporation, Japan, which is a high resolution video endoscope that has separate CCDs for WLE and AFI. 22 patients with HGD were examined with AFI and WLE. AFI detected additional lesions in 3 patients compared to WLE. The use of AFI was found to be feasible and promising in detecting dysplasia⁸³.

These earlier studies prompted to use AFI as a 'red flag' technique to highlight suspected areas in Barrett's which could be closely examined with WLE or NBI with and without magnification. One of the disadvantages observed was the high false positive rates for AFI and it was hypothesised that this could be improved by additional NBI use. Twenty patients with suspected HGD were observed with AFI and suspected areas were examined closely with NBI. All the 28 lesions in this cohort were picked up by AFI; however there was a false positive rate of 40%. This was reduced to 10% by the use of NBI, thus making a combined approach more specific⁸⁴. A randomised trial comparing AFI and WLE in Barrett's surveillance patients was performed where AFI was found to improve dysplasia detection rates. However this did not suggest replacing the standard four quadrant

biopsy protocols as in 11/19 patients dysplasia was detected only on random sampling⁸⁵. The combined use of WLE, AFI and NBI is possible with commercially available endoscopes with magnification. These different modalities could be used by the press of a button and the operator can switch back and forth in seconds. The value of this 'trimodal imaging' was investigated by the Amsterdam group. AFI was superior to WLE in detecting dysplastic lesions, but the false positivity was high as reported before (81%). This was reduced to 26% after inspection with NBI⁸⁶.

The role of AFI in colonic imaging is less well studied. Back to back colonoscopy with AFI and WLE examined the adenoma detection rates, which showed increased pick of adenomas in the right colon by AFI⁸⁷. However a study from Japan, which compared chromoendoscopy, NBI and AFI found that chromoscopy is superior to other modalities⁸⁸. More well designed studies are necessary in colon, to assess the utility of this technique.

It is possible that the AFI intensity changes with progressing dysplasia and also there is likely to be a difference with non-dysplastic and dysplastic Barrett's. This could not be easily differentiated endoscopically as areas of inflammation, scarring and dysplasia will show low intensity signals (magenta/purple) compared to the normal green mucosa on AF imaging (figure 3-4). However, a ratio of the 'red tone to the green tone' or vice versa analysis of images might be helpful to differentiate the true positives from the false positives.

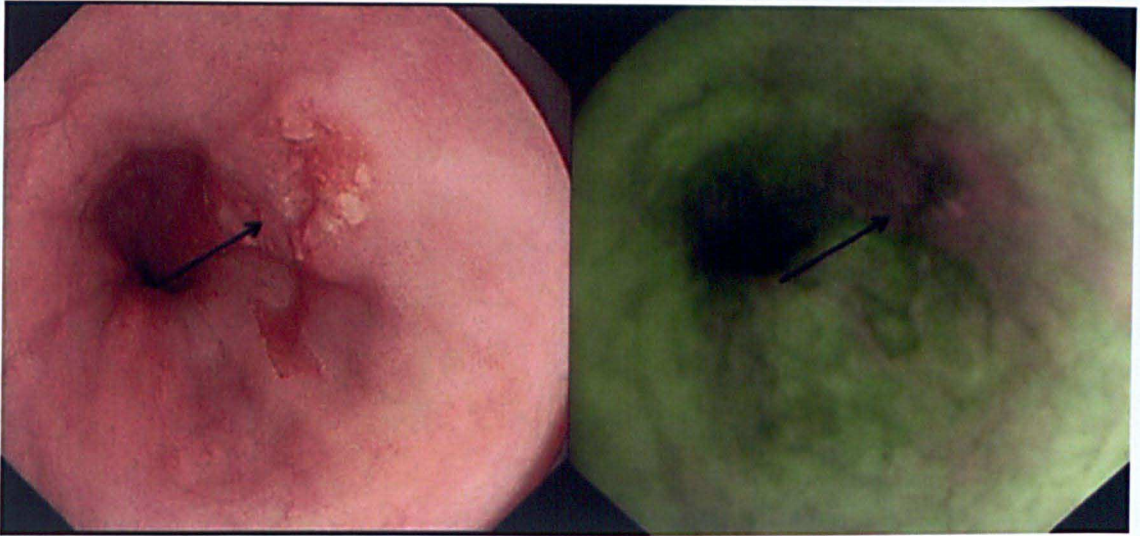


Figure 3: High definition white light endoscopy showing a Barrett's cancer highlighted in purple on autofluorescence imaging

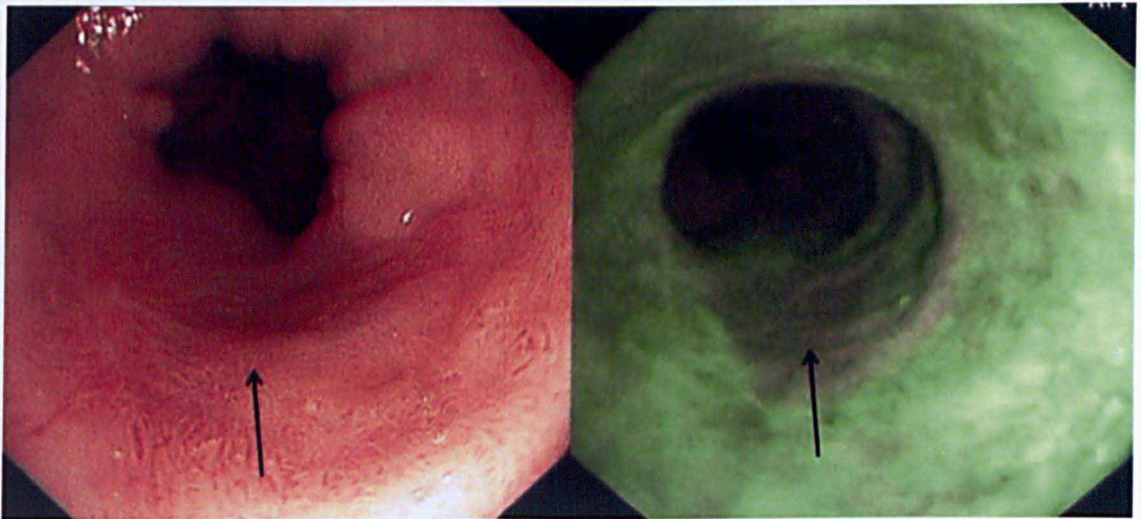


Figure 4: Barrett's high grade dysplasia seen as a subtle lesion on white light endoscopy highlighted in purple colour on autofluorescence imaging

1.2 Barrett's oesophagus

1.2.1 Epidemiology of Barrett's oesophagus and oesophageal adenocarcinoma

Barrett's oesophagus (BO) is named after Norman Barrett who first described this condition in 1950. Various investigators have described conditions similar to this since 1906. One of the first descriptions was by a pathologist named Tileston, who found 'peptic ulcer of the oesophagus' with surrounding mucosa simulating that of stomach. The anatomical origin of this abnormal lining was debated for a few decades. Norman Barrett himself believed that, this abnormal lining is in fact due to stomach tethered to chest with a congenitally short oesophagus ⁸⁹. A few years later, Allison and Johnstone, published their observations that the abnormal columnar lining is from the oesophagus. This was strengthened by their observations that the hollow organ contained submucosal glands and muscularis layer which are characteristic of oesophagus. Furthermore, they identified interspersed squamous islands in the columnar lining, strengthening the argument ⁹⁰. In 1957, Barrett agreed with these findings and his name was given to the condition where lower oesophagus was lined by columnar epithelium. In 1976, Paull *et al* published details of the various types of the columnar epithelium which was identified at the lower oesophagus. These included a gastric fundic type, a junctional type and a distinctive intestinal metaplasia, which was called specialised intestinal metaplasia ⁹¹. The complete specialised intestinal metaplasia with goblet cells are since then considered to be the hallmark of Barrett's oesophagus.

The endoscopic diagnosis remained challenging as the normal gastro-oesophageal junction (GOJ) was difficult to define in the presence of columnar epithelium. Many investigators argued that the distal oesophagus would normally contain some columnar epithelium. After years of contemplation, the Barrett's subgroup of the international working group for classification of oesophagitis (IWGCO) developed the Prague criteria to facilitate an internationally acceptable nomenclature for endoscopic description of Barrett's oesophagus in 2006 ⁹².

BO is characterised by replacement of the distal squamous oesophageal epithelium by columnar mucosa containing specialised intestinal metaplasia (SIM). The specialised intestinal metaplasia is considered to predispose to adenocarcinoma, and it could be argued that presence of SIM anywhere in the oesophagus could be called Barrett's and not necessarily the metaplasia at the lower oesophagus.

The average age of diagnosis of Barrett's is 55-65 years with a male preponderance at 2:1 ratio to females. Although Barrett's oesophagus can affect children, this is seldom seen below the age of 5 years, which strengthens the argument that Barrett's is an acquired condition. The condition is less often reported in the African Caribbean and Asian population compared to white Caucasians ^{93,94}. Thus white males in their middle age are the most predisposed patients, constituting 80% all cases. The role of smoking, obesity and alcohol in the pathogenesis of Barrett's is controversial. Some studies have reported progression from non-dysplastic BO to adenocarcinoma in patients with abdominal obesity and smoking habits ⁹⁵⁻⁹⁷.

The prevalence of Barrett's in the general population is variable depending on the population studied and the definition used. A Swedish population based study identified the prevalence as 1.6% of the general population ⁹⁸. Interestingly, around 45% patients with BO lacked significant reflux symptoms in this study, which suggests that screening programmes for detecting Barrett's in the population with reflux disease would be inadequate. There are reports of familial aggregation of Barrett's oesophagus and oesophageal adenocarcinoma. The presence of family history with first or second degree relatives having Barrett's oesophagus or oesophageal adenocarcinoma was significantly higher in cases than controls (24% Vs 5%) ⁹⁹. Germline mutations in MSR1, ASCC1 and CTHRC1 have been associated with BO and OA in a study conducted in 21 concordant affected sibling pairs ¹⁰⁰. However, larger cohort studies are necessary to validate these findings.

1.2.2 Aetiology and pathogenesis of Barrett's oesophagus

Barrett's oesophagus is a well recognised complication of long standing reflux disease. Patients who develop BO tend to have a combination of clinical features which include presence of hiatus hernia and reduced lower oesophageal sphincter pressure ¹⁰¹. These predispose to Gastro oesophageal reflux (GORD). Delayed oesophageal acid clearance time and duodeno-gastric reflux facilitating bile in the oesophageal lumen are also thought to be predisposing to development of BO ¹⁰². There are various oesophageal defence mechanisms in place. The anti-reflux barrier includes the high pressure zone at the gastro-oesophageal junction (GOJ) maintained by the tonic contraction of the lower oesophageal sphincter (LOS).

The external compression by the crus of the right diaphragm and the intra-abdominal location of the LOS also helps to maintain the high pressure at the lower oesophagus thus preventing reflux. However the LOS relaxes episodically and transiently in healthy persons. Reduction in the LOS pressure can be provoked by various dietary factors including chocolate, fatty foods, alcohol and smoking. These factors are seen to increase the transient LOS relaxations (TLOSRS). This predisposes to reflux of acid, bile, pepsin and pancreatic enzymes causing mucosal injury to the oesophagus ^{103, 104}.

The damage to the oesophageal lining is dependent on the duration of acid or other noxious substances contact with the mucosa rather than the number of episodes. Healthy individuals clear the oesophageal contents in various ways including the help of gravity, peristalsis and presence of bicarbonates in the salivary secretions. Dysmotility of the oesophageal musculature resulting in weak or ineffective peristalsis is an important contributing factor in the pathogenesis of GORD ¹⁰⁵.

BO develops through the process of metaplasia which implies that one kind of fully differentiated cell replaces another. Metaplasia occurs as a result of constant noxious substance exposure, where the injured mature cells are repaired by aberrant differentiation of immature proliferating cells. The metaplastic columnar epithelium seems to be a favourable adaptation for long standing reflux as columnar epithelium is resistant to reflux compared to squamous epithelium. The pattern of acid exposure to the metaplastic epithelium might play a role in the progression to dysplasia and cancer. An ex-vivo study showed that pulsed acid exposure to the metaplastic epithelium resulted in cellular proliferation as

compared to constant acid exposure when normal oesophageal, BO and duodenal cells were exposed to acid. The authors proposed a model in where diverse patterns of acid exposure may be contributing to the heterogeneity and unpredictability in progression of neoplasia in Barrett's ¹⁰⁶. A strong and probably causal relationship between gastro-oesophageal reflux and oesophageal adenocarcinoma was reported in a population study and they also suggested that the more frequent, more severe, and longer lasting symptoms of reflux are associated with higher risk of adenocarcinoma ¹⁰⁷. However, this was a case-control study based on personal interviews with regard to the severity of symptoms and is subject to bias. An association is definitely forthcoming but causal relationship is difficult to confirm. It was hypothesised that, given the propensity of severe reflux disease in patients with long segment BO, the metaplasia progressed in extent over the years. However, such extension of length of BO is only rarely seen and it is assumed that BO appears to develop to its full length over a short period of time ¹⁰⁸.

Traditionally, 3 different types of columnar epithelia have been described in Barrett's oesophagus ⁹¹.

1. Cardia type mucosa- This is also called junctional or cardiac epithelium and has a foveolar surface and glands that are lined by mucus secreting cells.
2. Gastric fundic type mucosa- This has a foveolar surface lined by mucus secreting cells and a deeper glandular layer containing chief and parietal cells.

3. Specialised intestinal metaplasia- This has intestinal type crypts lined by mucus secreting columnar cells and goblet cells.

The specialised intestinal metaplasia (SIM) was the only cellular type which was thought to have clear malignant potential. However, in a retrospective study, patients with SIM were compared with columnar lined oesophagus without SIM in terms of developing adenocarcinoma. No significant difference was seen between the groups. The authors concluded that SIM is not essential for cancer risk ¹⁰⁹. It is quite possible that the lack of SIM in some of the cases included in the study could be due to sampling error.

1.2.3 Development of neoplasia in Barrett's oesophagus

The development of dysplasia or cancer in Barrett's oesophagus is a step wise process going through a series of changes which are low grade intra-epithelial neoplasia or low grade dysplasia (LGD), high grade intra-epithelial neoplasia or high grade dysplasia (HGD) and finally cancer ^{110, 111}. The metaplastic epithelium (SIM) goes through a series of DNA alterations which gives the cells certain growth advantages leading to dysplasia. The changes including LGD, HGD and intra-mucosal cancer (IMC) are collectively referred to as early neoplasia (EN).

Dysplasia is recognised by pathologists as a collection of architectural and cytological abnormalities including nuclear enlargement, pleomorphism and hyperchromatism. Architectural changes include crowding of tubules and villiform surfaces. The severity of architectural and cytological changes differentiates low

and high grade dysplasia. However it is often difficult to identify dysplasia due to various reasons which include inadequate samples, sampling error and low inter-observer agreement (IOA) among histopathologists. The IOA for LGD is less than 50%, but this improves significantly in cases of HGD ^{112, 113}. The natural history of dysplasia in terms of progression to cancer is less well understood.

1.2.4 Preventive strategies for developing Barrett's oesophagus

The greatest morbidity with Barrett's oesophagus is development of oesophageal adenocarcinoma. It is unclear at what stage does Barrett's oesophagus occur in the natural history of reflux disease. There is no convincing evidence to suggest that regular medical treatment of GORD will prevent occurrence of Barrett's. This is also difficult to ascertain as in most of the cases, Barrett's is diagnosed on the first endoscopy in patients with symptoms of reflux disease.

Chemoprevention as the way to reduce development of dysplasia and adenocarcinoma has been widely studied. Regular use of Aspirin and non-steroidal anti-inflammatory drugs (NSAIDS) were found to influence the progression in epidemiological studies. One of the earliest case-control studies looked at patients diagnosed with oesophageal adenocarcinoma, squamous carcinoma, cardia adenocarcinoma and non-cardia gastric cancers as cases. The study was controlled for major co-morbidities and they found that current use of aspirin is associated with reduced OA (OR 0.37), oesophageal squamous cancers (OR 0.49) and non-cardia gastric cancers (OR 0.46). There was no protection noted for cardia adenocarcinoma. There was a similar reduced risk with current use of NSAIDS as

well in this cohort ¹¹⁴. An American epidemiological study from databases such as National Health and Nutrition Examination Survey (NHANES I) and the National Epidemiologic Follow-up Studies (NEFS) found that occasional usage of Aspirin and NSAIDS is associated with a 90% reduction in OA occurrence and none of the regular users developed cancer in the 12-16 year follow up ¹¹⁵. A more recent study using Barrett's animal models found beneficial effects of chemoprevention with selective and non-selective cyclo-oxygenase 2 inhibitors (COX 2) ¹¹⁶.

However prospective studies using COX-2 inhibitors did not show any commendable effect of chemoprevention on development of OA. A study by Heath *et al* called 'chemoprevention for Barrett's oesophagus trial' (CBET), included more than 200 patients with Barrett's oesophagus with low and high grade dysplasia in a phase II trial. They were randomised to receive Celecoxib or placebo. The primary outcome measure was change in proportion of biopsy specimens with dysplasia after 48 weeks of treatment. No statistically significant difference was seen between the groups. There was a suggestion that the lack of effect could have been due to the low doses of Celecoxib used (200 mg BD) ¹¹⁷.

The data on use of PPI as chemo protective agents to prevent dysplastic progression of Barrett's is also controversial. PPI is widely used in patients with Barrett's and the theoretical basis for this is the fact that acid exposure induces proliferation of cells and facilitates apoptosis. Considering the fact that acid reflux is thought to be a factor in developing intestinal metaplasia, PPI use seems sensible in the absence of any prospective controlled trials showing benefit ¹¹⁸.

Nevertheless, some observational studies suggest some benefit of PPI in the progression of Barrett's to cancer ¹¹⁹. A recent prospective cohort study also suggested a reduced risk of progression to HGD/cancer on regular PPI use ¹²⁰.

1.2.5 Surveillance strategies in Barrett's oesophagus

Endoscopic surveillance programme has been recommended in Barrett's oesophagus in the absence of any definitive preventive strategies and hoping that this would pick up early cancers and thus improve the outcome compared to symptomatic cancers. The reported annual incidence of cancer in BO is variable ranging from 0.1 to 2.0%. A recent Danish population based study in a cohort of 11,208 patients with Barrett's oesophagus from 1992 to 2009 found that the absolute annual risk for Barrett's cancer was 0.12% which is much lower than the widely described 0.5% ¹²¹. However, there are concerns that there is a significant regional variation in developing Barrett's cancers in the western world. A meta-analysis including studies from United Kingdom suggested that the conversion rate from non-dysplastic Barrett's to adenocarcinoma is around 1% ¹²². The prognosis of patients with advanced oesophageal adenocarcinoma who are treated with surgery remains poor at 10% five year survival rate ¹²³. Also, surveillance detected cancers are at a much earlier stage than symptomatic cancers which also have an impact on the survival rates of patients. In a meta-analysis, there was significantly improved survival in patients under surveillance at 1 year (88% Vs 67%) and at 5 years (80% Vs 31%) compared to symptomatic cancers ¹²⁴. This finding led to the suggestion of regular surveillance in Barrett's oesophagus by most national gastroenterological societies ranging from every 2-3 years. The

patients who are in a surveillance programme tend to be younger and generally in good health compared to those presenting with oesophageal adenocarcinoma. Thus controversy exists as to whether regular surveillance would reduce mortality from Barrett's cancer ¹²⁵. There are currently no studies that have addressed the issue whether the mortality from Barrett's cancer has reduced due to regular surveillance.

1.2.6 Endoscopic imaging techniques used in Barrett's surveillance

Endoscopic surveillance is usually done using white light endoscopy for assessment of any abnormal nodular lesions in BO followed by targeted and random four quadrant biopsies every 1-2 cm of the Barrett's length ¹²⁶. This is associated with significant sampling error as only 5-10% of the mucosal surface may be mapped ¹²⁷. In turn this has resulted in low yield of dysplasia in routine sampling questioning the role of regular Barrett's surveillance. Age and co-morbidities are important factors to consider before enrolling patients for regular surveillance.

The primary aim of regular surveillance is to identify early neoplastic changes such as dysplasia or early cancer which could then be treated expecting a better outcome compared to those with symptomatic cancers. While there is no evidence to suggest that regular surveillance reduces cancer related mortality, there is suggestion to limit surveillance to population at high risk. This includes patients who are > 45 years old, male sex, Barrett's segment > 8 cm, long duration of reflux symptoms and presence of ulceration or stricture ¹²⁸. The early neoplastic

lesions are often subtle and difficult to identify with white light endoscopy. Hence various image enhanced techniques are described to improve dysplasia detection¹²⁹. This includes chromoendoscopy, narrow band imaging, autofluorescence imaging, electronic chromoendoscopy and confocal endomicroscopy. These techniques are described in detail in section 1.1.

The photons interact with the tissue by elastic scattering or absorption which is wavelength dependent¹²⁵. Raman spectroscopy is based on the fact that some of the photons set up molecular vibrations and will provide molecular fingerprint for the identification of dysplasia and cancer¹³⁰. An endoscopic probe is developed for in-vivo diagnosis; however this remains mostly a research tool¹³¹.

1.2.7 Molecular markers in Barrett's oesophagus

Various genes and molecular biomarkers are identified in BO and the knowledge about these genetic changes in non-dysplastic Barrett's and adenocarcinoma could throw light into the molecular pathways of progression of BO.

Genetic instability induced by allelic loss, changes in DNA methylation and ploidy abnormalities are described in BO. One of the common genetic alterations in oesophageal adenocarcinoma is loss of heterozygosity (LOH). LOH at chromosomes 17p and 9p are the earliest alterations noted in BO. LOH at 3p21, 5q21, 9p21 and 17p13 chromosomal regions in non-dysplastic BO were found to be useful biomarkers for individuals with high risk of developing adenocarcinoma¹³². Various chromosomal changes include trisomy of chromosome 7 and 18, or loss of the Y chromosome^{133, 134}.

Widespread DNA changes occurring during malignant transformation of Barrett's to adenocarcinoma included ploidy abnormalities such as tetraploidy and aneuploidy. In patients with HGD and OA, 90% were found to have ploidy abnormalities. It is thought that increased ploidy alterations progress the development from HGD to OA. On the other hand tetra and aneuploidy were also detected in non-dysplastic BO ^{135, 136}. The earliest and most common genetic alterations in BO are LOH at 17p and 9p followed by tetraploidy and aneuploidy.

The life span of normal cells is closely related to the telomere length and telomerase activity. Normally cells undergo telomerase shortening during cell cycle which in turn induces cell senescence. However, in neoplastic cells this activity is altered and the telomere length is maintained which in turn leads to cell immortalisation ¹³⁷. Telomerase activity is associated with upregulation of human telomerase reverse transcriptase expression (hTERT) and high levels of telomerase and hTERT expression are seen in OA than patients without cancer ¹³⁸.

In patients with GORD and Barrett's, one of the most important hyper proliferative cell stimuli is gastric acid and bile acid. The most common and well described proliferation marker is Ki67 and proliferating cell nuclear antigen (PCNA). Suppression of acid exposure is found to induce cell differentiation and reduce cell proliferation ¹³⁹.

The p53 gene which is located on chromosome 17p is very commonly altered in human cancers. Alterations in p53 are associated with mutations and LOH and are well documented in Barrett's oesophagus. It was noted that p53 mutations are seen

1-5% non-dysplastic Barrett's, 65% in LGD, 75% in HGD and 50-90% in OA ¹⁴⁰,

141 .

1.2.8 Management of Barrett's oesophagus

1.2.8.1 Medical management of Barrett's oesophagus

The medical management in Barrett's is primarily treatment of associated GORD with proton pump inhibitors. There is no controlled trial to prove that use of PPI will reduce cancer progression in Barrett's oesophagus even though it is well known that gastric and bile acid reflux induces hyper proliferation, suppress apoptosis and promote carcinogenesis. In vitro studies using biopsy specimens from patients with BO at baseline and after 6 months of PPI therapy were found to have reduced expression of proliferating cell nuclear antigen (PCNA) and increased expression of a differentiation factor Villin, in those treated with acid suppression ¹⁴². The overall benefit of using PPI in patients with BO and no evidence of reflux, with a view to prevent progression to cancer, needs to be discussed individually weighing the benefit and risk.

Use of PPIs is beneficial to reduce symptoms of GORD in patients with Barrett's Oesophagus. Ph studies have shown persisting reflux in patients who were rendered asymptomatic on PPIs ¹⁴³. Patients with BO were considered to have resistance to anti-reflux therapy. This could be due to severe reflux rather than a true resistance to the anti-reflux properties of PPI therapy. A randomised cross over trial used 3 different doses of esomeprazole in patients with Barrett's. All three doses significantly reduced the intragastric acidity but in 16-23% of patients,

the oesophageal acid exposure continued ¹⁴⁴. The reflux diathesis is very strong that whatever acid in the stomach produces reflux.

A randomised controlled study showed partial regression of Barrett's with aggressive anti-reflux therapy. 68 patients with BO and ongoing reflux were enrolled to receive Omeprazole 40 mg BD or Ranitidine 150 mg BD. Reflux symptoms improved in both groups, but Omeprazole arm showed a statistically significant but small regression in length of Barrett's ¹⁴⁵. Whether these findings are a simple representation of changes in size of hiatus hernia or due to an inter-operator observation bias needs to be debated.

The role of anti-reflux surgery in regression of Barrett's and preventing development of oesophageal adenocarcinoma has been suggested mainly in uncontrolled trials. A systematic review of 25 studies showed regression of Barrett's and dysplasia with anti-reflux studies, but the evidence for reduction in incidence of adenocarcinoma was mainly from uncontrolled studies ¹⁴⁶.

1.2.8.2 Endoscopic resection of Barrett's neoplasia

Endoscopic resection (ER) could be offered as a therapeutic option in patients presenting with focal HGD and mucosal cancer. Those with submucosal invasion, vascular or lymphatic invasion should be referred for oesophagectomy. However, low risk submucosal invasion (T1sm1) is considered to be appropriate for endotherapy in many centres ¹⁴⁷. ER is considered to be therapeutic if lateral and deeper margins are clear of the tumour. Clearance of lateral margins is histologically difficult to assess, especially in cases of piecemeal resection. This is

usually achieved by making sure that all the marked areas are removed at the time of resection and follow up endoscopies are clear.

A large series published by the Wiesbaden group showed a complete remission of Barrett's cancer in 95% of patients treated with ER alone at 5 years follow up. A significant proportion of patients (20%) developed metachronous lesions during follow up, which were all managed endoscopically. The calculated 5 year survival rate was 84%¹⁴⁸. Stepwise radical endoscopic resection (SRER) to remove the entire segment of dysplastic Barrett's was attempted in another study. In 34 patients treated, all had complete eradication of HGD/early cancer and majority of them had complete eradication of Barrett's epithelium. However, a significant proportion of patients developed dysphagia secondary to stricture, which were all managed endoscopically¹⁴⁹. Two patients in this cohort developed perforations. Considering the higher rate of complications, SRER could not be recommended in all patients, except in those with short segment dysplastic BO. ER could be performed using an EMR-cap technique or a multi-band Mucosectomy device (MBM).

Multiband Mucosectomy kit (Duette®-Cook Medical, Bloomington, IN) includes a modified multiband ligator and a hexagonal polypectomy snare measuring 1.5 to 2.5 cm made of braided wire. The device is attached to the endoscope as in case of variceal ligation technique. The advantage is that multiple resections could be achieved. This is particularly useful in flat dysplasia, where a pseudo-polyp is formed by banding and this could be easily resected.

The use of a transparent distal attachment and suction, following local injection of saline to produce an elevation of the mucosal lesion, offers several significant advantages over alternative techniques, including secure, slip-free capturing of the target mucosa, and resection of a wider area at one time. This is the EMR cap technique. The distal attachment has an internal rim that allows easier positioning of the diathermy snare prior to resection. A straight cap and an oblique cap are available. A combination of Gelofusine, adrenaline and indigocarmine is useful for lifting the lesion; however saline in itself is used by many endoscopists. The EMR cap is especially useful for an en-bloc resection of a raised lesion. A comparison between these two techniques was done in 40 patients (80 resections) by the Amsterdam group. The time taken for procedure was significantly lower using a MBM kit, while the specimens were smaller in size with MBM compared to the EMR cap technique. The incidence of bleeding was also lower in the MBM group, and one perforation occurred with EMR cap. Multiband mucosectomy is, therefore, most suited for en-bloc resection of lesions smaller than 10 mm or for widespread resection of flat mucosa ^{150, 151}.

1.2.8.3 Endoscopic ablative therapies

Various ablation therapies are used to treat non-dysplastic and dysplastic Barrett's oesophagus. Thermal ablation therapies are the most commonly used which include multipolar electrocoagulation (MPEC), argon plasma coagulation (APC) and more recently radiofrequency ablation (RFA). MPEC is a contact ablation technique using an electrode passed through the accessory channel of the endoscope. Initial studies showed promise in ablating non-dysplastic BO with

reversal of Barrett's epithelium. The studies used concomitant acid suppression after ablation ^{152, 153}.

APC is a non-contact thermal technique using a probe passed through the accessory channel of the scope. The probe is usually placed 1-1.5 mm away from the mucosal lining before applying the thermal energy. 70 patients underwent high power APC ablation (90 W) of non-dysplastic BO followed by strong acid suppression with proton pump inhibitors. 69 treated patients had a complete squamous degeneration after a mean of 2 APC sessions and 12 months follow up ¹⁵⁴. After a 5 years follow up only 12% patients had evidence of intestinal metaplasia during surveillance endoscopies giving a histological relapse rates of 3% per year ¹⁵⁵. APC was also used to treat patients with Barrett's HGD ¹⁵⁶. Twenty nine patients with HGD underwent APC ablation and 86% responded to treatment. Over a follow up period of 7 years, 22 patients had a complete regression with neo-squamous epithelium ¹⁵⁷.

Radiofrequency ablation is a relatively new technique for eradication of non-dysplastic and dysplastic Barrett's. There are 2 different catheters available. One is a balloon based system (HALO³⁶⁰) and the other one is a paddle which could be attached to the tip of the scope (HALO⁹⁰). HALO³⁶⁰ is used for circumferential ablation of Barrett's using closely packed electrodes distributed circumferentially over a 3 cm long balloon and delivering a short burst of energy. HALO⁹⁰ is useful for focal ablation of residual Barrett's or islands ¹⁵⁸.

A randomised, sham-controlled trial investigated the efficacy of RFA in eradicating Barrett's dysplasia and preventing progression of disease. This study included 127 patients, 64 with low-grade dysplasia (LGD) and 63 with high-grade dysplasia (HGD), from 19 different centres in the USA. Complete eradication of dysplasia was achieved in 86% (92% for per protocol analysis) with no statistical differences between the LGD and HGD groups. Total eradication of SIM was achieved in 77% (83% for per protocol analysis), again, irrespective of the grades of dysplasia ¹⁵⁹. Various other uncontrolled trials have also shown that RFA is safe and efficacious in eradicating dysplasia and intestinal metaplasia ^{160, 161}. A systematic review including 9 studies and 429 patients, found that complete eradication of Barrett's dysplasia and metaplasia was achieved respectively for 71-100% and for 46-100% of the patients. There were no serious adverse events reported and buried glands were noted only in one case ¹⁶².

Photodynamic therapy was one of the first ablative therapies used for Barrett's dysplasia ^{163, 164}. This technique involves intravenous administration of a photosensitising agent such as porfimer sodium many hours before the endoscopy ¹⁶⁵. A laser light is used through a fibre passing through the accessory channel of the endoscope to activate the photosensitising agent to achieve ablation in Barrett's oesophagus ^{166, 167}. A randomised trial compared PDT with Omeprazole in patients with Barrett's HGD. The PDT arm was successful in eradicating dysplasia in 77% as opposed to Omeprazole which eradicated dysplasia in 39% ¹⁶⁸. The significant drawbacks of this modality are stricture formation and photosensitisation.

1.2.8.4 Surgical management of Barrett's neoplasia

Oesophagectomy is the only definitive treatment which clearly removes the all neoplastic epithelium along with adjacent lymph nodes. However, oesophagectomy is associated with significant morbidity and mortality compared to other less invasive endoscopic therapies such as endoscopic resection and ablative therapies. A Dutch study suggested that the mortality improves with increasing number of surgeries performed by the hospital and thus suggesting centralisation of services ¹⁶⁹. The patient needs a 10-15 days hospital stay after surgery and up to 30% patients develop at least one serious complication such as pneumonia, myocardial infarction, heart failure or anastomotic leak ¹⁷⁰. The improvement in healthcare has resulted in significant reduction of morbidity which still remains substantial. The long term problems include dysphagia, weight loss and chronic GORD. Minimally invasive oesophagectomy tends to have lesser hospital stay but morbidity and mortality depends on the expertise.

1.2.9 How to improve outcome in patients with Barrett's oesophagus

The previous discussions have made it clear that dysplasia in Barrett's oesophagus progresses in a stepwise manner progressing through low grade dysplasia, high grade dysplasia and finally oesophageal adenocarcinoma. The only management strategy in the absence of any definitive preventive measures, either by medical or surgical measures, is to detect neoplasia early and treat accordingly. The surveillance strategy by doing four quadrant random biopsies every 2 cm is

associated with sampling error and the yield of dysplasia is sub-optimal. In this setting, image enhanced endoscopy techniques might provide additional benefit in terms of identifying and targeting dysplasia during surveillance. This thesis will address the value of multimodal imaging during Barrett's surveillance endoscopies.

CHAPTER 2

AIMS

1. To determine the role of high definition endoscopy, narrow band imaging and autofluorescence imaging in detection of dysplasia in Barrett's oesophagus
2. To determine whether autofluorescence imaging technique has sufficient inter-observer reliability in Barrett's surveillance
3. To determine the biological basis of autofluorescence and the role of collagen and elastin in autofluorescence
4. To develop an objective measurement of autofluorescence to reliably identify dysplasia in Barrett's oesophagus

CHAPTER 3

HIGH DEFINITION VERSUS STANDARD DEFINITION WHITE LIGHT ENDOSCOPY FOR DETECTING EARLY NEOPLASIA IN BARRETT'S OESOPHAGUS SURVEILLANCE

3.1 Abstract

Introduction

High definition (HD) endoscopy systems provide superior image resolution compared to the older standard definition (SD) endoscopy systems. However, the utility of this new technology in dysplasia detection during Barrett's surveillance has not been evaluated.

Aims and Methods

The aim was to assess whether using HD endoscopy system translates to better outcomes compared to the SD system in terms of detecting dysplastic lesions in patients with Barrett's oesophagus (BO) undergoing surveillance.

A retrospective cohort study of patients with non-dysplastic BO undergoing surveillance endoscopy with biopsies was performed. Data was retrieved from the central hospital electronic database. Procedures performed for non-surveillance indications; BO Prague C0M1 classification with no specialised intestinal metaplasia (SIM) on histology; patients diagnosed with dysplasia or cancer on index endoscopy and procedures where any other advanced imaging techniques was used were excluded from the study. Logistic regression was performed to estimate adjusted odds ratios (aOR) and 95 % confidence intervals (CI) comparing outcomes with SD and HD systems.

Results

The HD system was superior to the SD system in targeted detection of dysplastic lesions (aOR 3.27, 95% CI 1.27-8.40) as well as all dysplasia detected on random and target biopsies (aOR 2.36, 95% CI 1.50-3.72). More false positive lesions were detected with the HD system (aOR 1.16, 95% CI 1.01-1.33) and it had a marginally higher yield of dysplasia on random biopsies alone (aOR 1.07, 95% CI 1.00-1.15). There was no difference between HD and SD in diagnosing all (random and target) high grade dysplasia (HGD) or cancers (aOR 0.93, 95% CI 0.83-1.04).

Trainee endoscopists, number of biopsies and male sex were all significantly associated with a higher yield of dysplastic lesions. Trainees were also more likely to detect false positive lesions (aOR 5.26, 95% CI 2.11-13.15) compared to non-trainees.

Conclusions

The use of the HD endoscopy system is associated with better targeted and any dysplasia detection during BO surveillance. HD endoscopy cannot replace random biopsies during BO surveillance.

3.2 Introduction

The advances in electronics over the past few decades have improved the endoscopic resolution and definition considerably. The standard definition signals offer images in a 4:3 aspect ratio with image resolutions up to 700 X 525 pixels. SD endoscopes are equipped with CCDs that produce an image signal of 100,000 to 400,000 pixels. Advances in the technology have resulted in smaller chips with higher number of pixels in the CCD which can offer images with resolutions that range from 850,000 to over a million pixels³. These are called high resolution endoscopes. The images generated from such endoscopes are viewed on high definition television transmitted via HD cables to obtain the HD endoscopy systems. This would improve the mucosal details seen on the monitor and could potentially improve detection of early neoplastic lesions in BO.

A prospective randomised cross-over trial comparing high resolution endoscopy (HRE) with indigocarmine or narrow band imaging (NBI) showed that most patients with HGD or early cancer could be identified by high resolution endoscopy alone with no additional advantage from chromoscopy or NBI¹⁶. Similarly an inter-observer study using high resolution endoscopy, chromoscopy and NBI suggested that addition of enhancement techniques did not improve the yield of dysplasia compared to HRE alone²¹. A more recent randomised study compared endoscopic trimodal imaging (ETMI) with SD endoscopy and found that ETMI is superior to SD in targeted detection of Barrett's dysplasia¹⁷¹. All these studies are performed in an enriched population with high incidence of dysplasia and not on routine surveillance population. Moreover these studies are

from a few centres of excellence. It is difficult to extrapolate this data to the general surveillance population. There is no data comparing standard definition to high definition endoscopy in BO surveillance and thus the aim of this study was to compare the HD and SD systems in detecting dysplasia during Barrett's surveillance

3.3 Material and methods

3.3.1 Data collection

The data for this study was retrospectively collected from the endoscopic and clinical database at Nottingham University Hospitals. Clinical and demographic data of all patients undergoing Barrett's surveillance between September 2008 and August 2012 were reviewed. All patients over the age of 18 years undergoing surveillance endoscopy and biopsy for Barrett's oesophagus were included. The exclusion criteria were, BO with Prague C0M1 classification with no SIM on histology; patients diagnosed with dysplasia or cancer on index endoscopy; procedures where any other advanced imaging techniques was used; non-surveillance endoscopies and patients with no histological confirmation.

Patient data including age, sex, diagnosis, length of Barrett's C&M classification, any visible lesions, number of lesions, biopsies taken, whether targeted or random biopsies, endoscopic system used and grade of endoscopist (ie. consultant/trainee) were recorded. Endoscopies performed using a high resolution endoscope H260 (Olympus-Keymed UK) using an Olympus Lucera Spectrum processor and an HD 1080i capable monitor (Olympus OEV 191H) were classified as high definition

endoscopies. All other procedures using endoscopes GIF Q230, XQ240, Q240, and Q260 were classified as standard definition endoscopies. During BO surveillance, targeted biopsies are taken in the presence of any identifiable mucosal abnormalities. This was followed by random biopsies from four quadrants every 2 cm as per the Seattle protocol ¹⁷². Biopsies were sent for histopathological analysis in 10% formalin, and they were reported according to Vienna classification as no dysplasia, indefinite for dysplasia, low grade dysplasia, high grade dysplasia and invasive cancer ¹⁷³.

3.3.2 Statistical analysis

Logistic regression was performed to estimate odds ratios (ORs) and 95 % confidence intervals (CI) comparing outcomes with standard and high definition endoscopy (PASW version 19, IBM Corp). Separate regression models for (i) dysplasia detected on target biopsy; (ii) all high grade dysplasia/cancer; (iii) dysplasia detected on random biopsy alone; (iv) number of false positive lesions; and (v) all dysplastic lesions detected were performed.

Statistical models included the following potential confounders, chosen a priori based on the literature: age at the index exam, sex, trainee endoscopist or consultant, length of Barrett's oesophagus and the number of biopsies taken. The goodness of fit for the logistic regression model was determined using the Hosmer-Lemeshow test ¹⁷⁴. The collinearity between the confounder variables using correlation matrices was tested. If collinearity was detected ($\rho > 0.6$) we

planned to minimise this by inputting the variable separately in the multivariate analysis

3.4 Results

A total of 521 endoscopies were performed of which 266 were done using SD endoscopy systems in 227 patients undergoing Barrett's surveillance. 255 endoscopies were performed in 208 patients using HD endoscopy systems during the study period. 111 endoscopies during the study period were performed using autofluorescence and narrow band imaging (trimodal) and they were excluded (Figure 1). Patients with non-surveillance indications such as those for EMR, post EMR follow up and other therapeutic procedures were excluded. Patient demographics are shown in Table 1.

3.4.1 Dysplasia detection on target biopsies

The total number of targeted biopsies taken in the HD arm was 51, and that in the SD arm was 20. There were a total of 6 dysplastic lesions identified on target biopsy in the HD group and 2 dysplastic lesions in the SD group. This included 4 cancers and 2 LGD in the HD arm and 2 cases of indefinite for dysplasia (ID) in the SD arm. The high definition endoscopy was superior to standard definition endoscopy in targeted detection of dysplastic lesions (aOR 3.27, 95% CI 1.27-8.97) (Table 2)

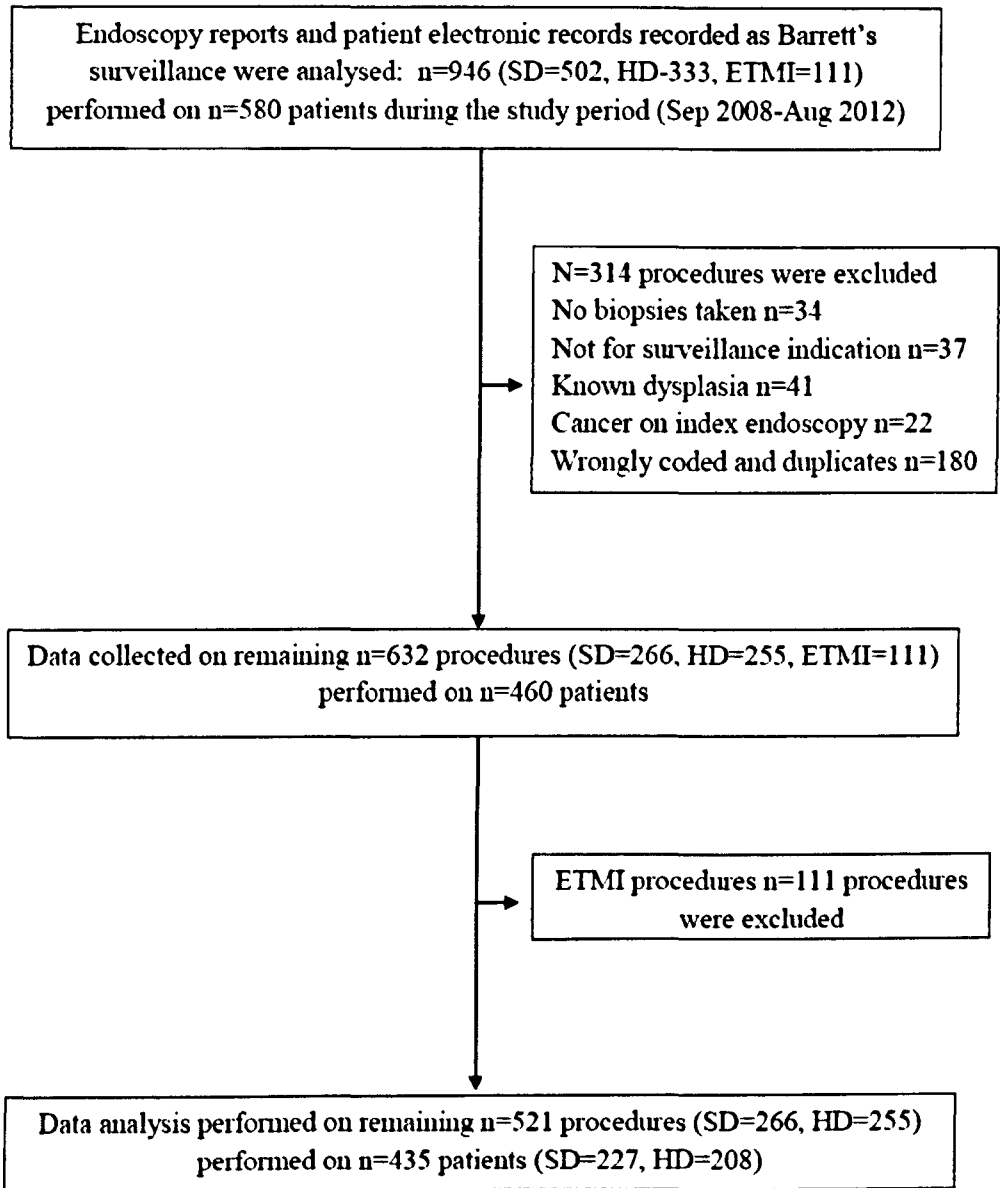


Figure 1: Flow chart of study procedures

Table 1: Demographic and clinico-pathological details of endoscopy procedures

Variable	Total n=521	HD group n=255	SD group n=266
Age (mean ±SD) years	68.0 (11.9)	68.8 (12.1)	67.3 (11.7)
Male sex (%)	356 (68.3)	166 (65.1)	190 (71.4)
PPI users (%)	415 (84.5)	220 (88.7)	195 (80.3)
Endoscopist grade			
Consultant	371 (71.2)	161 (63.1)	210 (78.9)
Trainee (GI fellow)	149 (28.6)	93 (36.5)	56 (21.0)
Barrett's Prague class			
C length (median, IQR)	3 (1-5)	2 (0-4)	3 (1-6)
M length (median, IQR)	4 (2-6)	4 (2-6)	4 (2-6)
Hiatus hernia	327 (62.8)	172 (67.5)	155 (58.3)
Oesophagitis	89 (17.1)	48 (18.8)	41 (15.4)
SIM	379 (76.6)	178 (70.9)	201 (82.4)
Target biopsies	71(13.6)	51(20)	20 (7.5)
Random biopsies	481 (92.3)	238 (93.3)	243 (91.4)
No. of random biopsies (median, IQR)	8 (4-8)	4 (3-6)	4 (4-8)
Dysplasia on random biopsies (%)	46 (8.8)	25 (9.8)	21 (7.9)
Any Dysplasia (random and target) (%)	53 (10.1)	31 (12.2)	23 (8.7)
Total no. of lesions detected (%)	23 (4.4)	18 (7.1)	5 (1.9)
No. of dysplastic lesions (dysplasia on target biopsy) (%)	8 (1.5)	6 (2.4)	2 (0.8)
No. of false positive lesions (false positive on target dysplasia) (%)	15 (2.9)	12 (4.7)	3 (1.1)
Any HGD/cancer (random and target) (%)	19 (3.7)	15 (5.9)	4 (1.5)

HD: High definition, SD; Standard definition, IQR: Inter-quartile range, SIM: specialised intestinal metaplasia, HGD: High grade dysplasia

Table 2: Logistic regression for all dysplasia detected on targeted biopsies

Variable	Odds Ratio	95% CI	P value
Total biopsies	1.43	1.22-1.68	< 0.001
Male Gender	5.32	2.18-12.99	< 0.001
Trainee	4.69	1.05-20.82	0.042
HD Scope	3.27	1.27-8.39	0.014
Barrett's length	0.98	0.85-1.15	0.872
Age	1.07	1.05-1.1	<0.001

CI-Confidence interval, HD-High definition

3.4.2 Dysplasia detection on random and targeted biopsies

There were 25 endoscopies in the HD arm which detected dysplasia on random biopsies alone which included 2 cancers, 8 HGD, 11 LGD and 4 ID as compared to 21 endoscopies in the SD arm with dysplasia on random biopsies alone including 1 cancer, 1 HGD, 11 LGD and 8 ID. The HD arm detected significantly more number of dysplasia by target and random biopsies combined together as compared to the SD arm (aOR 2.36, 95% CI 1.50-3.72) (Table 3)

High definition endoscopy identified significantly more number of dysplastic lesions when analysis was done excluding indefinite for dysplasia on random and target biopsies as compared to SD endoscopy (aOR 1.12, 95% CI 1.04-1.2).

However, there was no significant difference between HD and SD in detection of HGD or cancer on both targeted and random biopsies (aOR 0.93, 95% CI 0.83-1.04) (Table 4). There was a marginally higher pick up of all dysplasia on random biopsies alone using HD endoscopy compared to the SD arm (aOR 1.07 95% CI 1.0-1.15) (Table 5).

More number of false positive lesions was identified by HD endoscopy on target biopsies compared to SD (aOR 1.16, 95% CI 1.01-1.33). On multivariate analysis, endoscopies performed by trainee endoscopists, number of biopsies taken and male sex were significantly associated with increased yield of targeted dysplasia (Table 2). Trainees also detected more number of false positive lesions compared to non-trainees (aOR 5.26 95% CI 2.11-13.16).

Table 3: Logistic regression for all dysplasia detected on random and targeted biopsies

Variable	Odds Ratio	95% CI	P value
Total biopsies	1.08	1.01-1.15	0.017
Male Gender	3.58	2.32-5.52	< 0.001
Trainee	1.77	0.99-3.16	0.053
HD Scope	2.36	1.5-3.71	<0.001
Barrett's length	0.96	0.88-1.05	0.399
Age	1.04	1.02-1.05	<0.001

CI-Confidence interval, HD-High definition

Table 4: Logistic regression for HGD/Cancer for random and targeted biopsies

Variable	Odds Ratio	95% CI	P value
Total biopsies	4.9	2.55-9.44	<0.001
Male Gender	4.49	1.53-13.19	0.006
Trainee	1.98	1.04-3.77	0.037
HD Scope	0.93	0.83-1.04	0.174
Barrett's length	1.31	1.17-1.46	<0.001
Age	1.05	1.04-1.07	<0.001

HGD-High grade dysplasia, CI-Confidence interval, HD-High definition

Table 5: Logistic regression for all dysplasia on random biopsies only

Variable	Odds Ratio	95% CI	P value
Total biopsies	3.96	2.49-6.29	<0.001
Male Gender	1.72	0.93-3.18	0.082
Trainee	2.79	1.71-4.56	<0.001
HD Scope	1.07	1-1.15	0.50
Barrett's length	3.96	2.49-6.29	<0.001
Age	1.04	1.03-1.05	<0.001

CI-Confidence interval, HD-High definition

3.5 Discussion

This study compared the yield of dysplasia during Barrett's surveillance using high definition and standard definition endoscopy systems. The principal findings include a higher yield of any dysplasia in the HD arm. This was significant both in the targeted yield of dysplasia as well as combined targeted and random detected dysplasia. The number of random biopsies taken was similar in both arms, but the HD endoscopy facilitated more number of target biopsies. This could be due to the fact that HD images provide more detailed views of the Barrett's epithelium and subtle lesions were picked up. On the other hand, some of the inflammatory changes would have been more prominent on HD endoscopy thus leading to higher number of targeted biopsies. This is highlighted by the fact that there were higher false positive targeted biopsies in the HD arm. Nonetheless, this has led to increased dysplasia detection in the HD arm at the expense of more false positive lesions compared to SD endoscopy. A consensus statement on HGD in Barrett's oesophagus suggested the use of high resolution endoscopy in Barrett's surveillance with four quadrantic biopsies every 1-2 cm¹⁷⁵. The evidence itself for this recommendation was poor as there are no direct studies comparing HD Vs SD. However, one of the studies compared SD endoscopy with NBI in 65 patients with Barrett's oesophagus where NBI identified more number of patients with dysplasia as well as higher grades of dysplasia compared to SD endoscopy⁷⁵. The NBI used in this study is a high resolution endoscopy system, but it is difficult to predict whether high resolution white light would deliver such results.

There was no difference in targeted or random detection of HGD and cancer between the HD and SD arm. This could be related to the small absolute number of HGD or cancer detected in the cohort as this was a surveillance population. Or else, this could be related to the fact that most HGD or early cancer lesions could be visualised with SD endoscopy itself and there is no additional role for HD endoscopy in this setting.

Endoscopies performed by trainee endoscopists/fellows were found to detect more number of dysplasia compared to non-trainee endoscopists. This is a very interesting finding which could be explained in various ways. First of all, there is significantly more number of trainees/fellows who performed endoscopies in the HD arm ($P < 0.001$). Hence the increased dysplasia detection would be a result of better performance of HD endoscopy compared to the SD arm. However, we adjusted these findings for the type of endoscopy (HD Vs SD) and the results remain significant. Secondly, there was increased number of false positive lesions detected by trainees. This is due to overcalling dysplasia in this cohort thus leading to more number of targeted and overall biopsies. The other reason would be a higher representation of research fellows with interest in Barrett's oesophagus performing endoscopies compared to generalist non-trainee gastroenterologists. This would also relate to the more time spent on examination of Barrett's by the trainees/fellows compared to non-trainees.

The other factor which improved dysplasia detection was the number of biopsies taken. This is an anticipated outcome as we are aware that there is significant sampling error in Barrett's surveillance biopsies. Hence, when more number of

biopsies is taken, it is likely to yield higher number of dysplasia. A retrospective study which analysed patients with Barrett's HGD/early cancer found that a significant number of patients undergoing surveillance did not have adequate number of biopsies taken, thus missing dysplasia during surveillance period and indicating sampling error ¹⁷⁶. However, a more intensive Seattle protocol biopsies taken from every 1 cm of the Barrett's does not seem to reliably predict adenocarcinoma in patients undergoing oesophagectomy for HGD ¹⁷⁷. This finding could not be extrapolated to non-dysplastic surveillance population and there is no evidence to suggest that a less intensive protocol is sufficient to identify any dysplasia. A significant number of dysplastic areas were detected by random biopsies alone and this indicates that HD endoscopy cannot replace random biopsies. Male sex was associated with higher yield of dysplasia. This is also an expected finding in the light of our knowledge that Barrett's dysplasia/cancer is higher in males compared to females ¹⁷⁸⁻¹⁸¹.

There are various limitations associated with this study. The study was conducted using data collected retrospectively from the electronic case records and endoscopy reports of patients. In this setting it is difficult to standardise all the data. An ideal way of doing such a study would be a prospective randomised controlled study. However, the retrospective design could also be considered as strength. We have utilised actual clinical data of routine surveillance practice and this could represent a true picture as opposed to a clinical trial in controlled settings. It is also argued that endoscopists are naturally biased during a randomised trial and would perform endoscopies more diligently than in routine

clinical practice. As with all non-randomised trials, it is difficult to exclude all confounding variables; however appropriate statistical methods are used to adjust the variables within the limits of such a study. The other limitation for this retrospective study is that the endoscopists are not blinded to the clinical data and the pathologists are not blinded to endoscopy and clinical data.

3.5.1 Conclusions

In conclusion, the overall yield of dysplasia during Barrett's surveillance was better with HD endoscopy compared to SD endoscopy. HD endoscopy has 3 times higher chance of picking up targeted dysplasia compared to SD, which is at the expense of higher false positive lesions. There was no difference in detection of HGD or early cancer between the groups. Randomised controlled trials are necessary to examine these findings. It is difficult to recommend routine use of HD endoscopy for regular Barrett's surveillance based on these observations, but certainly should be considered as a valuable option.

CHAPTER 4

NARROW BAND IMAGING FOR CHARACTERISATION OF HIGH GRADE DYSPLASIA AND SPECIALISED INTESTINAL METAPLASIA IN BARRETT'S OESOPHAGUS. A META-ANALYSIS

Mannath J, Subramanian V, Hawkey CJ, Ragnath K. Endoscopy. 2010 May;
42(5):351-9

4.1 Abstract

Background

Narrow band imaging (NBI), a novel endoscopic technique that highlights mucosal surface structures and microvasculature is being increasingly advocated as a tool to detect and characterise neoplasia and intestinal metaplasia in patients with Barrett's oesophagus (BO)

Aim

To assess the diagnostic accuracy of NBI with magnification for the diagnosis of high grade dysplasia (HGD) and specialised intestinal metaplasia (SIM) in patients with BO.

Methods

A meta-analysis of studies which compared NBI based diagnosis of HGD and SIM with histopathology as the gold standard was performed.

Results

Eight studies including 446 patients with 2194 lesions met the inclusion criteria. The pooled sensitivity, specificity, diagnostic odds ratio (DOR) and the area under the curve (AUC) for diagnosing HGD was 0.96 (95% CI 0.93-0.99), 0.94 (95% CI 0.84-1.0), 342.49 (95% CI 40.49-2896.89) and 0.99 (SE 0.01) on a per-lesion analysis and 0.95 (95% CI 0.88-1.0), 0.97 (95% CI 0.97-0.98), 343.45 (95% CI 77.88-1514.70) and 0.99 (SE 0.01) on a per-patient analysis. For the characterisation of SIM, the pooled sensitivity, specificity, DOR and AUC was 0.95 (95% CI 0.87-1.0), 0.65 (95% CI 0.52-0.78), 37.53 (95% CI 6.50-217.62) and 0.88 (SE 0.08) on a per-lesion analysis and 0.97 (95% CI 0.94-1.0), 0.78 (95%

CI 0.56-1.0), 100.97 (95% CI 33.62-303.22) and 0.97 (SE 0.02) on a per-patient analysis.

Conclusion

NBI with magnification is accurate with high diagnostic precision for diagnosis of HGD in BO using irregular mucosal pit patterns and/or irregular microvasculature.

NBI has high sensitivity but poor specificity for characterising SIM.

4.2 Background

Barrett's Oesophagus is a complication of long standing gastro-oesophageal reflux disease (GORD) and is known to affect 10-15% of those with GORD. Patients with BO have a 30-125 times higher risk of developing adenocarcinoma compared to the general population ¹⁸². BO is characterised by endoscopically identifiable 'salmon' coloured columnar epithelium containing specialised intestinal metaplasia (SIM) ^{182, 183}. The metaplastic epithelium accumulates genetic changes over a period of time and can progress through low grade dysplasia (LGD), high grade dysplasia (HGD) and then to oesophageal adenocarcinoma (OA) ¹⁸⁴. Early dysplastic lesions can be endoscopically resected or ablated. This will reduce the risk of progression without the need for radical surgery with its associated morbidity and mortality ¹⁵⁹.

Regular surveillance of BO with random 4 quadrant biopsies every 1-2 cm is the standard practice, however the yield of dysplasia with such an intensive endoscopic biopsy protocol is suboptimal ^{185, 186}. Chromoendoscopy with methylene blue, crystal violet, acetic acid and indigocarmine has been advocated to improve the yield of intestinal metaplasia and dysplasia. However chromoendoscopy with methylene blue was found to be no better than random biopsies in a recent meta-analysis ³⁸. Narrow band Imaging (NBI), a novel endoscopic technology, uses narrowed bandwidths of blue (440-460nm) and green (540-560nm) light waves with the help of a special filter that deletes the red light spectrum from the emitted light ⁷¹. This facilitates delineation of surface pit patterns and micro-capillaries, and by assessing their changes, it is possible to

identify abnormal areas and target biopsies accordingly. The filter is activated electronically by pressing a switch on the hand control and the endoscopists can easily switch between white light and NBI. It offers similar benefits in terms of characterisation to magnification chromoendoscopy, but without the need for dye spray. NBI is widely used in characterisation of lesions in colon, oesophagus and lungs with high in-vivo diagnostic precision ¹⁸⁷.

Observational studies using NBI and magnification have identified various micro-structural and capillary patterns in Barrett's oesophagus. Regular micro-structural patterns include round, linear, tubular or villous/ridged type. Irregular patterns and absent pit patterns are also reported. Micro-vascular patterns are classified either regular or irregular. Sensitivity and specificity of the irregular micro-vascular and micro-structural patterns for prediction of HGD was as high as 90 and 100% in a recent study ¹⁸⁸. Similarly the villous/ridged/absent pit patterns were thought to be highly suggestive of specialised intestinal metaplasia (SIM) and the round patterns associated with columnar lined epithelium.

The aim of this meta-analysis is to assess the diagnostic accuracy, sensitivity and specificity of NBI with magnification in characterising HGD and SIM associated with BO.

4.3 Methods

4.3.1 Selection of studies

We included all studies assessing the accuracy of narrow band imaging with magnification (NBI-Z) for characterising dysplasia or SIM in BO. Histology from the area of interest is used as the gold standard. The inclusion criteria were 1) prospective clinical studies where NBI-Z is used to assess BO 2) typical mucosal pit patterns and vascular patterns of the assessed areas are described 3) diagnostic accuracy in terms of sensitivity and specificity of mucosal patterns are compared against gold standard and 4) real time assessment of lesions or post hoc digital images characterisation is used. Studies using NBI for detection of lesions in BO without lesion characterisation and those with no extractable data were excluded. Also, studies without histological confirmation of lesions were excluded as were case reports, editorials, commentaries and data reported as abstracts only.

4.3.2 Search strategy

Bibliographical searches were performed up to June 2009 in MEDLINE, EMBASE, Web of Science, Google Scholar and Cochrane library using search terms 'Narrow Band Imaging' and 'Barrett's oesophagus'. Articles in all languages were included. We also searched for any abstracts from international conferences and hand searched references from published articles. Two investigators independently searched the databases and studies which were duplicated, reviews and case reports were excluded.

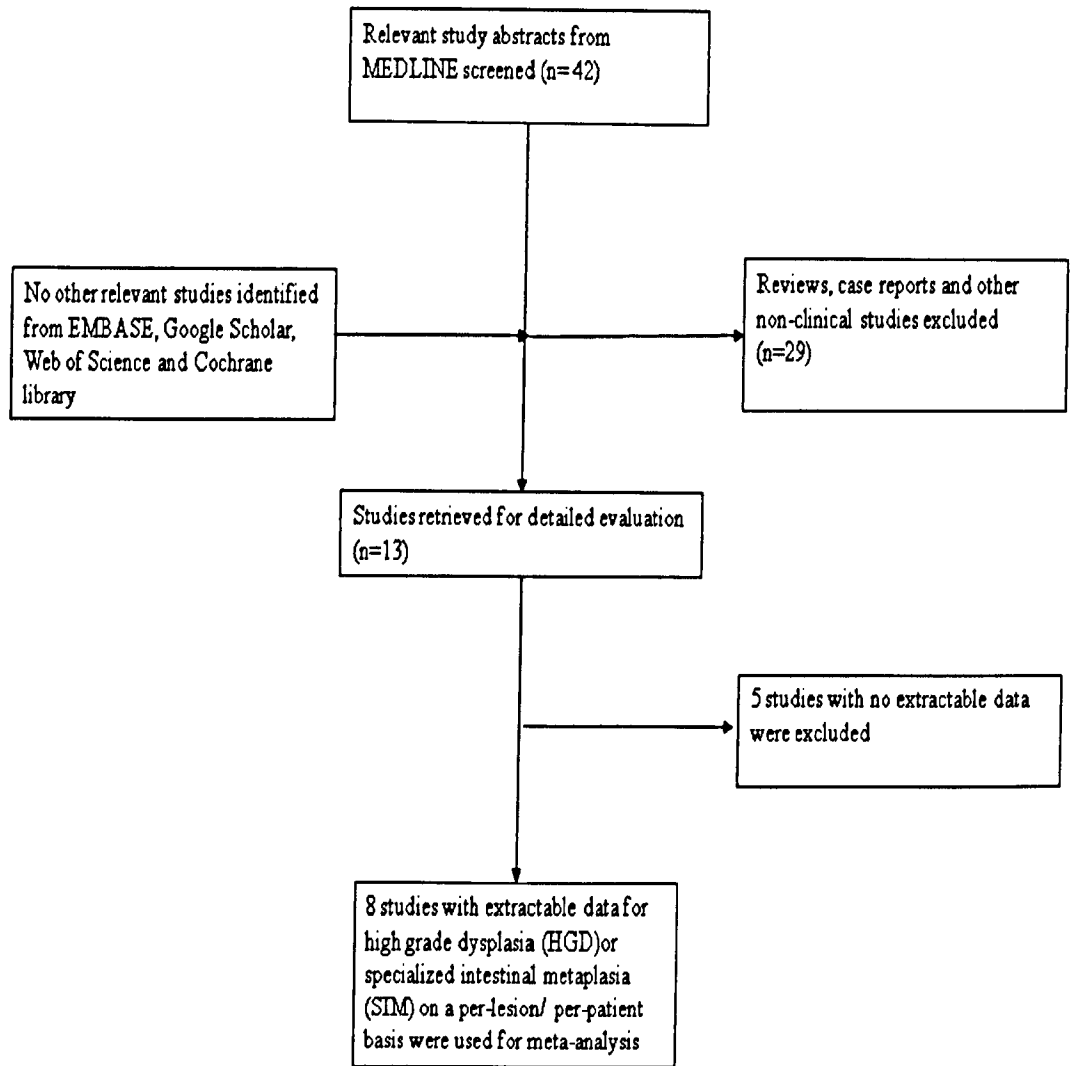


Figure 1: Flow chart of study selection for meta-analysis

4.3.3 Data extraction and assessment of study quality

All included studies were assessed by two reviewers independently and data extracted using a predefined data extraction form. The following variables were assessed; author, year of publication, publication format, type of study, number of centres, endoscopes used, number of endoscopists and whether pit patterns/microvasculature was used to characterise lesions. True positives, false positives, false negatives and true negatives were extracted using histology as gold standard. The data were extracted both on 'per-patient' and 'per-lesion' basis wherever available. Where studies reported mucosal pattern and micro-vascular characteristics, the measures with highest accuracy was used for the overall analysis.

The quality of the studies was assessed using the "Quality Assessment of Diagnostic Accuracy Studies" (QUADAS) tool ¹⁸⁹. The tool is based on 14 item questionnaire summarised in Table 1, which should each be answered "yes," "no," or "unknown." The tool does not incorporate a global quality score ¹⁸⁹. Quality assessment of studies was done independently by two reviewers and discrepancies in the interpretation were resolved by consensus (table 1).

Table 1: 'Quality Assessment of Diagnostic Accuracy Studies' (QUADAS)

Author	1	2	3	4	5	6	7	8	9	10	11	12	13	14
Kara <i>et.al</i>	N	Y	Y	Y	Y	Y	Y	Y	Y	U	U	N	Y	Y
Kara <i>et.al</i>	N	Y	Y	Y	Y	Y	Y	Y	Y	Y	Y	Y	Y	Y
Sharma <i>et. al</i>	N	N	Y	Y	Y	Y	Y	Y	Y	Y	Y	Y	Y	Y
Curvers <i>et.al</i>	N	Y	Y	Y	Y	Y	Y	Y	Y	Y	Y	Y	Y	Y
Singh <i>et.al</i>	Y	Y	Y	Y	Y	Y	Y	Y	Y	U	Y	Y	Y	U
Goda <i>et.al</i>	N	Y	Y	Y	Y	Y	Y	Y	Y	U	Y	Y	Y	Y
Anagnostopoulos <i>et.al</i>	N	Y	Y	Y	Y	Y	Y	Y	Y	Y	Y	Y	U	U
Hamamoto <i>et.al</i>	U	Y	U	U	U	Y	Y	Y	N	U	U	N	U	U

Y = yes; N = no; U = unknown.

1. Was the spectrum of patients representative of the patients who will receive the test in practice?
2. Were selection criteria clearly described?
3. Is the reference standard likely to classify the target condition correctly?
4. Is the period between reference standard and index test short enough to be reasonably sure that the target condition did not change between the two tests?
5. Did the whole sample or a random selection of the sample receive verification using a reference standard?
6. Did patients receive the same reference standard regardless of the index test result?
7. Was the reference standard independent of the index test (*i.e.*, the index test did not form part of the reference standard)?
8. Was the execution of the index test described in sufficient detail to permit replication of the test?
9. Was the execution of the reference standard described in sufficient detail to permit its replication?
10. Were the index test results interpreted without knowledge of the results of the reference standard?
11. Were the reference standard results interpreted without knowledge of the results of the index test?
12. Were the same clinical data available when test results were interpreted as would be available when the test is used in practice?
13. Were uninterruptable/intermediate test results reported?
14. Were withdrawals from the study explained?

4.3.4 Data synthesis

Data analysis was performed using the Meta-Disc (version 1.4) software ¹⁹⁰.

Sensitivity and specificity were used as measures of diagnostic accuracy of NBI in differentiating HGD and SIM. These were computed using a two-by-two table with NBI based diagnosis of high grade dysplasia by irregular pit patterns ± irregular vascular patterns and diagnosis of SIM with ridge/villous/absent pit patterns with regular microvasculature plotted against targeted histology as gold standard. Sensitivity (true positive rate [TPR]) is defined as the proportion of sites/patients determined to be having HGD or SIM based on NBI correctly to the reference standard histology. Specificity (True negative rate or 1-false positive rate [FPR]) is defined as the number of sites/patients who are identified as not having HGD/SIM on NBI correctly compared to the reference standard.

Forest plots were formulated to display estimates of accuracy and examine the heterogeneity of the summary measures of sensitivity and specificity by random-effect model with correction for over dispersion. The joint distribution of TPR and FPR is summarised with a summary receiver operating characteristic (SROC) curve. SROC curves used in analyses of diagnostic accuracy are intended to represent the relationship between TPR and FPR across studies when test performance is evaluated at varying diagnostic thresholds ¹⁹¹. Each study is a separate unit of analysis and contributes an estimate of TPR and FPR. Overall diagnostic performance of a test can be judged by the position and appearance of the SROC curve. The area under the curve (AUC) represents an overall summary measure of the curve and the test's overall ability to accurately distinguish cases

from non-cases. The Q* index, the highest point on the SROC curve that intersects the anti-diagonal, represents a summarisation of test performance where sensitivity and specificity are equal (so the probability of an incorrect test result is the same for cases and non-cases). An AUC of one represents perfect discriminatory ability, while a Q* index of one represents perfect accuracy¹⁹¹. A value of 0.5 infers a test that is equally likely to diagnose a positive result as either positive or negative and most clinical tests have a value between 0.5 and 1.0.

Likelihood ratios (LRs) state how many times more likely particular test results are in patients with disease than in those without disease. Positive LR >10 and negative LR <0.1 provide convincing diagnostic evidence, whereas those >5 and <0.2 give strong diagnostic evidence¹⁹². To calculate LR, if the event of one of the cells of the cross table contained a zero value; 0.5 points were added to all the cells.

Heterogeneity in meta-analysis refers to a high degree of variability in study results, a fairly common finding in diagnostic meta-analyses. Such heterogeneity could be due to variability in thresholds, disease spectrum, test methods, and study quality across studies. In the presence of significant heterogeneity, pooled, summary estimates from meta-analyses are not meaningful. A test for heterogeneity examines the null hypothesis that all studies are evaluating the same effect. The usual test statistic (Cochran's Q) is computed by summing the squared deviations of each study's estimate from the overall meta-analytic estimate, weighting each study's contribution in the same manner as in the meta-analysis. The test is known to be poor at detecting true heterogeneity among studies as

significant. Meta-analyses often include small numbers of studies and the power of the test in such circumstances is low. An alternative method is measuring inconsistency (I^2), which describes the percentage of total variation across studies that are due to heterogeneity rather than chance¹⁹³. We investigated the sources of heterogeneity using meta-regression and subgroup analyses.

4.4 Results

4.4.1 Description of studies

The study selection process is summarised in Figure 1. After the initial screening (excluding case reports, reviews and other irrelevant articles by reading titles and abstracts) 13 studies were selected. A total of 8 prospective studies met the inclusion criteria either for a 'per-patient' or 'per-lesion' analysis or both^{76, 84, 86, 188, 194-197}. 5 studies were excluded^{21, 75, 198-200} as there were no extractable data for calculations of sensitivity and specificity. Three of the excluded studies were inter-observer studies with no data available on true negatives or false positives to calculate sensitivity and specificity^{21, 198, 199}. Two other excluded studies were dysplasia detection studies and did not follow the mucosal morphological patterns for differentiation^{75, 200}. Out of the 8 studies included, 6 studies gave details of HGD characterisation on per-lesion basis^{76, 84, 86, 188, 194, 195} and 4 studies yielded data for per-patient analysis^{76, 84, 188, 195}. 6 studies reported characterisation of SIM on per-lesion basis^{76, 188, 194-197} and 3 studies compared NBI based diagnosis of SIM on per-patient basis^{76, 188, 195}. The details of included studies are summarised in table 2.

4.4.2 Diagnostic accuracy of NBI in HGD

6 studies including a total of 1904 lesions in 377 patients were analysed for differentiation of HGD lesions on per-lesion analysis. The pooled sensitivity and specificity were 0.96 (95% CI 0.93-0.99) and 0.94 (95% CI 0.84-1.0) respectively (figure 2). The pooled diagnostic odds ratio (DOR) was 342.49 (95% CI 40.49-2896.89) using a random effects model. As shown in figure 3, the area under the curve (AUC) was 0.99 (SE 0.01) with Q^* of 0.95 (SE 0.02), indicating a high level of diagnostic accuracy of NBI. The pooled positive LR was 15.248 (95% CI 3.917-59.350) and negative LR was 0.75 (95% CI 0.040-0.141).

On a per-patient analysis, 4 studies with 216 patients and 1616 lesions were pooled. The pooled sensitivity, specificity and DOR were 0.95 (95% CI 0.88-1.0), 0.97 (95% CI 0.97-0.98) and 343.45 (95% CI 77.88-1514.70) respectively (figure 4). The AUC and Q^* were 0.99 (SE 0.01) and 0.95 (SE 0.02), again indicating the high accuracy of NBI characterisation of HGD on a per-patient basis as well (figure 5).

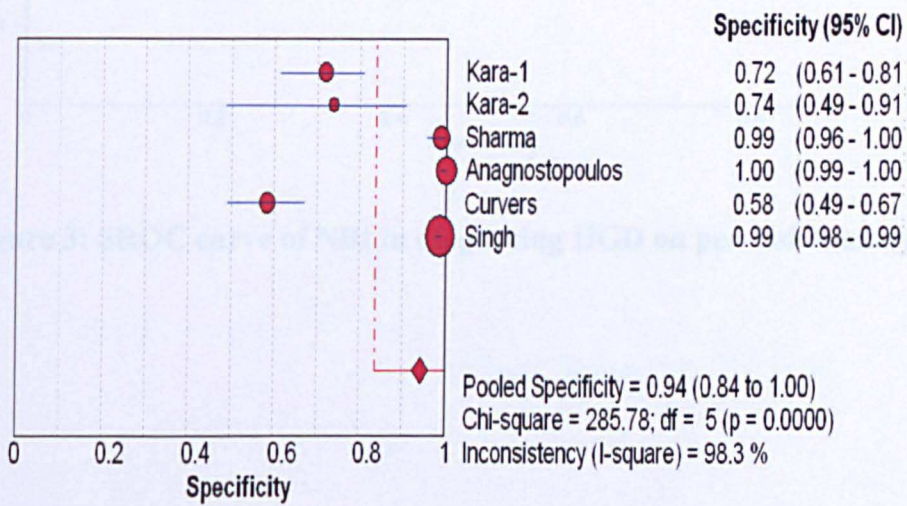
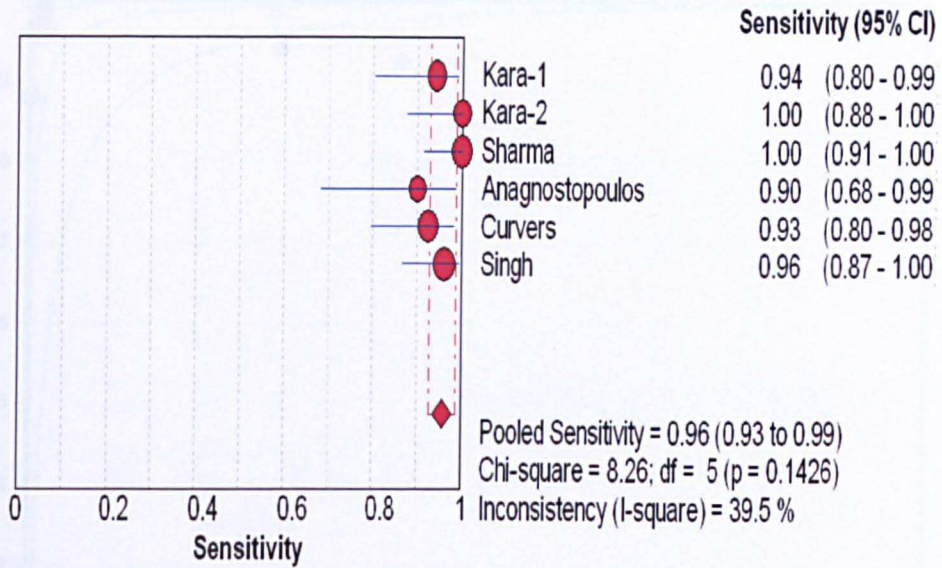


Figure 2: Pooled sensitivity and specificity of NBI in diagnosing HGD on per-lesion analysis

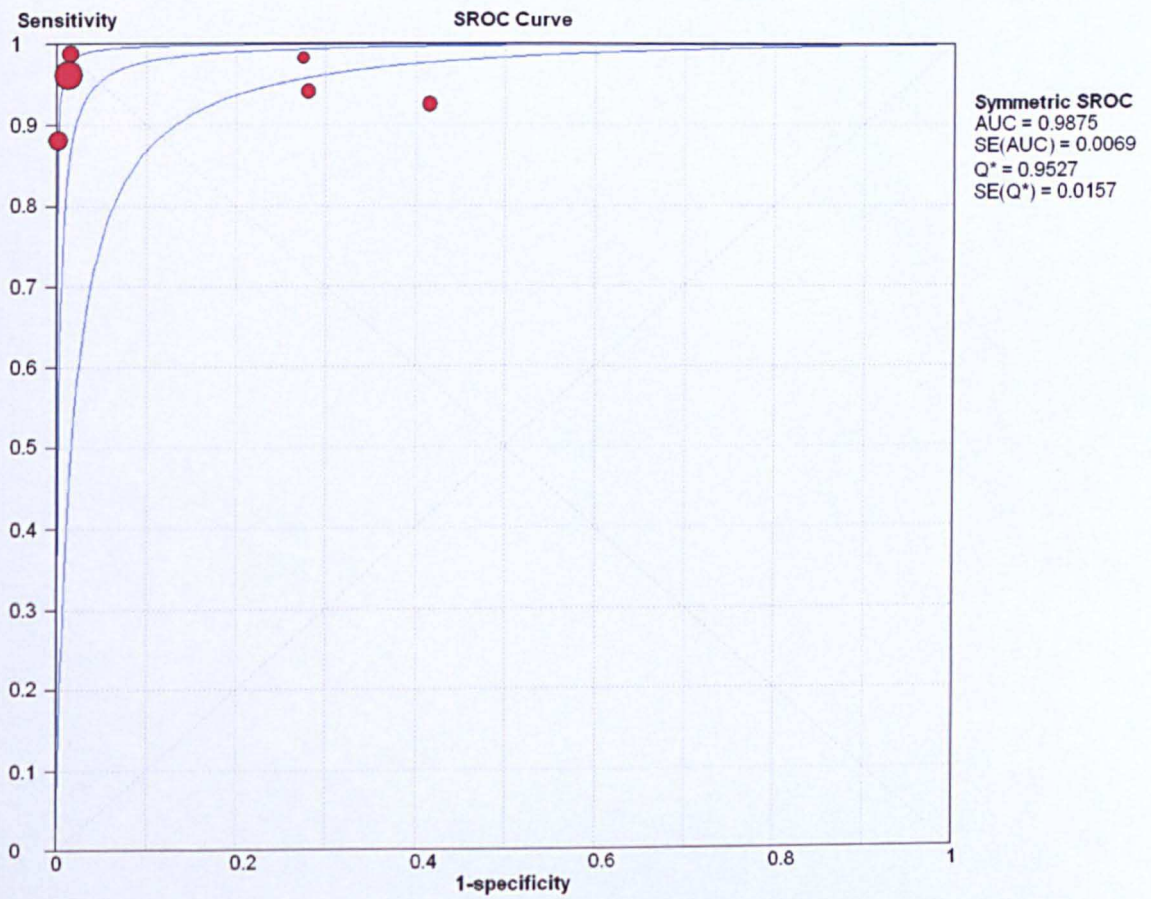


Figure 3: SROC curve of NBI in diagnosing HGD on per-lesion analysis

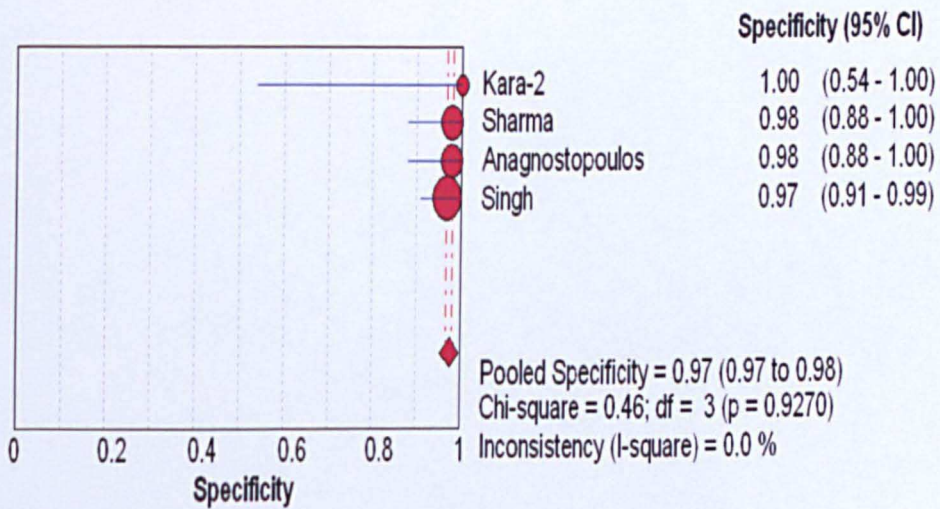
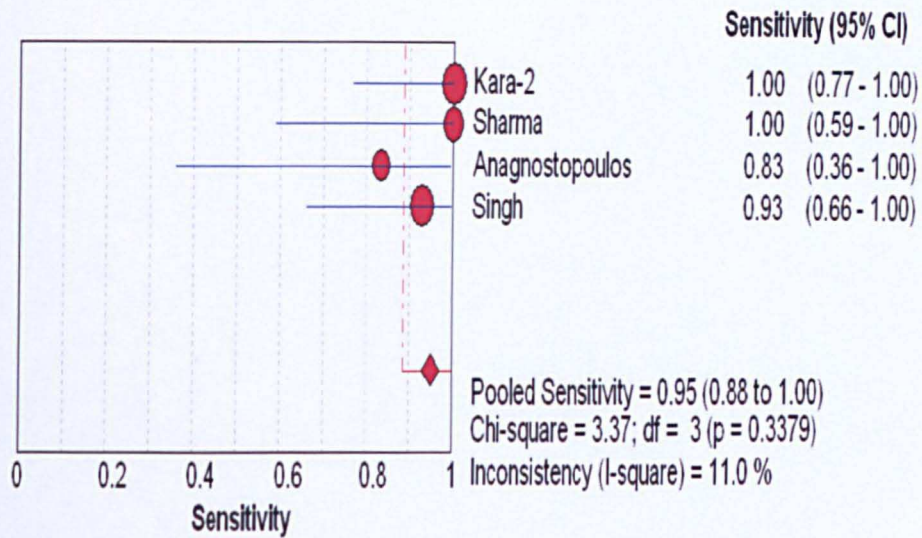


Figure 4: Pooled sensitivity and specificity of NBI in diagnosing HGD on per-patient analysis

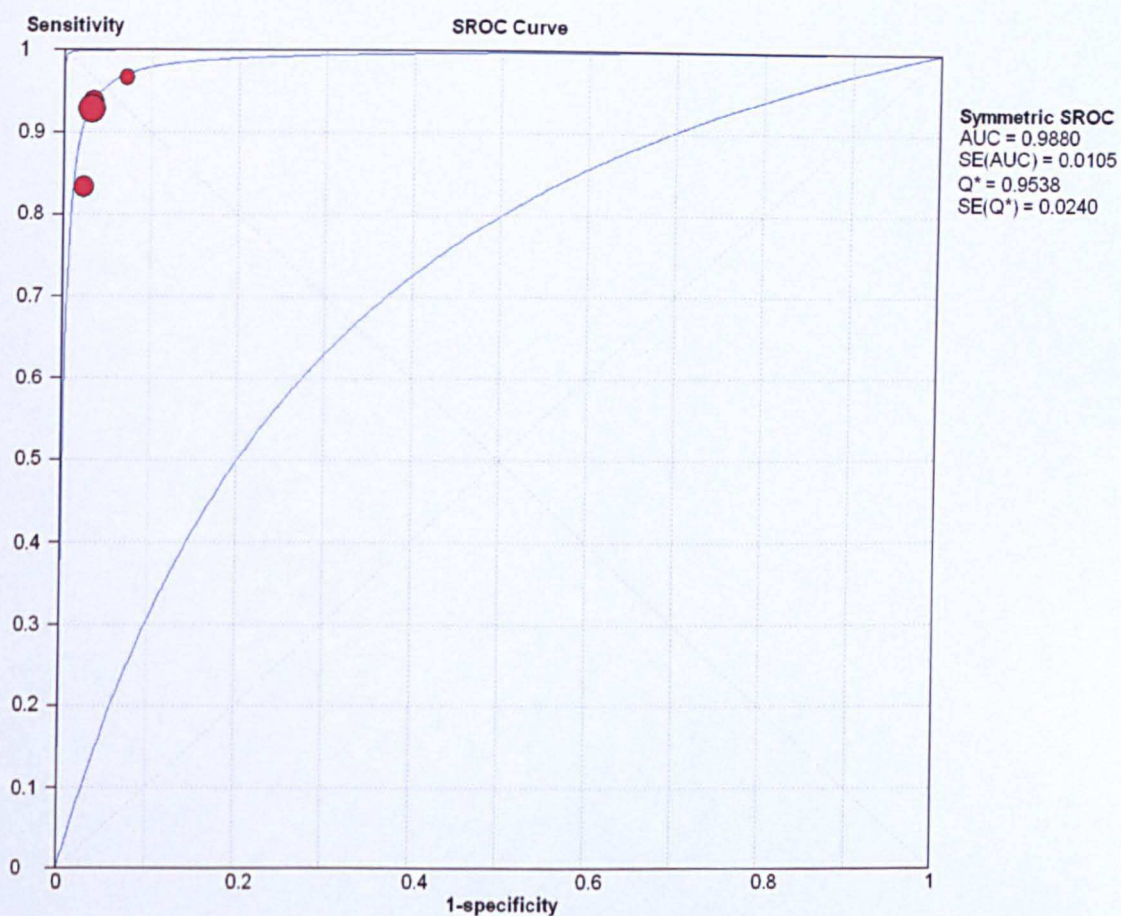


Figure 5: SROC curve of diagnostic accuracy of NBI in characterising HGD on per-patient analysis

4.4.3 Diagnostic accuracy of NBI in SIM

A total of 1938 lesions in 342 patients from 6 studies were used to analyse the data on characterisation of SIM using NBI on a per-biopsy basis (figure 6). Pooled sensitivity and specificity were 0.95 (95% CI 0.87-1.0) and 0.65 (95% CI 0.52-0.78) with a modest DOR of 37.53 (95% CI 6.50-217.62). The AUC was 0.88 (SE 0.08) and Q^* was 0.80 (SE 0.08) which were lower compared to the diagnostic accuracy of characterising HGD (figure 7). Pooled Positive LR was 3.111 (95% CI 1.870-5.17) and negative LR was 0.107 (95% CI 0.26-0.44).

3 studies with 210 patients and 1569 lesions were pooled to assess the accuracy on per-patient analysis (figure 8). Pooled sensitivity 0.97 (95% CI 0.94-1.0), specificity 0.78 (95% CI 0.56-1.0) and DOR 100.97 (95% CI 33.62-303.22) were similar to per-lesion analysis. The AUC and Q^* were 0.97 (SE 0.02) and 0.92 (SE 0.04) respectively (figure 9). The sensitivity of NBI in differentiating SIM appears to be high; however the specificity is poor.

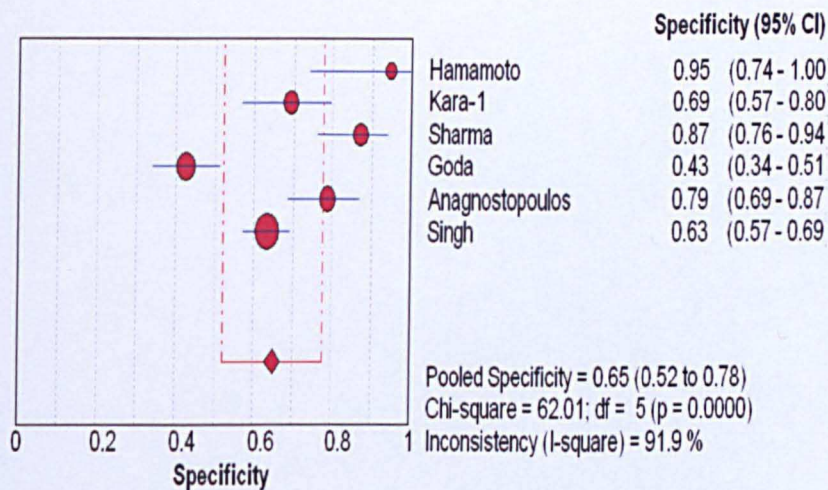
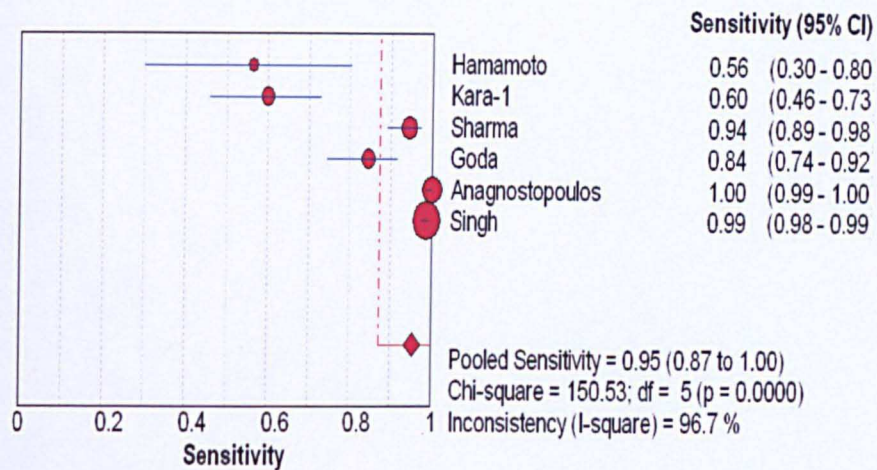


Figure 6: Pooled sensitivity and specificity of NBI diagnosis of SIM on per-lesion analysis

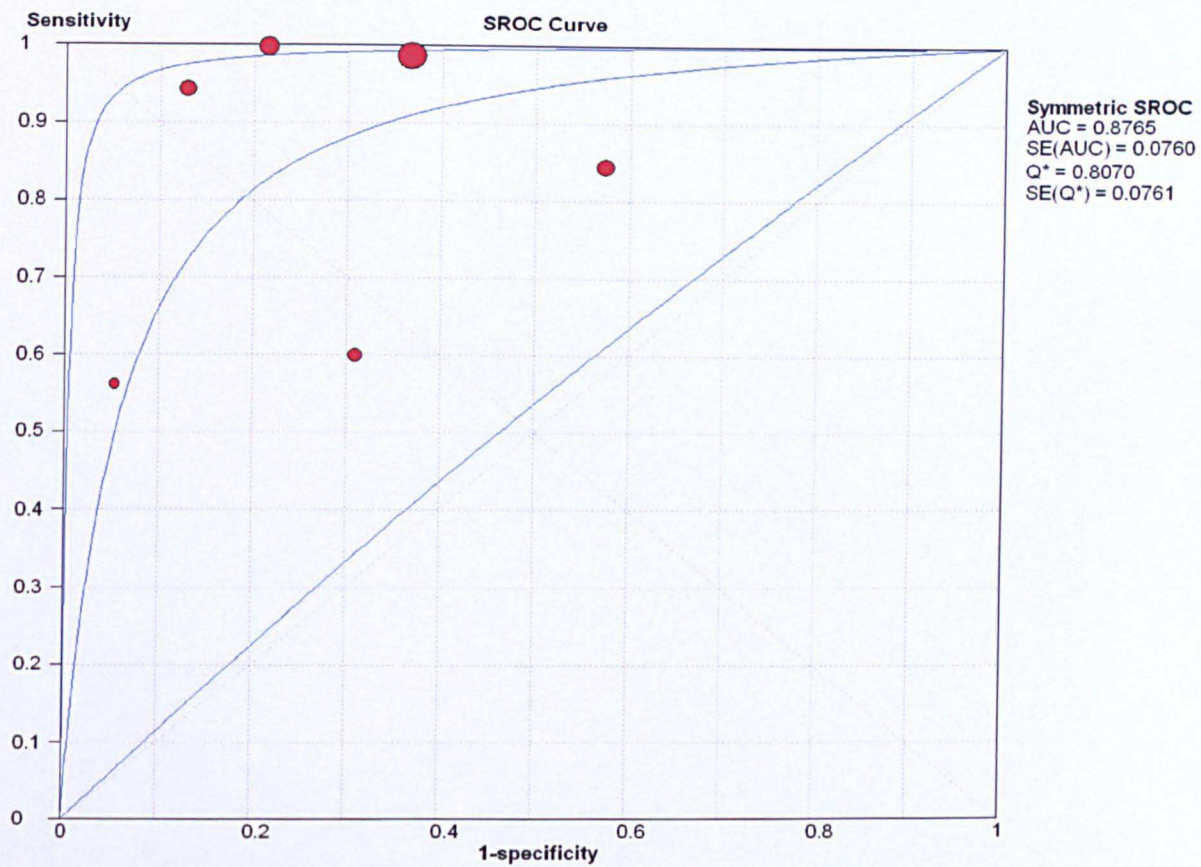


Figure 7: SROC curve of NBI diagnosis of SIM on per-lesion analysis

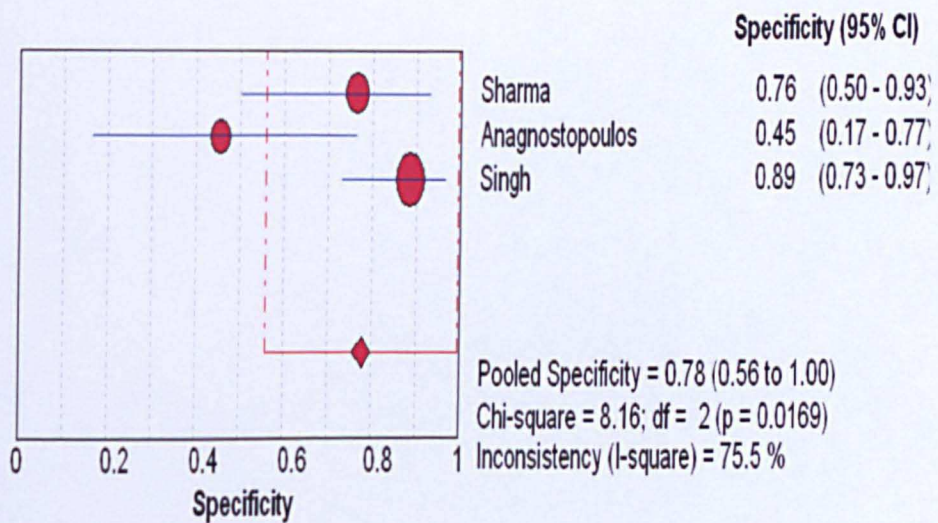
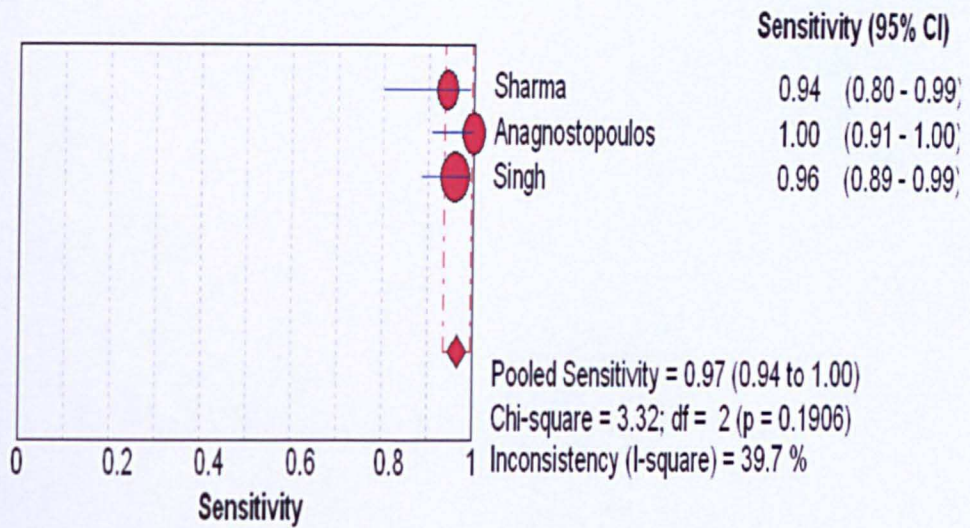


Figure 8: Pooled sensitivity and specificity of NBI diagnosis of SIM on per-patient analysis

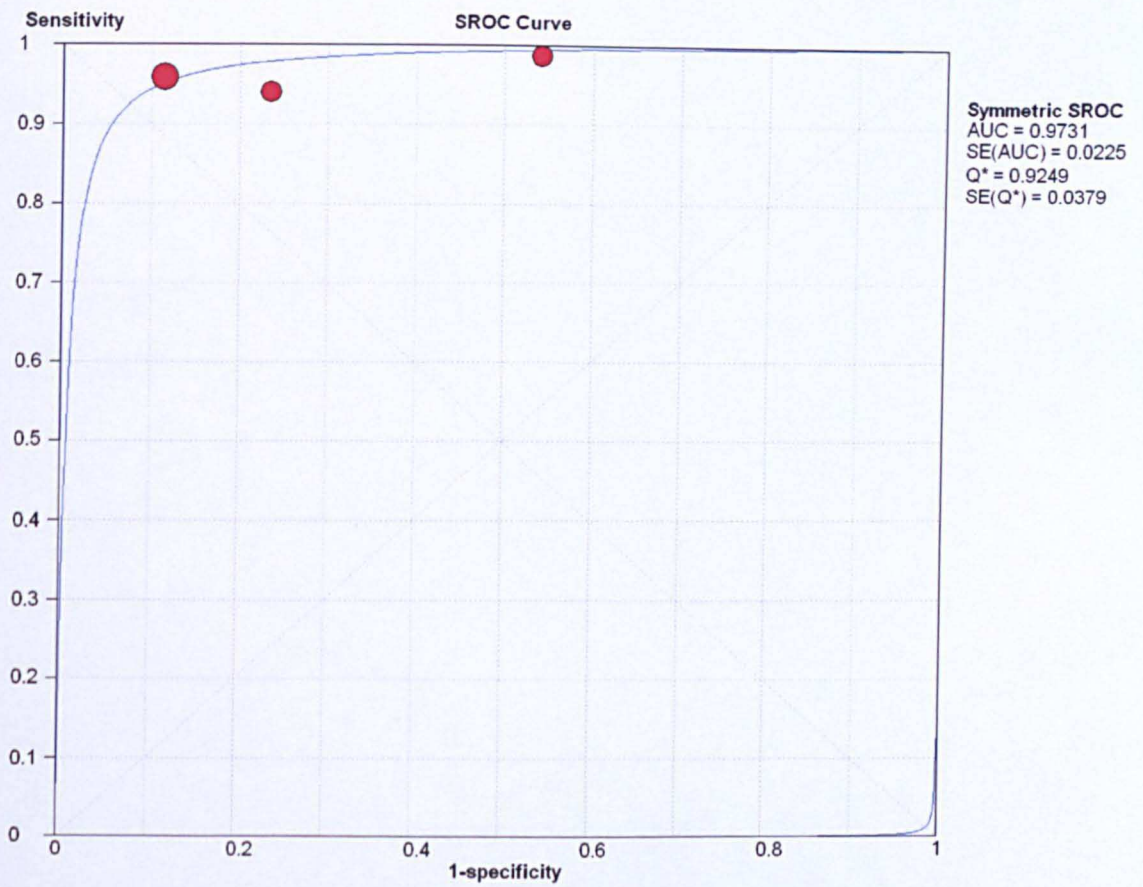


Figure 9: SROC curve of NBI accuracy in diagnosing SIM on per-patient analysis

4.4.4 Heterogeneity of studies

Studies used in HGD analysis: Heterogeneity was observed among studies which were pooled for a per-lesion analysis of HGD characterization with an I^2 of 86.2%. However, there was no heterogeneity among studies which were pooled together for a per-patient analysis ($I^2=0\%$). We used meta-regression and subgroup analysis to identify the source of heterogeneity. The following subgroups were analysed separately; single centre or multicentre study, number of endoscopists <2 or ≥ 2 , number of patients <50 or ≥ 50 , number of lesions examined <200 or ≥ 200 , Quality of studies (<12 or ≥ 12 scores on QUADAS) and whether autofluorescence imaging (AFI) is used along with NBI. The number of lesions was the only significant variable identified as to the cause of heterogeneity ($P=0.005$, relative DOR 88.52 [95% CI-10.04-781.36]) (table 3). When those studies with ≥ 200 lesions^{76, 188, 195} were pooled together, the sensitivity and specificity was 0.97 (95% CI 0.91-0.99) and 0.99 (95% CI 0.98-0.99). The DOR was 2566.8 (95% CI 741.38-8886.5) with an I^2 of 0% (decreased from 86% when all 6 studies included).

Studies used in SIM analysis: The studies used for analysis of SIM characterisation on per-patient basis showed good homogeneity ($I^2=0\%$), however, when studies were pooled on per-lesion basis there was significant heterogeneity ($I^2=94.7\%$). The subgroup analysis showed that the number of SIM lesions examined (<100 or ≥ 100) was the only significant variable responsible for the

Table 3: Meta-regression analysis to identify sources of heterogeneity

Variables	HGD-per-lesion analysis		SIM-per-lesion analysis	
	P	Relative DOR (95% CI)	P	Relative DOR(95% CI)
Number of endoscopists <2 or ≥2	0.33	0.04 (0.0-136.21)	0.59	3.31(0.01-920.28)
Number of patients <50 or ≥50	0.77	2.70 (0.0-21604.19)	0.84	1.86 (0.0-6065.47)
Number of lesions (for HGD analysis <200 or ≥200 lesions, for SIM <100 or ≥100 SIM lesions evaluated)	0.005	88.57 (10.04-781.36)	0.001	34.23 (11.92-98.30)
Quality of studies <12 or ≥12 on QUADAS	0.412	4.68 (0.03-821.54)	0.99	0.97 (0.0-323.66)

DOR- Diagnostic odds ratio, CI- Confidence interval

heterogeneity (P=0.001, RDOR 34.23 [95% CI 11.92-98.30]) (table 3). When we pooled the studies with >100 SIM lesions, the sensitivity and specificity was 0.99 (95% CI 0.97-0.99) and 0.7 (95% CI 0.65-0.74). The DOR was 158.63 (95% CI 62.54-402.33) with an I² of 47% (decreased from 97% when all 6 studies included).

4.5 Discussion

4.5.1 Principal findings

Narrow Band Imaging offers the advantages of chromoscopy without the need for any additional dye spray and is easy to use. However to obtain clear mucosal views in order to assess the pit patterns and microvasculature, magnification is necessary. In this meta-analysis we reported pooled analysis on a per-lesion and per-patient basis, as it is important to see whether NBI-Z analysis is beneficial from a patient perspective as well, rather than just in diagnosing lesions. Results suggest that NBI with magnification has a high diagnostic accuracy in characterising HGD both on per-lesion and per-patient analysis with sensitivity and specificity over 90%. The sensitivity of NBI-Z in differentiating SIM is high but the specificity is poor.

4.5.2. Clinical implications

The high diagnostic accuracy of NBI-Z for characterising HGD suggests that it is useful in accurately targeting biopsies and therapy of early neoplasia. This will reduce the need of multiple random biopsies and increase the yield of dysplasia. Also, in patients referred for endoscopic resection of early neoplastic lesions, NBI-Z will help delineating the lesion and assist in determining the margins of endoscopic resection. On the other hand, patients with BO who are on surveillance, endoscopic resection for abnormal dysplastic areas detected by NBI-Z will be useful for accurate local staging and as a curative therapy, without waiting for biopsy results and avoiding multiple endoscopies. In suspected or

small BO, NBI-Z could be useful in identifying SIM and targeting biopsies, even though the diagnostic accuracy is comparatively low. The pooled sensitivity is 95%, but the specificity (65%) needs to be improved. One of the reasons for this could be the various novel classification systems used by observers including linear, ridged, villous and absent patterns as a marker of SIM. Once diagnostic patterns are standardised, the diagnostic accuracy could improve. For HGD, irregular micro-structural and vascular patterns have been accepted as the standard diagnostic patterns and consequently the diagnostic accuracy is high.

4.5.3 Study limitations

Like most meta-analysis of diagnostic accuracy, this study has a few limitations. We have not compared the diagnostic accuracy of NBI-Z against white light (WLE), white light with zoom (WLE-Z) or chromoendoscopy as there is a paucity of data in the literature on this. Further comparative studies are necessary in order to advocate NBI-Z over other modalities.

In order to include all relevant articles and reduce the effect of potential publication bias, we reviewed a range of electronic databases. We also included studies in all languages and hand searched references from the published studies. Assessment of publication bias is challenging in meta-analysis of diagnostic accuracy as the accuracy is assessed against reference standard and as such the outcome is not compared between two tests. In this context funnel plots are not useful. Smaller number of primary studies available for this meta-analysis also makes it difficult to interpret funnel plots²⁰¹. Incorporation bias is unlikely as

most studies indicate that histopathological interpretation is done without knowledge of the NBI findings. Verification bias is excluded as all lesions/patients included have index (NBI) and reference (histology) test.

Heterogeneity was observed among studies, which is usual with meta-analysis of diagnostic accuracies. We performed meta-regression and sub-group analysis to identify the sources of heterogeneity. The number of lesions examined was the only variable which showed significance in the meta-regression and the consistency improved when studies with larger numbers of lesions were pooled together. Several slightly varied classification systems were used for the characterisation of SIM in each of the studies, which also would add to the heterogeneity.

Narrow band imaging itself has disadvantages. It needs a video processor and additional light source which will increase the cost of the procedure. Moreover, a detailed examination of mucosa to differentiate various micro-structural and vascular patterns needs a magnification scope, adding to the capital cost. Presence of blood on the mucosa will make characterisation by NBI very difficult and hence operators have to be careful to avoid suction trauma to the lesions. Also, once biopsies are done, it becomes difficult to examine the rest of the dysplastic area. Inflammation with increased vascularity can be misinterpreted for dysplasia, based on the vascular characteristics. The studies in this meta-analysis used the older generation GIF Q240Z endoscope. Currently high definition and higher resolution endoscopes are available and further studies looking at the additive value of these endoscopes are needed.

4.5.4 Conclusions

NBI-Z has a high diagnostic precision in lesion characterisation of high grade dysplasia in BO. NBI-Z will help target endoscopic biopsies and in delineating resection margins during endotherapy of dysplastic areas. Use of NBI in lesion characterisation for specialised intestinal metaplasia seems to be less accurate, probably due to the different classification of micro-structural patterns used, but could be improved with adoption of standardised classification systems.

Author (year)	Mean Age (Y)/ Males (%)	No. Of subjects	Total No. Of lesions examined	Study design	Endoscope type	Index test (NBI classification)	Reference standard (histology)	Number of endoscopists	QUADAS score
Kara et.al 2006 (194)	65/50(79%)	63	198	Cross sectional, Post hoc Image evaluation	GIF Q240Z	Mucosal pattern, Vascular pattern	High grade dysplasia, specialised intestinal metaplasia	2	10/14
Kara et.al 2006 (84)	66/17(85%)	20	47	Cross sectional, real time evaluation	GIF Q240Z	Mucosal pattern, Vascular pattern	High grade dysplasia	2	13/14
Sharma et.al 2007 (195)	64/50(98%)	51	204	Cross sectional, image evaluation	GIF Q240Z	Mucosal pattern, Vascular pattern	High grade dysplasia, Specialised intestinal metaplasia	Not stated	12/14
Curvers et.al 2008 (86)	67/70(83%)	84	165	Cross sectional, real time evaluation	GIF Q240Z	Mucosal pattern, Vascular pattern	High grade dysplasia	5	13/14
Singh et.al 2008(76)	61.9/77(71%)	109	1021	Cross sectional, post hoc image evaluation	GIF Q240Z	Mucosal pattern, vascular pattern	High grade dysplasia, specialised intestinal metaplasia	4	12/14
Goda et.al 2007 (196)	60/51(88%)	58	217	Cross sectional, real time evaluation	GIF Q240Z	Mucosal pattern, Vascular pattern	Cancer, Specialised intestinal metaplasia	1	12/14
Anagnostopoulos et.al 2007 (188)	62.1/34(68%)	50	344	Cross sectional, realtime evaluation	GIF Q240Z	Mucosal pattern, Vascular pattern	High grade dysplasia, Specialised intestinal metaplasia	3	11/14
Hamamoto et.al 2004(197)	61.2/6(55%)	11	35	Case series, Post hoc image evaluation	GIF Q240Z	Mucosal pattern, Vascular pattern	Specialised intestinal metaplasia	1	4/14

Table 2: Characteristics of studies included in the meta-analysis

CHAPTER 5

ROLE OF VIDEO AUTOFLUORESCENCE ENDOSCOPY IN DETECTION OF DYSPLASIA IN BARRETT'S OESOPHAGUS; A META-ANALYSIS

5.1 Abstract

Background and aims

Autofluorescence imaging (AFI) is a novel technique which highlights abnormal or dysplastic areas in Barrett's oesophagus and is used as a 'red flag' technique. Various published studies have shown conflicting results regarding the accuracy of this technique. The aim of this study was to compare the diagnostic yield of Barrett's dysplasia between AFI and white light endoscopy (WLE).

Method

A meta-analysis of all prospective studies which compared lesions detected by AFI with histopathology as the gold standard was performed. Electronic databases were searched with key words "Autofluorescence and Barrett's". Forest plots were formulated to display estimates of accuracy. The pooled incremental yield for dysplasia detection of AFI over WLE was calculated.

Results

An initial search provided 54 studies and 5 studies met our inclusion criteria. 350 patients with 521 AFI detected lesions were included in the final analysis. The incremental yield for detecting high grade dysplasia/cancer by AFI over WLE was 49% (95% CI 42%-56%). For detection of all dysplasia, the incremental yield was 46% favouring AFI (95% CI 25%-67%) when 3 studies with available data were

included. The event rates for false positive detection of lesions were 75% (95% CI 58%-86%) for AFI and 70% for WLE (95% CI 54%-82%). White light endoscopy is more likely to miss HGD/cancer (OR 3.58, 95% CI 1.8-7) and all dysplasia (OR 4.26, 95% CI 0.88-20.7) compared to AFI.

Conclusion: Autofluorescence imaging is more likely to detect high grade dysplasia/cancer and all dysplasia compared to white light endoscopy in Barrett's surveillance. This is at the expense of significant false positive lesion detection.

5.2 Introduction

Regular surveillance in Barrett's oesophagus is performed with a view to identify early dysplastic lesions which could be treated at an early stage^{202, 203}. This is likely to improve clinical outcome for patients compared to those presenting with symptomatic cancers. The routine practice in BO surveillance is to observe for any early lesions, which could then be target biopsied. In the absence of any obvious lesions, random four quadrant biopsies are taken every 2 cm as recommended by various national Gastroenterology societies^{126, 204}. The random biopsy technique is associated with significant sampling error. Image enhanced endoscopy techniques as well as chromoendoscopy were used with a view to improve the detection of subtle early lesions with variable results.

Autofluorescence video endoscopic imaging is a relatively new technique which was introduced in 2005⁸³. This endoscope is equipped with two CCD, one for the white light imaging and the other for AF imaging. The basis of this technique involves the fact that, when certain endogenous fluorophores in the gastrointestinal tract is excited with light of short wavelength, they emit light of long wavelength. This is captured after filtering the short wavelength light to incorporate into a pseudo colour image. The normal mucosa appears green related to the absorption spectrum of haemoglobin and the abnormal or dysplastic tissue will have reduced fluorescence seen in magenta/purple colour.

The AF imaging was studied predominantly in enriched Barrett's population and the results were suggestive of high sensitivity in picking up early dysplastic lesions. However, this is associated with a high false positive rate and hence low

specificity. This meta-analysis was aimed to assess the incremental yield of detecting dysplastic lesions by AFI compared to white light endoscopy (WLE).

5.3 Methods

5.3.1 Search strategy

Literature search was done in various databases including Medline, Google Scholar, Web of Science and Cochrane databases. The search terms used were 'Autofluorescence and Barrett's'. Articles in all languages were searched. We also hand-searched references from published articles. Abstracts were not included.

5.3.2 Selection of studies

All studies reporting the accuracy of AF imaging and WLE in Barrett's oesophagus with histology as gold standard were included. The inclusion criteria were a) prospective evaluation of autofluorescence imaging in BO, b) histological confirmation of the abnormal lesions c) real time assessment of lesions or post-hoc analysis and d) video autofluorescence endoscopic system is used.

Studies without histological confirmation and those without extractable data were excluded. Also, case reports, case series, editorials, inter-observer studies, commentaries and data reported as abstracts only were excluded. Moreover, studies which used light induced fluorescence endoscopy (LIFE) and laser induced spectroscopy systems were excluded. Data from studies were independently extracted by two investigators and any discrepancies were resolved by discussion.

5.3.3 Meta-analysis

A meta-analysis was performed with the following outcomes; the yield of AFI and WLE in detecting HGD/cancer and all dysplasia. Furthermore, the event rates for false positive detection of lesions were calculated for AFI and WLE. Finally, the miss rates of HGD/cancer and all dysplasia by AFI and WLE were analysed. The incremental yield of AFI was calculated by subtracting the yield of WLE from that of AFI and a 95% confidence interval was calculated. A fixed effects model was used unless there was significant heterogeneity, in which case the DerSimonian–Laird random effects model was used²⁰⁵. Comprehensive Meta Analysis version 2.2 (Biostat, Englewood, New Jersey, USA) statistical package was used for the data analysis.

5.3.4 Heterogeneity analysis

The Cochran's Q was used to test heterogeneity among the pooled estimates. Statistical heterogeneity was also assessed using I^2 (inconsistency) that quantifies the proportion of inconsistency in individual studies that cannot be explained by chance. Values of I^2 such as 25%, 50% and 75% represent inconsistency which is low, moderate or high respectively. To test publication bias, a test for asymmetry of the funnel plots as suggested by Egger *et al* was used²⁰⁶.

5.4 Results

A Pubmed search revealed 54 potentially relevant articles. 49 articles were excluded by reading the abstracts and/or the full text articles. These included

reviews, commentaries, case reports, correspondence and inter-observer studies.

Articles pertaining to the light induced fluorescence (LIFE), laser fluoroscopy and spectroscopy were also excluded and finally 5 papers which used the video autofluorescence endoscopy and have extractable data were included in the analysis^{83, 84, 86, 171, 207}. No additional articles were retrieved from other sources.

All 5 studies provided data on the detection of lesions containing HGD/early cancer. Only 3 studies provided data on all dysplastic lesions detected by these modalities^{83, 171, 207}. All 5 studies had sufficient data to analyse the false positive rates (FPR) of AFI and 4 studies provided the information on FPR of WLE^{84, 86, 171, 207}. The miss rates for HGD/cancer were calculated from 4 studies^{83, 86, 171, 207} and that of all dysplasia were calculated from 3 studies which provided sufficient data^{83, 171, 207}.

5.4.1 Detection of high grade dysplasia/cancer

Five studies with 350 patients and 521 lesions were included in the analysis. The pooled incremental yield of AFI over WLE for detecting HGD/cancer was 49% (95% CI 42%-56%). Figure 1 shows the Forest plot for the incremental yield of AFI over WLE in the selected studies.

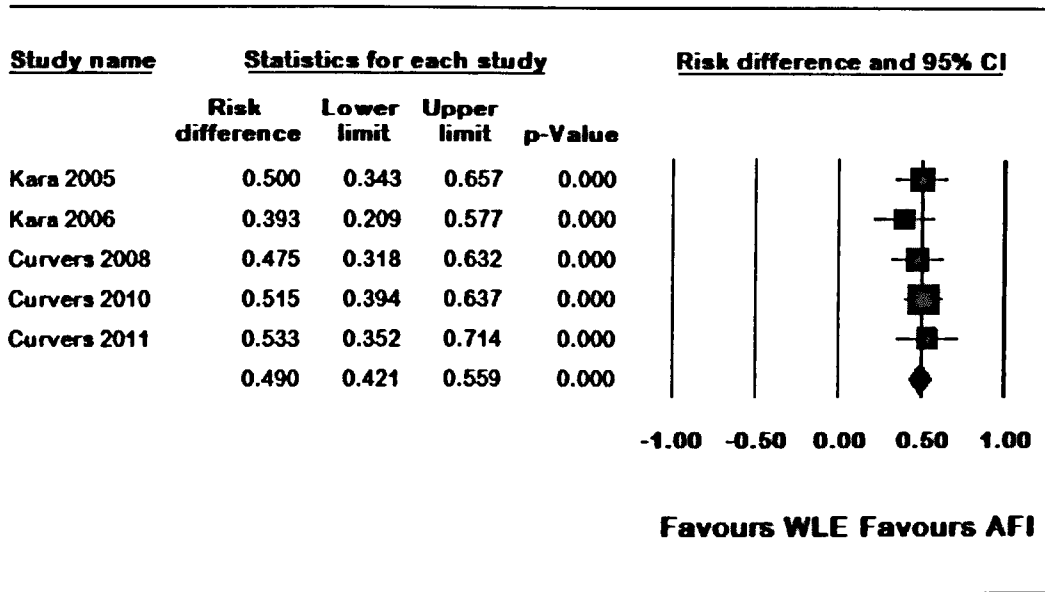


Figure 1: Pooled incremental yield of AFI compared to WLE in detecting HGD/cancer

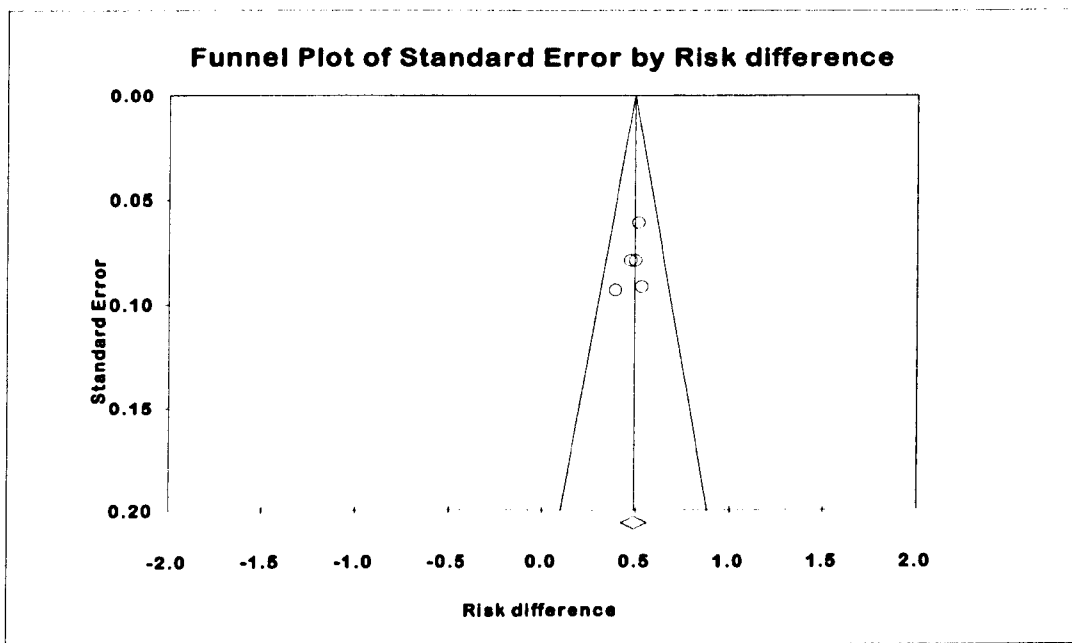


Figure 2: Funnel plot for publication bias for detection of HGD/cancer comparing AFI and WLE

A fixed effect model was used for analysis as the heterogeneity was low (Cochran's Q 1.5, $p=0.83$, $I^2=0\%$). Publication bias was excluded by a funnel plot (figure 2) and Egger's regression asymmetry test ($p=0.4$, intercept= -1.72, 95% CI -7.36 to 3.91)

5.4.2 Detection of all dysplasia

3 studies with a total of 372 lesions were included in the analysis for all dysplastic lesions. The pooled incremental yield for AFI for detecting all dysplastic lesions compared to WLE was 46% (95% CI 25%-67%). Figure 3 shows the Forest plot for the incremental yield of AFI over WLE in the selected studies. A random effect model was used as the heterogeneity between the studies was high (Cochran's Q 15.69, $P<0.001$, I^2 87%). Publication bias was excluded by Egger's regression symmetry ($p=0.40$, intercept= -6.50, 95% CI -67.1 to 54.1).

5.4.3 False positive rates

The pooled false positive rates (FPR) for each modality were calculated as event rate or the proportion of lesions which were false positive. All 5 studies were included in the analysis for AFI and 4 studies with available data were used for FPR of WLE. The pooled false positive rates for AFI in detecting dysplastic lesions was 75% (95% CI 58-86%) on a random effects model (figure 4). For WLE, the pooled FPR was 70% (95% CI 54-83%) (figure 5). Random effects model was used as heterogeneity among studies were high (AFI-Cochran's $Q=48.9$, I^2 92%, for WLE-Cochran's $Q=15.7$, I^2 81%).

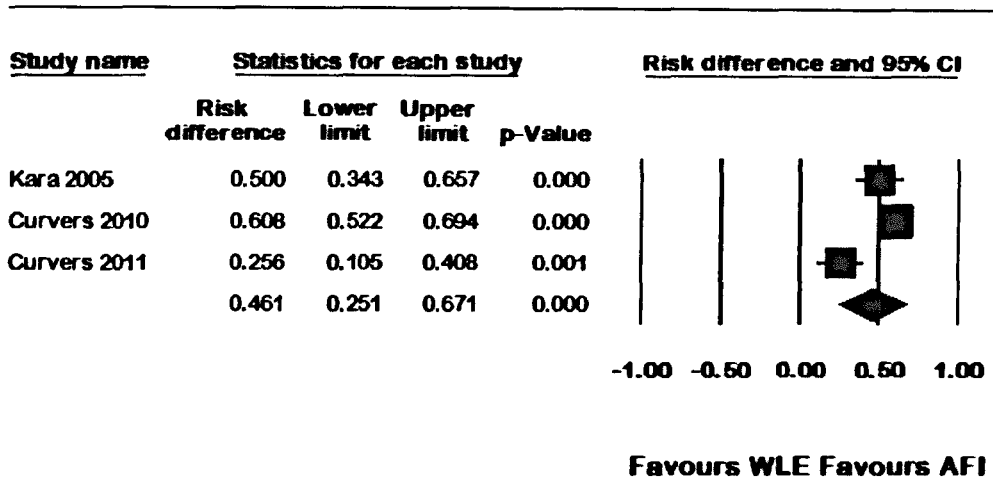


Figure 3: Pooled incremental yield of AFI compared to WLE in detecting all dysplasia

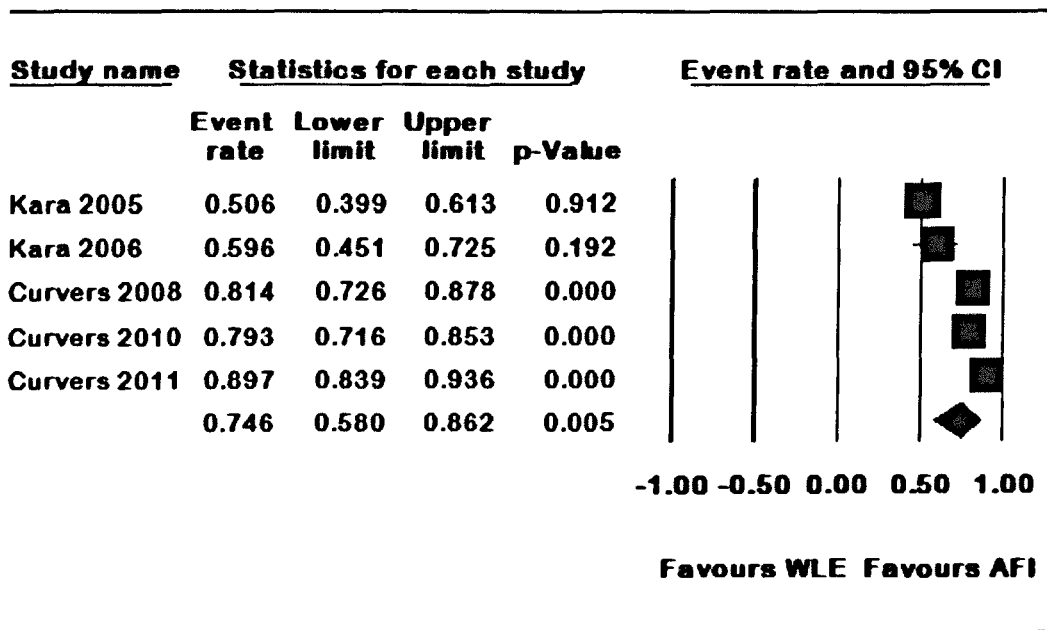


Figure 4: Pooled false positive rates for autofluorescence imaging detected lesions

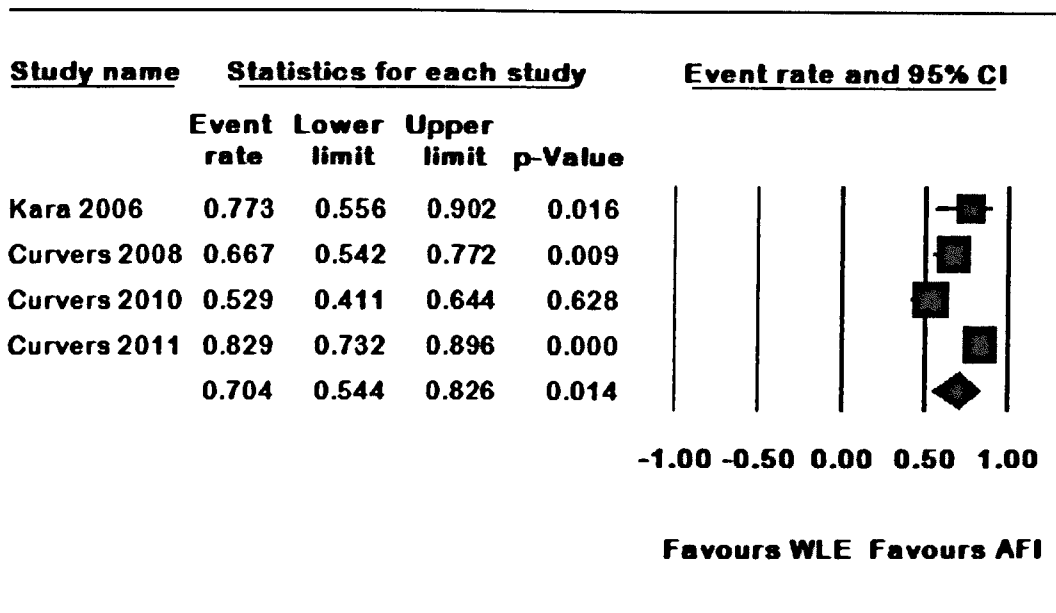


Figure 5: Pooled false positive rates for white light endoscopy detected lesions

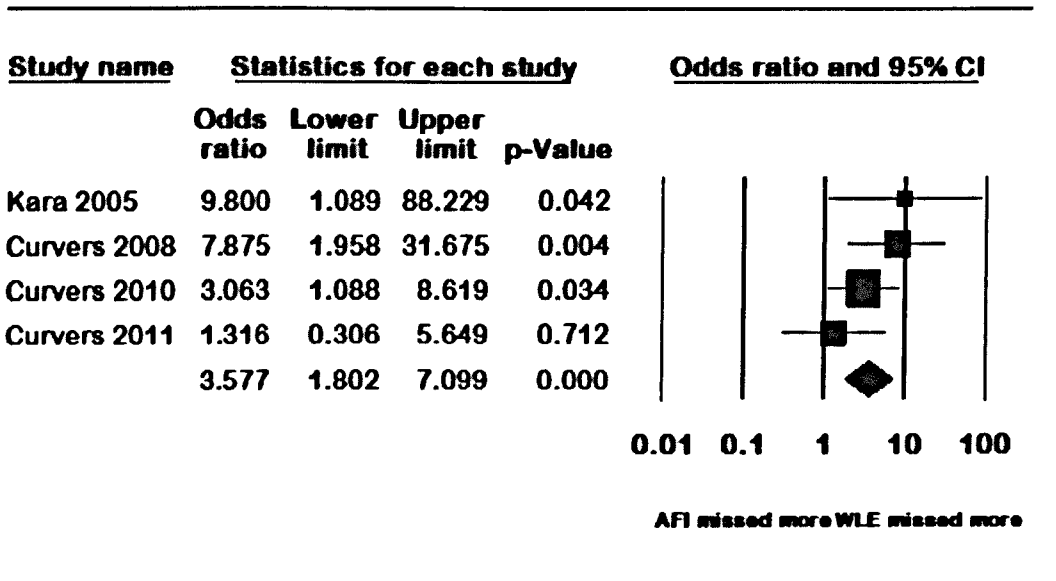


Figure 6: Pooled Odds ratio of miss rates of high grade dysplasia or cancer compared between AFI and WLE

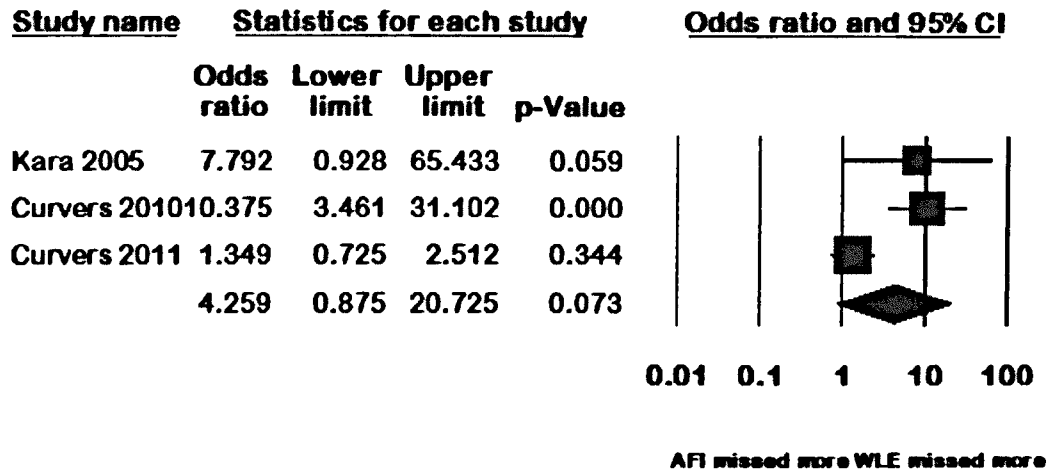


Figure 7: Pooled Odds ratio of miss rates of all dysplasia compared between AFI and WLE

5.4.4 Miss rates of high grade dysplasia and all dysplasia

The odds of missing a lesion was calculated with number of patients with HGD for the calculation of HGD miss rates and the total number of patients for the miss rates of all dysplasia. The pooled Odds ratio of missing HGD or early cancer was 3.57 (95% CI 1.8-7.1) with WLE missing more number of lesions compared to AFI (Figure 6). A fixed effects model was used as the heterogeneity of studies was low (Cochran's $\chi^2 = 3.93$ $p=0.27$, I^2 24%). Similarly the OR for all dysplastic lesions were 4.26 (95% CI 0.87-20.73) favouring AFI on a random effects model (figure 7). The heterogeneity among the 3 studies included in this analysis was high (Cochran's $Q = 11.3$, $p=0.004$, I^2 82%). There was no evidence of publication bias on the Egger's regression asymmetry analysis ($p=0.44$, intercept=1.50, 95% CI - 9.7 to 12.7).

5.5 Discussion

This study was aimed to evaluate the added benefits of autofluorescence endoscopy compared to white light endoscopy in terms of detection of lesions containing primarily high grade dysplasia and cancer. AFI is found to identify more number of dysplastic lesions during BO surveillance compared to WLE, but high false positive rates were reported. This indicates that the more number of lesions identified are at the expense of over calling dysplasia during surveillance. This study showed that the incremental yield of AFI in detecting HGD/cancer was 49% compared to WLE. The studies included in the analysis did not show significant heterogeneity or publication bias. It could be argued that, more time is

spent on the endoscopic procedure by switching between AFI and WLE and the careful examination itself would have contributed to the higher pick up of HGD/cancer. The other argument is whether the higher HGD pick up is related to more number of biopsies taken as there are significantly higher false positive lesions detected during AFI. However, in this study, the pooled FPR rates for AFI and WLE was not significantly different (75% Vs 70%). The pooled incremental yield for AFI in detecting all dysplasia was 46% (95% CI 25%-67%) compared to WLE. This analysis included only 3 papers with significant heterogeneity and hence the results should be viewed with caution.

The pooled FPR for AFI was 75%. This has been a consistent finding in all the clinical studies. A study by Curvers *et al* attempted to identify predictive factors for true positive lesions detected during BO surveillance²⁰⁸. The study suggested that opaque intensity, abnormality in WLE and remoteness to gastric folds are potential factors predicating the true positive nature of the lesions. These factors should be considered during endoscopic examination which might help to reduce the false positive rates.

White light endoscopy is more likely to miss HGD/cancer compared to AFI (OR 3.6, 95% CI 1.8-7.1). Similarly, the miss rates for WLE in detecting all dysplasia were 4.3 times higher than the AFI. This is particularly significant finding in an enriched Barrett's population, but whether this would be applicable in routine Barrett's surveillance is not clear. The use of white light endoscopy in studies was heterogeneous; some of the studies used high resolution endoscopy^{83, 84, 86} and

other studies used standard definition endoscopy^{171,207}. However, all studies showed a higher detection of dysplasia by AFI.

5.5.1 Limitations of the study

As with any meta-analysis there are several potential limitations to this study especially by pooling data from different trials. The variations in the study designs, inclusion and exclusion criteria, operator experience and interpretation of findings could have all contributed to the heterogeneity. Some of the studies have included small number of patients and are potentially subject to selection bias. By pooling data from such studies, selection bias would be amplified.

5.5.2 Conclusions

Autofluorescence imaging is more likely to detect high grade dysplasia, cancer and all dysplasia in an enriched Barrett's population compared to white light endoscopy. The miss rates for dysplasia by white light endoscopy were significantly higher compared to autofluorescence imaging. However, the increased dysplasia detection rate of AFI was at the expense of high false positive lesion detection. The use of AFI could improve the overall yield of dysplasia, but could not replace random biopsy sampling.

CHAPTER 6

AN INTER-OBSERVER AGREEMENT STUDY OF AUTOFLUORESCENCE ENDOSCOPY IN BARRETT'S OESOPHAGUS AMONG EXPERT AND NON-EXPERT ENDOSCOPISTS

Mannath J, Subramanian V, Telakis E, Lau K, Ramappa V, Wireko M, Kaye PV,
Ragunath K. Dig Dis Sci. 2013 Feb; 58(2):465-70

6.1 Abstract

Background

Autofluorescence imaging (AFI) is a 'red flag' technique during Barrett's surveillance to identify subtle abnormal lesions. AFI is associated with significant false positive results, but the reported sensitivity is high. The aim of this study was to assess the inter-observer agreement (IOA) in detecting AFI positive lesions and to assess the overall accuracy of AFI.

Materials and methods

Anonymised AFI and high resolution white light (HRE) images were prospectively collected. The AFI images were presented in random order, followed by corresponding AFI+HRE images in a second folder. Three AFI experts and 3 AFI non-experts scored images after a training presentation. The IOA was calculated using kappa and accuracy was calculated with histology as gold standard.

Results

74 sets of images were prospectively collected from 63 patients (48 males, mean age 69). The IOA for number of AF positive lesions was fair when AFI images were presented. This improved to moderate when corresponding AFI and HRE images were presented (experts 0.57 [0.44-0.70], non-experts 0.47 [0.35-0.62]). The IOA for the site of AF lesion was moderate for experts and fair for non-

experts using AF images, which improved to substantial for experts (k 0.62 [0.50-0.72]) but remained at fair for non-experts (k-0.28 [0.18-0.37]) with AFI+HRE.

Among experts, the accuracy of detecting dysplasia was 0.76 (0.7-0.81) using AFI images and 0.85 (0.79-0.89) using AFI+HRE images. The accuracy was 0.69 (0.62-0.74) with AFI images alone and 0.75 (0.70-0.80) using AFI+HRE among non-experts.

Conclusion

The IOA for AF positive lesions is fair to moderate using AFI images which improved with addition of HRE. The overall accuracy of identifying dysplasia was modest which was better when AFI and HRE images were combined.

6.2 Introduction:

Regular endoscopic surveillance in Barrett's oesophagus (BO) is recommended to detect dysplastic changes or early cancer at a curable stage which in turn could improve the prognosis^{126, 209}. These dysplastic lesions are often difficult to identify with conventional endoscopy and various image enhanced techniques are now available. Autofluorescence imaging (AFI) endoscopy is a relatively new technique which utilises the endogenous fluorophores of the gastrointestinal tract. When a light of short wavelength interacts with these fluorophores, they emit light of longer wavelength. A composite pseudo colour image is formed by the processor of the endoscope using the emitted light⁸³. Earlier studies in Barrett's oesophagus have shown that, AFI has a high sensitivity in diagnosing dysplastic areas in Barrett's oesophagus. The abnormal areas are seen in 'magenta' or 'purple' colour compared to the normal tissue in 'green' colour depicting the absorption spectrum of haemoglobin. However, the specificity of AFI was low with significant false positive rates in all the studies^{86, 171, 207, 210}. The AFI is thus predominantly used as 'red flag' technique to highlight suspicious areas which could then be closely observed with HRE or NBI with magnification to look at the vascular and pit patterns^{76, 199}. There is limited data on what constitutes an abnormal area in the AFI as there are various factors which could cause false positive signals. Previous studies have shown that a 'purple' colour area away from gastro-oesophageal junction, which is opaque and ill defined, might suggest dysplasia²⁰⁸. AFI is an easy to use technique in regular surveillance of Barrett's and potentially can pick up flat and inconspicuous dysplasia. We aimed to assess

the inter-observer agreement in detecting AF positive lesions among AFI experts and AFI non-experts. We also aimed to assess the diagnostic accuracy of dysplasia using AFI images between these groups.

6.3 Methods

6.3.1 Patients

Patients included in this study were those undergoing routine Barrett's surveillance and those referred to our centre for dysplasia work up and management. All patients were included in various single centre and multicentre ethically approved Barrett's trials involving imaging and endotherapy. This study conforms to the ethical guidelines of the World Medical Association Declaration of Helsinki ²¹¹ and signed informed consent was obtained from all patients prior to the procedure. The endoscopic images were obtained by experienced endoscopists and were stored as high quality anonymised JPEG images in our central database. Corresponding biopsy specimens were taken from areas of interest which was imaged.

6.3.2 Endoscopic equipment

High resolution endoscopes GIF Q240 FZ and GIF Q260 FZ (Olympus Keymed, UK) with a Olympus Lucera spectrum processor (Olympus Keymed, UK) equipped with a red, green and blue (RGB) sequential illumination xenon light source (XCLV-260HP), RGB filters and a high definition television monitor (Olympus OEV181H) were used for the procedures. These endoscopes have an

additional autofluorescence chip at the tip. The operator could easily alternate between white light endoscopy and AFI by pressing a button on the hand control. When AFI is switched on, the mucosa is sequentially excited with blue light (390-470 nm) and green light (540-560 nm). A barrier filter placed in front of the AFI CCD allows only passage of fluorescence light with a wavelength between 500 and 630 nm after blue light excitation and of the green reflected light after green light excitation. The video processor subsequently constructs a pseudo colour image on the basis of the total AF and green reflectance²⁰⁸.

6.3.3 Endoscopic procedure

All endoscopies were done under topical anaesthesia with 2% lignocaine spray or sedation using midazolam or diazepam with or without pethidine. During endoscopy, any suspicious areas are noted and separately sampled after capturing high quality HRE and AFI images (using a Sony BZMD-1 DICOM Capture station or Sony HD Video GV-HD700E). Non-suspicious areas in BO are also imaged prior to random sampling. These images are stored as JPEG files (300 kb, 1280 X 1024 pixel array and 32-bitcolour). All images were then anonymised and added to a database with corresponding HRE and AFI images of each area.

6.3.4 Selection of images for the study

The images for this study were selected from the database (total of 447 images, HRE=211, AFI= 236,) by a single endoscopist based on image quality, number of lesions, availability of corresponding set of AFI and HRE images for the same area and histological diagnosis. Images showing large lesions and obvious

cancers were excluded from the study. These images were imported into a training power point presentation (Microsoft Power Point 2007, Redmond, WA) and two separate folders containing AFI images alone and corresponding AFI and HRE images were inserted into Microsoft power point in a random fashion. All images were anonymised, presented without any changes to the original images and were of the same size and resolution.

6.3.5 Image evaluation

Three endoscopists experienced in advanced imaging (KR, VS, and ET) each of whom had done more than 200 advanced imaging procedures using AFI (AFI experts) and 3 experienced endoscopists (MW, KL, and VR) with no prior experience of AFI (AFI non-experts) but with significant experience in Barrett's surveillance using HRE (> 150 procedures) took part in the assessment of the anonymised images. Before starting the image evaluation a short automated power point presentation was provided to each endoscopist showing images of non-dysplastic Barrett's oesophagus, false positive AFI areas (non-dysplastic) and true positive AFI areas (dysplastic), in both HRE and AFI modes.

After the training, all endoscopists independently assessed all images (74 AFI and 74 corresponding AFI and HRE) presented in a random order. The endoscopists were instructed to record the findings *a priori* including a) presence of any abnormal AFI signal (positive), b) site of abnormal AFI signal, c) whether dysplastic or not, and d) Quality of images on a visual analogue scale of 1-10. Finally the HRE and AFI images from corresponding regions were displayed as

pairs and similar questions were repeated. Endoscopists were asked to answer these questions based on AFI images alone and were not asked to rate HRE images. All data were inserted into a separate Microsoft excel file by each endoscopist, which were analysed. The endoscopists were blinded to the histological diagnosis of these patients.

6.3.6 Histological assessment

Targeted biopsies were taken from abnormal areas as seen in AFI or HRE and in cases where there were no obvious mucosal abnormalities; random four quadrant biopsies were taken every 2 cm from the entire Barrett's mucosa. Random biopsies were also taken even if there were abnormal areas targeted. The specimens are fixed in 10% formalin and sent for histopathological assessment. The specimens were assessed by a specialist gastrointestinal pathologist (PVK) and in cases of dysplasia, by two different gastro-intestinal pathologists. The histopathological reporting was done according to Vienna classification ¹⁷³.

6.3.7 Statistical analysis

The inter-observer agreement was expressed by the percentage of overall agreement among all observers, AFI experts and AFI non-experts as well as by an overall kappa (κ) statistic with 95% confidence interval ²¹². The interpretation of κ -values was done according to the values provided by Landis and Koch who characterised values < 0 as indicating no agreement and 0–0.20 as slight, 0.21–0.40 as fair, 0.41–0.60 as moderate, 0.61–0.80 as substantial, and 0.81–1 as almost perfect agreement ²¹³. Bootstrapping techniques (k=2000 bootstrap samples) was

used to obtain a bias corrected confidence intervals²¹⁴. On account of the correlated nature of the data we used bootstrapping techniques (k=2000 bootstrap samples) to obtain P values for differences in κ -values between experts and non-experts. Stata version 9 (Stata Corporation, College Station, Texas) and PASW® version 17 (SPSS Inc, Chicago, Illinois) were used for the analysis. Continuous outcomes variables are given as mean \pm standard deviation and were analysed using the t test. P < 0.05 was considered statistically significant. Sensitivity, specificity and accuracy were calculated with histopathology as gold standard. For analytical purposes LGD was grouped with non dysplastic Barrett's and HGD/IMC was analysed as dysplastic Barrett's.

6.4 Results

74 sets of anonymised images of AFI and HRE were collected from 63 patients (males 48, mean age 69). The histopathological diagnosis in these 74 sets were; Intramucosal cancer (IMC) =16, High grade dysplasia (HGD) =16, Low grade dysplasia (LGD) =11, and Non-dysplastic Barrett's (NDBO) =31.

6.4.1 Number of AF positive lesions

The inter-observer agreement (IOA) (kappa) for number of true AFI positive lesions when only AFI images were shown was fair for all observers, experts and non-experts which improved to moderate when both AFI and HRE images were shown. Percentage of full agreement is shown in Table 1.

Table 1: Inter-observer agreement κ (95% CI) for the number of AF positive lesions

	AFI κ(95% CI)	Full agreement AFI (%)	AFI + HRE κ(95% CI)	Full agreement AFI+HRE (%)	P value
All observers	0.301 (0.235- 0.384)	16	0.484 (0.401- 0.584)	38	0.002
Experts	0.392 (0.272- 0.518)	46	0.567 (0.443- 0.700)	65	0.044
Non-experts	0.259 (0.142- 0.381)	36.5	0.473 (0.347- 0.615)	61	0.02
P value	0.08		0.32		

AFI-Autofluorescence imaging, HRE-High resolution imaging, κ -Kappa

6.4.2 Site of AF positive lesions

The kappa for all observers for the site of AF positive lesion was 0.392 (95% CI 0.316-0.474) with AFI images alone which improved to 0.435 (95% CI 0.358-0.518) with corresponding AFI + HRE images. Among experts, the kappa for site of AF positive lesion was moderate which was significantly higher than non-experts ($P=0.01$) when AFI images were presented. When corresponding AFI + HRE images were shown, kappa for experts improved to substantial ($k = 0.615$ [95% CI 0.498-0.721]), but remained at fair for non-experts ($k= 0.275$ [95% CI 0.182-0.377]). Percentage of full agreement is shown in Table 2.

6.4.3 Inter-observer agreement for dysplasia

The IOA for presence of high grade dysplasia or early cancer was moderate ($k = 0.410$ [95% CI 0.300-0.527]) for all observers with AFI images which improved to substantial ($k= 0.614$ [95% CI 0.509-0.717]) with corresponding AF and white light images. Among experts, the kappa with AFI images alone was 0.492 (moderate, 95% CI 0.339-0.654) and 0.781 (substantial, 95% CI 0.646-0.874) with combined AFI + HRE images. Among non-experts, the kappa with AFI images alone was 0.381 (95% CI 0.225-0.551) and 0.478 (95% CI 0.333-0.627) with AFI + HRE images. Percentage of full agreement is shown in Table 3.

Table 2: Inter-observer agreement κ (95% CI) for the site of AF positive

lesions

	AFI κ(95% CI)	Full agreement AFI (%)	AFI + HRE κ(95% CI)	Full agreement AFI+HRE (%)	P Value
All observers	0.392 (0.316- 0.474)	15	0.435 (0.358- 0.518)	15	0.45
Experts	0.478 (0.372- 0.595)	45	0.615 (0.498- 0.721)	62	0.09
Non-experts	0.276 (0.167- 0.384)	24	0.275 (0.182- 0.377)	20	0.98
P value	0.01		<0.001		

AFI-Autofluorescence imaging, HRE-High resolution endoscopy, K-Kappa

Table 3: Inter-observer agreement κ (95% CI) for dysplasia

	AFI κ(95% CI)	Full agreement AFI (%)	AFI + HRE κ(95% CI)	Full agreement AFI+HRE (%)	P value
All observers	0.410 (0.300- 0.527)	38	0.614 (0.509- 0.717)	57	0.01
Experts	0.492 (0.339- 0.654)	62	0.781 (0.646- 0.874)	84	0.004
Non-experts	0.381 (0.225- 0.551)	57	0.478 (0.333- 0.627)	64	0.38
P value	0.33		0.001		

AFI-Autofluorescence imaging, HRE-High resolution endoscopy, k-kappa

Table 4: Sensitivity, specificity and accuracy (95% CI) of dysplasia with histology as gold standard

	Experts		Non-experts		All observers	
	AFI	AFI + HRE	AFI	AFI + HRE	AFI	AFI + HRE
Sensitivity	0.75 (0.68 – 0.81)	0.84 (0.78 – 0.89)	0.56 (0.49 – 0.62)	0.64 (0.57 – 0.69)	0.66 (0.6- 0.7)	0.74 (0.69- 0.78)
Specificity	0.76 (0.71 – 0.81)	0.85 (0.80 – 0.89)	0.78 (0.72 – 0.83)	0.83 (0.78 – 0.88)	0.77 (0.73- 0.8)	0.84 (0.81- 0.87)
Accuracy	0.76 (0.70 – 0.81)	0.85 (0.79 – 0.89)	0.69 (0.62 – 0.74)	0.75 (0.70 – 0.80)	0.72 (0.68- 0.76)	0.8 (0.76- 0.83)

AFI-Autofluorescence imaging, HRE-High resolution endoscopy

6.4.4 Accuracy of dysplasia detection

Using histopathology as gold standard the sensitivity and specificity for dysplasia detection was calculated. Among experts, the sensitivity and specificity was 0.75 (95% CI 0.68-0.81) and 0.76 (95% CI 0.71-0.81) when AFI images were used alone. When both AFI and IIRE images were shown together, the sensitivity and specificity improved to 0.84 (95% CI 0.78-0.89) and 0.85 (95% CI 0.80-0.89). Among non-experts the sensitivity and specificity were 0.56 (95% CI 0.49-0.62) and 0.78 (95% CI 0.72-0.83) with AFI images alone. The sensitivity and specificity were 0.64 (95% CI 0.57-0.69) and 0.83 (0.78-0.88) when AFI + HE images were presented among non-experts. The overall accuracy is shown in Table 4.

6.4.5 Quality of AFI images

The overall quality of AFI images on a visual analogue score of 1-10 (1=Poor, 10=Best) were 6.27 ± 1.64 (mean \pm SD) for all observers when AFI images were presented on its own. For experts, the mean VAS score was 6.44 ± 1.53 and for non-experts it was 6.1 ± 1.73 . When AFI + HRE images were shown the mean (\pm SD) VAS scores for AFI images for all observers, experts and non-experts were 6.83 ± 1.62 , 6.65 ± 1.3 , 7 ± 1.87 respectively.

6.5 Discussion

This study has directly assessed the inter-observer agreement of AFI positive lesions in patients with BO and has ascertained the accuracy of detection of high

grade dysplasia and early cancer with histology as gold standard. This image enhanced technique is user friendly and is used as a 'red flag' technique during BO surveillance. It is important to assess the IOA among experts and non-experts in identifying such abnormal areas to understand the value of this technique in routine clinical practice. The predictive factors for dysplasia in AFI were studied earlier and the investigators found that abnormal AF signals (magenta or purple) with opaque AF intensity and mucosal abnormalities in HRE images are highly suggestive of dysplasia. They also found that abnormal AF signals in proximity to gastric folds are likely to be false positive²⁰⁸. We included these three criteria in the training session along with presenting other common false positive signals in the context of scarring, inflammation and squamous mucosal islands to prevent reporting false positive areas.

The consistent finding is the improvement in IOA and dysplasia detection by experts and non-experts when combined AFI and HRE images were shown. This finding is in agreement with the previously discussed study²⁰⁸. The clinical importance is that, switching between AFI and HRE is essential in real time endoscopy. However, the likelihood of dysplasia in the presence of an abnormal AFI signal and normal HRE findings needs to be ascertained in prospective studies. Also, the value of AFI imaging in itself as a tool for BO surveillance is questionable and should be combined with HRE. It is very easy for the operator to switch back and forth between AFI and HRE and the suspicious areas should be carefully examined by both modalities.

The non-experts demonstrated a low agreement on the number of AF positive signals and the site of AF positive areas compared to experts. This indirectly indicates a learning curve. A previous study indicated that NBI in differentiation of colonic polyps could be learned in 20 minutes by didactic lecturing²¹⁵. In our study, a power point presentation for 15 minutes does not seem to be sufficient to improve the IOA and accuracy of AFI in dysplasia detection. This needs to be clarified in prospective study with definitive aim directed towards it.

The AFI non-experts have significant experience in Barrett's surveillance using HRE only. This might explain the statistically significant improvement in the IOA of number of AF positive lesions when both AFI and HRE images were shown compared to AF images alone. Nonetheless, there was no significant improvement in the IOA of site of AF positive lesions or dysplasia with combined images. This reflects the learning curve in identifying the areas of true positive AFI signals. This argument is strengthened by the fact that, AFI experts significantly improved IOA when HRE were added.

There was no significant difference between experts and non-experts in the reported quality of AFI images and the VAS score was above average. This could be due to selection bias as only good images were selected for the study. The AFI experts however, scored the images similar to that of non-experts.

The strength of this study is that 3 expert and 3 non-expert endoscopists participated in the study with a comparable number of dysplastic and non-dysplastic Barrett's images. The overall accuracy of dysplasia among experts was

good at 0.76 with AFI images and 0.85 with AFI+HRE images. This indicates that the technique is valuable in correctly identifying dysplasia by experts. However, no comparison was done between HRE and AFI and thus results does not reflect that AFI is better than HRE in indentifying dysplasia. Nevertheless, the combined use of AFI and HRE seems to be of value in the context.

The quality of images assessed by both experts and non-experts were between 6.27-7.0 (mean) on a VAS scale of 1-10. Arguably, an improvement in quality of images could improve the IOA and possibly the identification of dysplasia. Further studies with improved quality of images are necessary to ascertain this.

6.5.1 Limitations of the study

As with many previous inter-observer studies, endoscopic images were used in this study. This does not reflect routine clinical practice where real time images are displayed on high definition monitors. However, in real time, many endoscopists assess the abnormal areas by freezing the images and this was mimicked in our study. Video clips of the relevant areas would have been a better way of assessment.

The sensitivity and specificity is assessed using targeted histology as gold standard. Random biopsies were taken if there were no abnormal areas to target. This does not reflect the true sensitivity and specificity of the modality as there is significant sampling error in Barrett's and occult dysplasia would have been overlooked. The other limitation of the study is that for analytical purposes we have included low grade dysplasia along with non-dysplastic Barrett's as there are

no definitive AFI abnormalities described in cases of LGD. This study was done in enriched population and thereby is not a true reflection of Barrett's surveillance. The images were selected from a database of images and only good quality of images was selected. Also, there is no time pressure on endoscopists to comment on images unlike in real time settings.

Considering the facts that this study was done using selected images and not a real time study, focused on dysplasia identification rather than detection and the significant but modest accuracy of dysplasia, it would not be possible to recommend AFI for routine use in Barrett's surveillance

6.5.2 Conclusions

The inter-observer agreement for AF positive lesions is fair to moderate using AFI images which improved with addition of HRE. The overall accuracy of dysplasia identification using AFI images was modest, but was better among experts and with combined AFI and HRE images. Better understanding of what constitutes an AF positive signal and improvement in technology to increase the quality of images could enhance the value of this endoscopic technique in BO surveillance.

CHAPTER 7

UTILITY OF AN AUTOFLUORESCENCE INDEX TO DETECT EARLY NEOPLASIA IN BARRETT'S OESOPHAGUS; A PILOT STUDY

7.1 Abstract

Background

Auto-fluorescence imaging (AFI) endoscopy is a novel imaging technique that can identify neoplastic tissue by highlighting differences in tissue fluorescence properties and detect early neoplasia not detectable by conventional white light endoscopy. Although it has a high sensitivity, it is associated with a high false positive rate up to 80%

Aims

To determine if autofluorescence index defined as the ratio of the intensity of red and green tone between normal and abnormal AFI areas in patients with Barrett's oesophagus (BO) can improve the specificity and accuracy of AFI endoscopy.

Methods

Images of patients with both AFI true and false positive areas of BO were selected from a prospectively collected dataset using the Olympus Lucera-Hyperpro prototype video endoscopy system and GIF Q240FZ gastroscope. Biopsies from these areas had been confirmed by an experienced GI pathologist. The intensity of the red and green tone at the abnormal and 2 separate normal areas were read blinded using the NIS Elements AR 2.30 imaging software (Nikon instruments, Japan). Statistical analysis was done using SPSS version 16 (SPSS Inc, USA).

Results

There were 82 images of AFI abnormalities. Of these 19 had high grade dysplasia (HGD), 18 had carcinoma (Ca), 38 had specialised intestinal metaplasia without dysplasia (SIM) and 7 were that of columnar epithelium without SIM. The area under the receiver operating curve (AUROC) for the auto-fluorescence index (AF index) was 0.881 (95% CI 0.81-0.95) and 0.91 (95% CI 0.84-0.97) when utilising the two different normal AFI areas respectively for calculating the index. The two separate readings made were highly correlated (Spearman's rho 0.82). Using an AF index cut off of 1.32 the sensitivities for readings 1 and 2 were 92% (95% CI 82-99) and 95% (95% CI 85-99) respectively, specificities were 76% (95% CI 67-80) and 62% (95% CI 54-65).

Conclusions

The AF index shows promise as a tool to improve the diagnostic capabilities of AFI endoscopy. Further prospective studies with real time determination of the ratio during video AFI endoscopy will serve to confirm its utility in clinical practice.

7.2 Background

Oesophageal adenocarcinoma (OA) has the fastest rising incidence in the western world and Barrett's oesophagus is the only known precursor lesion. The incidence of OA has increased 4-6 folds over the past 4 decades^{216,217}. When diagnosed at an advanced stage, OA has a poor prognosis²¹⁸. Early detection of lesions will facilitate endotherapy or surgery and improve the prognosis. Due to this reason regular surveillance of BO is recommended²¹⁹. In recent years, various advanced endoscopic imaging techniques have facilitated the assessment and early detection of lesions. Autofluorescence imaging (AFI) is a technique which can potentially differentiate dysplastic from non-dysplastic areas in BO. Normal and neoplastic tissues have different characteristics in AFI⁷⁸. The initial use of AFI was limited to autofluorescence spectroscopy and use of fibre optic endoscopes. However these modalities produced poor picture quality of white light imaging. The new generation of AFI endoscopes has two high resolution chips, one for the white light and one for the autofluorescence imaging. The non-dysplastic area of the BO appears 'green' and the dysplastic areas appear 'pink or magenta'. However most of the studies with the new system have reported a high false positive rates ranging from 40% to 80%^{84,86}. The additional use of NBI has found to reduce this false positivity.

We investigated to identify an autofluorescence index which could enable to differentiate the truly dysplastic areas from false positive areas in AFI images.

7.3 Methods

7.3.1. Images

AFI images from dysplastic and non dysplastic Barrett's, which were prospectively collected, were retrieved from existing database. All lesions were confirmed by target biopsies as to whether they harbor dysplasia. The criteria for selecting the images were a) adequate AFI image quality for analysis, b) the lesions seen were correlated with white light images, c) target biopsies were reviewed by a gastrointestinal pathologist, and d) only images with non dysplastic BO or that with early neoplasia.

7.3.2 Endoscopy system

The autofluorescence endoscope (XGIF-240FZ, Olympus, Tokyo, Japan) has 2 separate CCDs, one for WLE and one for AFI. The system uses sequential red-green-blue illumination for WLE. While using the AFI system, the mucosa is sequentially excited with blue light (390-470 nm) and green light (540 nm-560 nm). A blue light filter is placed in front of the AFI CCD to allow only passage of reflected fluorescence light with a wavelength between 500 and 630 nm after blue light excitation and of the green reflected light after green light excitation. The video processor (XCV-260 HP3P, Olympus) receives the reflected light and constructs a pseudo colour image on the basis of the total autofluorescence and green reflectance. The pseudo colour image is produced by allocating the AF signal to the green (G) channel and the reflected signal of green light to the red (R)

and blue (B) channels in a 1 to 0.5 ratio²²⁰. Non dysplastic Barrett's epithelium appears green during AFI, whereas suspicious areas appear red or magenta.

7.3.3 Image analysis

Digital images of AFI positive areas were captured using a digital video cassette recorder (Sony Mini DV GV-D100e PAL; Sony Corp., Tokyo Japan) and were stored as JPEG files (200-300kb, 1280 x 1024 pixel array and 32 bit colour). Gamma corrected images were analysed using NIS Elements AR 2.30 imaging software (Nikon instruments, Japan). All analysis was done blinded to the histopathological diagnosis. The region of interest, which shows low intensity signal (red or magenta), was traced using the software. The intensity of the red tone and green tone were calculated at this area. Two normally appearing areas (green) away from the suspected area were also traced. The mean red tone intensity and green tone intensity of both these areas were also calculated. The ratio of red tone to green tone (AF ratio) in the abnormal area to that of normal areas was pragmatically considered as the autofluorescence index (AF index). Two different sets of values obtained using the abnormal area and two normal areas in this manner.

7.3.4 Statistical analysis

Diagnostic test statistics of sensitivity, specificity, and predictive values were calculated by using histopathology determination as the gold standard. Statistical analysis was done using SPSS version 16 (SPSS Inc, USA). The two separate readings of AF indices were correlated using Spearman's rank correlation

coefficient. Receiver operating curves (ROC) analysis was used to find optimal cut off values for assessing dysplastic areas. Area under the receiver operating characteristic curve (AUROC) was obtained plotting the sensitivity on the X axis and 1-specificity on the Y axis for both sets of recordings.

7.4 Results

There were 82 images of AFI abnormalities which were selected as per the criteria taken from 49 patients with BO (40 males, median age 68 years (IQR 57-76)). 19 images were from areas of high grade dysplasia (HGD), 18 from areas of cancer, 38 from non dysplastic Barrett's with specialised intestinal metaplasia and 7 were that of columnar epithelium. The AF index was calculated using the AF positive area and 2 normal background areas. The results were plotted to obtain a ROC (figure 1). The area under the receiver operating curve (AUROC) for the auto-fluorescence index was 0.881 (95% CI 0.81-0.95) and 0.91 (95% CI 0.84-0.97) when utilising the two different normal AFI areas respectively for calculating the index (table 1). The two separate readings made were highly correlated (Spearman's ratio 0.82). Using the ROC curve, optimal AFI index cut off of 1.32 was derived, which represents a sensitivity of 86% and specificity of 88%.

The AF index value of 1.32 was used to define the sensitivity and specificity of the 82 images with histology as gold standard. The sensitivities for readings 1 and 2 were 92% (95% CI 82-99) and 95% (95% CI 85-99) respectively, specificities were 76% (95% CI 67-80) and 62% (95% CI 54-65) and likelihood ratio of a positive test was 3.8 (95% CI 2.5-4.6) and 2.5 (95% CI 1.9-2.8). None of the

cancers and only 3 and 2 HGD's respectively were misclassified by the AFI index of 1.32.

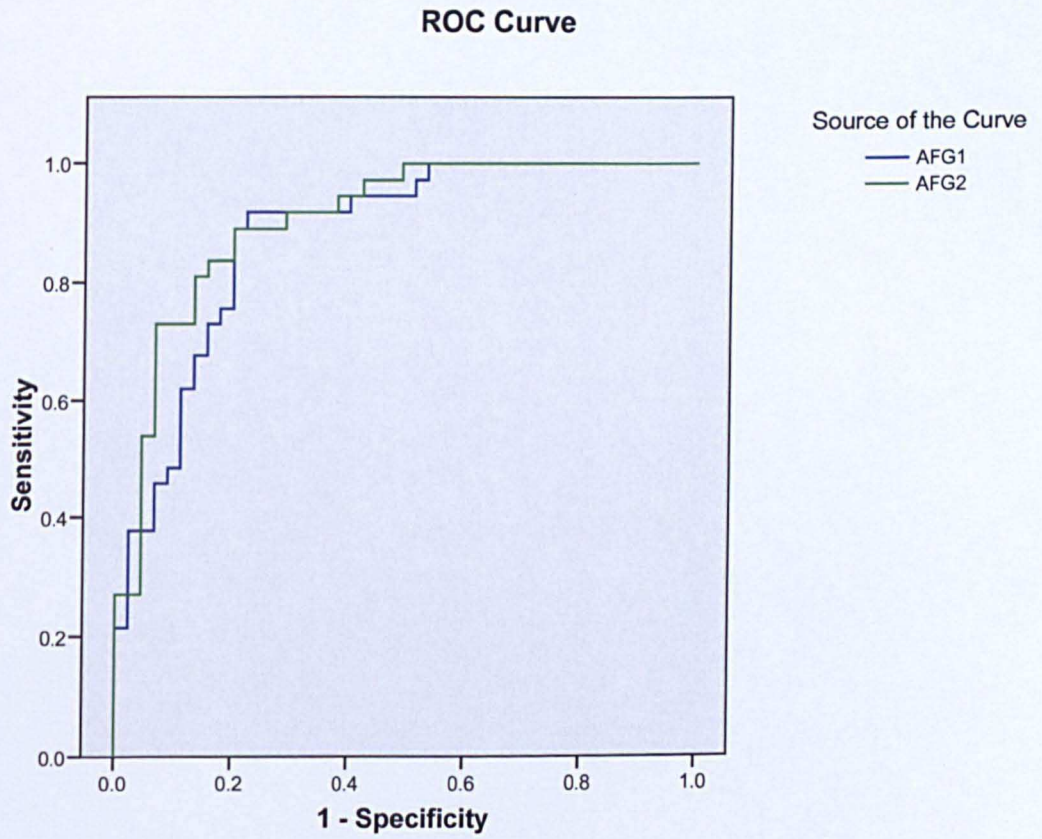


Figure 1: ROC of two different sets of autofluorescence index ratios

Coordinates of the ROC Curve

Test Result Variable: Autofluorescence index ratios

Autofluorescence index ratio	Sensitivity	1 - Specificity
-.8438	1.000	1.000
.3815	.973	1.000
.6120	.973	.978
.7668	.973	.956
.9664	.973	.933
1.0218	.973	.911
1.0364	.973	.889
1.0461	.973	.867
1.0474	.973	.844
1.0514	.973	.822
1.0567	.973	.800
1.0613	.973	.778
1.0676	.973	.756
1.0799	.973	.733
1.0892	.973	.711
1.0937	.973	.689
1.1025	.973	.667
1.1138	.973	.644
1.1284	.973	.622
1.1451	.973	.600
1.1554	.973	.578
1.1619	.973	.556
1.1791	.973	.533
1.1931	.946	.533
1.1946	.919	.533
1.1957	.919	.511
1.2155	.892	.511
1.2366	.892	.489
1.2397	.892	.467
1.2411	.892	.444
1.2477	.892	.422
1.2542	.892	.400
1.2622	.865	.400
1.2801	.865	.378
1.2921	.865	.356
1.2957	.865	.333
1.2989	.865	.311
1.3007	.865	.289
1.3038	.865	.267
1.3119	.865	.244
1.3280	.865	.222
1.3466	.838	.222
1.3566	.838	.200
1.3687	.811	.200
1.3798	.784	.200
1.3810	.757	.200
1.3853	.730	.200
1.3933	.703	.200
1.4068	.703	.178

Autofluorescence index ratio	Sensitivity	1 - Specificity
1.4191	.703	.156
1.4376	.676	.156
1.4550	.649	.156
1.4624	.649	.133
1.4696	.622	.133
1.4739	.595	.133
1.4773	.595	.111
1.4990	.568	.111
1.5422	.541	.111
1.5653	.514	.111
1.5809	.486	.111
1.5978	.486	.089
1.6077	.459	.089
1.6206	.459	.067
1.6347	.432	.067
1.6565	.405	.067
1.6827	.378	.067
1.7133	.378	.044
1.7334	.378	.022
1.7368	.351	.022
1.7795	.324	.022
1.8377	.297	.022
1.8655	.270	.022
1.8775	.243	.022
1.8790	.216	.022
1.8976	.216	.000
1.9286	.189	.000
1.9692	.162	.000
2.0069	.135	.000
2.0439	.108	.000
2.1091	.081	.000
2.1803	.054	.000
2.6582	.027	.000
4.1038	.000	.000

Table1: Coordinates of the receiver operating characteristic curve showing the sensitivity and 1-specificity for various autofluorescence index ratios of one set of recordings.

7.5 Discussion

AFI exploits differences in fluorescence properties of normal and abnormal gastrointestinal mucosa and facilitates the detection of early pre-invasive cancer. Although AFI is highly sensitive, it is associated with a very high false positive rate which can lead to excessive biopsies, longer procedure time and greater costs. Clinical studies have shown that as high as 75% of lesions with abnormal fluorescence were false positive when correlated with histology^{86, 171}. In this study we have shown that an autofluorescence index might be of value in differentiating dysplastic areas from non dysplastic BO. The sensitivity, specificity, and predictive values were calculated for several autofluorescence index ratios and, by using the ROC, a value of 1.32 was chosen as the best value to separate dysplastic area from a non-dysplastic area. This will help in reducing the high false positive rates associated with a subjective examination of the autofluorescence. The current system of autofluorescence video endoscopy does not provide an in vivo measurement of AF index and we hypothesised that there is a biological plausibility of increase in the index with increasing dysplasia. Thus, a cut off index ratio would be helpful to differentiate between normal and dysplastic areas. Light induced fluoroscopy system (LIFE) was used in the past to differentiate adenomatous polyps from non-adenomatous polyps using an index. They found cut off value of 2.3 for their index, which has a sensitivity and specificity 85% and 81%²²¹. However this system produced poor quality images and is outdated now by the video autofluorescence endoscopy system. In the fibre optic system it was

possible to do the measurements of the index in vivo, producing immediate results to take clinical decisions.

This study has a few limitations. The images were retrieved from a pre collected database and only those with good quality were obtained. There is selection bias involved in this. Also, the images are from patients referred to a tertiary referral centre and do not represent the true Barrett's surveillance population, causing referral bias. Moreover the images are gamma corrected and pseudo colour images. The value of in vitro assessment using image analysis software might not represent a clinical scenario. Also, as a pilot study, we have used a dataset to derive a cut off value of autofluorescence index and used this value on the same dataset for validation. The assessment of such an index is incomplete without validating in a different dataset. Nonetheless, we have identified a method to improve the diagnostic specificity of this emerging technology which is used currently as a 'red flag' system than a diagnostic method by itself due to the high false positive results. More studies using images from a prospective cohort would provide a better understanding of the index, which in the future could be incorporated into the endoscopy system to enable better in vivo diagnostic accuracy.

CHAPTER 8

CORRELATION OF QUANTITATIVE MEASURES OF

AUTOFLUORESCENCE FROM VIDEO

AUTOFLUORESCENCE ENDOSCOPY WITH

COLLAGEN AND ELASTIN AND CHANGES OVER

WITH TIME IN A MOUSE MODEL OF COLON

CANCER (APC^{MIN} MICE)

8.1 Introduction

The theory of autofluorescence is based on the presence of natural fluorophores in the gastrointestinal tract. When light of a specific wavelength is focussed on tissue, several interactions occur at the cell interface. The light (consisting of photons) could be either reflected at the cell surface or penetrate the tissue and get absorbed by chromophores. The main chromophore in tissue which absorbs the visible wavelength of light is haemoglobin. Absorption of light occurs both with oxygenated or deoxygenated forms of haemoglobin ^{77,222}. The third outcome from the interaction of light and tissue is absorption of the light followed by light of a longer wavelength being emitted by the tissue: a phenomenon termed as autofluorescence. During white light endoscopy, reflection and absorption are the main interactions between light and tissue. During white light video endoscopy in patients with Barrett's oesophagus, the mucosa appears 'salmon' pink in colour as most of the red light is reflected, but on the other hand green and blue light are absorbed by chromophores in the tissue.

Fluorophores are biological substances which emit longer wavelengths (fluorescent light) when excited by short wavelength light such as blue light. Some of the fluorophores which are thought to be responsible for tissue autofluorescence include collagen, aromatic amino acids, nicotinamide adenine nucleotide (NADH) and porphyrins ⁷⁷. However, this phenomenon is poorly understood. The changes in fluorescent properties in normal, metaplastic and dysplastic tissue would vary due to the different types, concentrations and distribution of various fluorophores and chromophores.

The phenomenon of reduced autofluorescence in dysplastic Barrett's compared to non-dysplastic Barrett's was thought to be related to the changes in mucosal thickening. This would attenuate the strong fluorescence from collagen rich sub-mucosa. An ex-vivo study on snap-frozen mucosal biopsies from patients with Barrett's oesophagus scanned with confocal fluorescence microscopy showed that both dysplastic and non-dysplastic epithelium showed predominantly green fluorescence. The main source of the fluorescence was from both cytoplasm and lamina propria²²³. Contrary to this, clinical studies have shown reduced autofluorescence in dysplastic Barrett's compared to non-dysplastic Barrett's. There are various mechanisms proposed as to the cause for this⁷⁷;

1. The nuclear-cytoplasmic ratio increases in dysplastic cells and nuclei have little or no autofluorescence properties compared to cytoplasm
2. The dysplasia is associated with increased mucosal thickness which would prevent the light from penetrating into the submucosal layer where the abundant collagen is thought to have the highest fluorescence in gastrointestinal tract
3. An increased concentration of tissue haemoglobin in the mucosal layer associated with dysplastic process attenuates the autofluorescence

This study was aimed to understand the biological basis and role of collagen and elastin in the process of autofluorescence

8.2 Materials and methods

8.2.1 Endoscopic equipment

The autofluorescence endoscope (GIF-240FZ, Olympus, Tokyo, Japan) has 2 separate CCDs, one for WLE and one for AFI and the process of producing autofluorescence image is described in chapter 7 under materials and methods.

The video processor (XCV-260 HP3P, Olympus) receives the reflected light and constructs a pseudo colour image on the basis of the total autofluorescence and green reflectance.

8.2.2 Mouse colon cancer model (APC^{min} mouse)

Formalinised colonic specimens from Apc^{min} mice were used for this study as there are currently no acceptable animal models for Barrett's neoplasia. Familial adenomatous polyposis is a rare condition associated with multiple gastrointestinal polyposis and nearly 100% risk of colorectal cancer in humans. This is caused by a germline mutation in the adenomatous polyposis coli (APC) gene²²⁴. Min (multiple intestinal neoplasia) is a mutant allele of the murine Apc locus, which encodes a nonsense mutation at codon 850²²⁵. These APC^{min} strain are highly susceptible to intestinal adenoma and cancer formation. It is reported that nearly 100% of the APC^{min} heterozygotes who are fed with high fat diet would develop more than 30 adenomas and they die by 120 days²²⁶.

The APC^{min} mice used in the study were taken from a study approved by the Nottingham Research Ethics Committee on the effect of chemo preventive agents

on colonic cancer formation and were in the placebo arm of the study. As part of the ethically approved protocol these mice were sacrificed at 12, 18 and 24 weeks and their colons preserved in formalin for histopathological analysis. These specimens were used for imaging and histopathological studies. No additional mice were sacrificed or used for the purpose of this study. A total of 30 mice colons of which 10 sacrificed at 12 weeks, 10 sacrificed at 18 weeks and another 10 mice colons sacrificed at 24 weeks were used in the study.

8.2.3 Mice colonic imaging

The mice colons were stored in labelled formalin containers with details of the time of sacrifice of the animals. The mice colons were imaged according to the age at sacrifice. 10 each of the colons from 12 weeks, 18 weeks and 24weeks were imaged. These colons were dissected along the length to open the mucosal layer and pinned down to the board exposing the mucosal layer prior to imaging.

The images were obtained using a GIF 240 FZ gastroscope (Olympus medical, Keymed UK) connected to a Olympus Lucera Spectrum processor (Olympus Keymed, UK) with a red-green-blue sequential illumination xenon light (XCLV 260HP) and a high definition monitor (Olympus OEV181H). All images were captured with a Sony HD video GV HD700E and stored as JPEG files (300 Kb, 1280 X 1024 pixel arrays). The original files were used for further analysis without any modification to the resolution of the images. Corresponding white light and autofluorescence images were obtained. Only AFI images were used for further evaluation.

8.2.4 Image analysis using soft ware

A freely downloadable software called ImageJ (Image processing and analysing in Java) version 4.3 (National Institute of Health (NIH), USA) was used to do analysis of the mice colonic autofluorescence images. This software is a public domain java image processing programme which was inspired from NIH image which was developed by research services branch (RSB). The colonic images were opened with ImageJ. They were cropped to include only the colonic part and excluded the mounting board and needle points. The image was split into red, green and blue channels. Free hand technique was used to identify the area of lesion in the red and green channels, followed by marking a similar sized area of the background from the macroscopically normal area on white light imaging in the red and green channels. The autofluorescence ratio and index were then calculated. First of all the red to green ratio of the lesion was measured by dividing the mean colour tone of the lesion in the red channel to that of the mean green channel (AF ratio). Similarly, the red to green ratio of the normal background was measured in the red and green images. The AF ratio of the lesion to the background value was taken as the Autofluorescence index or colour contrast index (CCI)

8.2.5 Staining mice colons for elastin and collagen

The mice colons were stored in formalin after AF imaging and were subsequently embedded into paraffin and cut into sections including the lesions and the background of the imaged colon. These sections were stained with Verhoeff's Van

Gieson (EVG) stain. The principle of this staining technique is not well known. It is hypothesised that hydrogen bond is formed between certain parts of elastic fibre and phenolic group of resorcin in the EVG stain. Elastin is stained blue-black and the collagen fibres appear as red (Figures1-4). The rest of the tissue including muscle fibres would appear yellow.

8.2.6 Quantifying the amount of collagen and elastin with ImageJ

The amount of collagen and elastin was quantified using ImageJ software. A plug-in known as 'threshold colour' plug-in was installed into the software for analysis. The EVG stained colonic images were magnified up to 20 times and were opened by ImageJ. All images were standardised with regards to the resolution and size. The original images were 24 bit in RGB format. For the purpose of analysis, they were changed to 8 bit on the ImageJ software. The images were then analysed using the 'threshold' where the area of interest would appear in red. Prior to measurement it was confirmed that the 'red' area includes both the elastin and collagen as depicted in the original images (stained in red and blue-black) (Figure 5, 6). Analysis was done by 'analyse particles' prompt on the software which provides the measure of the percentage of the total image area covered by the measured object and is termed as area fraction. The area fraction in our analysis is a measure of the area of tissue covering collagen and elastin and represents what fraction of the tissue it comprises.

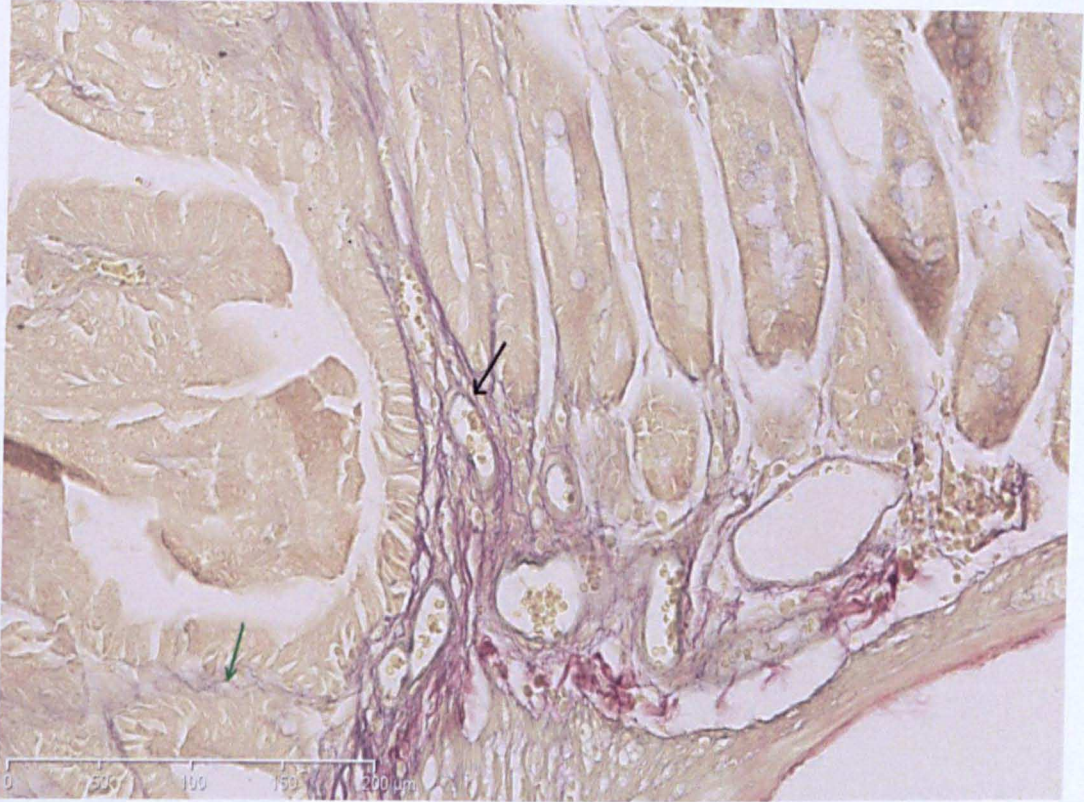


Figure 1: Image of mice colonic lesions stained with EVG, showing collagen stained in red (black arrow) and elastin in blue-black (green arrow)

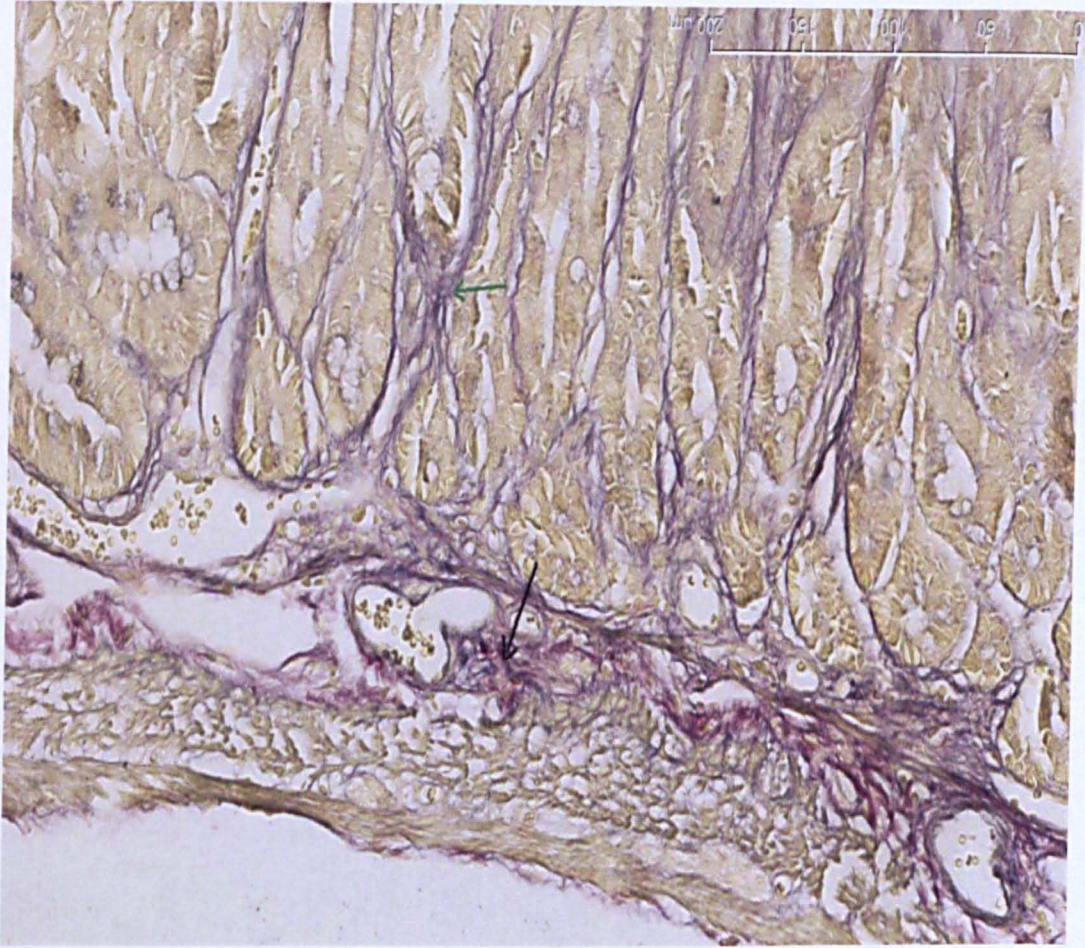


Figure 2: Image of mice colonic lesions stained with EVG, showing collagen stained in red (black arrow) and elastin in blue-black (green arrow)

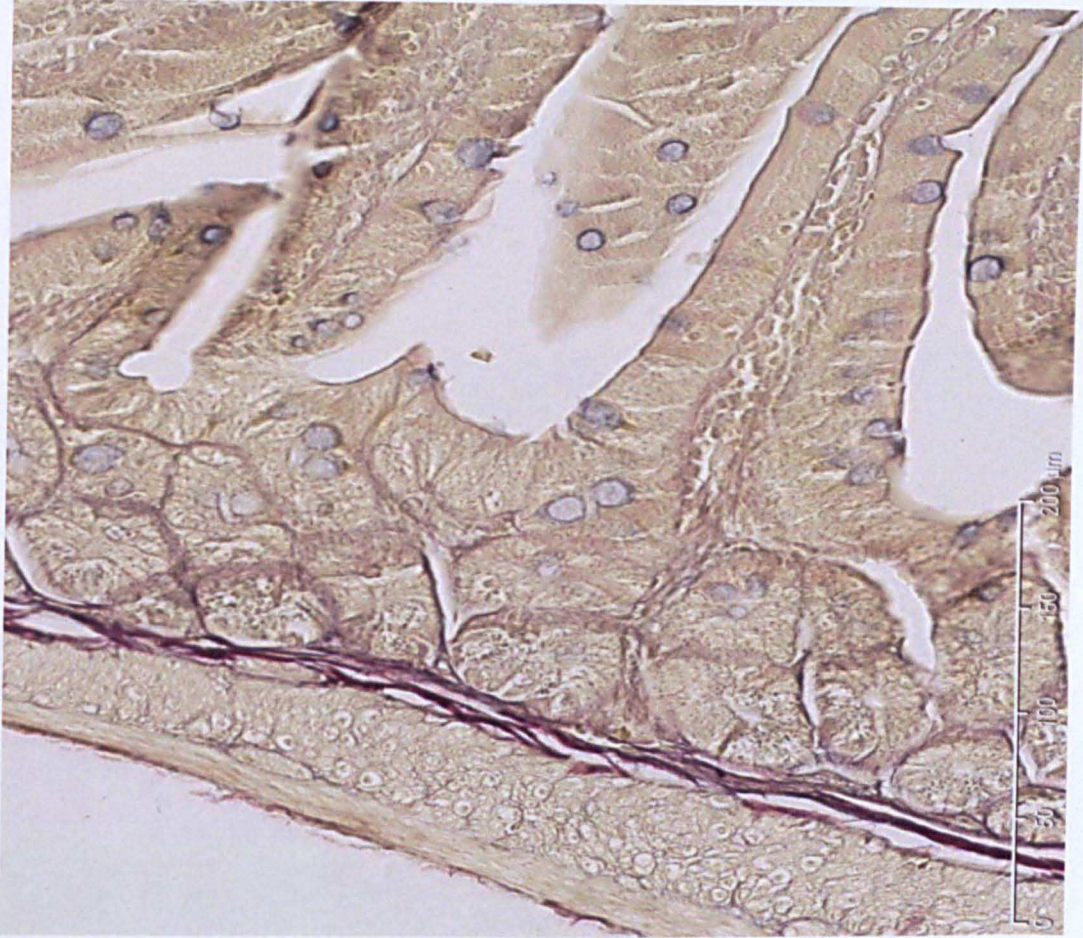


Figure 3: Background colonic mucosa stained with EVG stain with collagen in red and elastin in blue-black

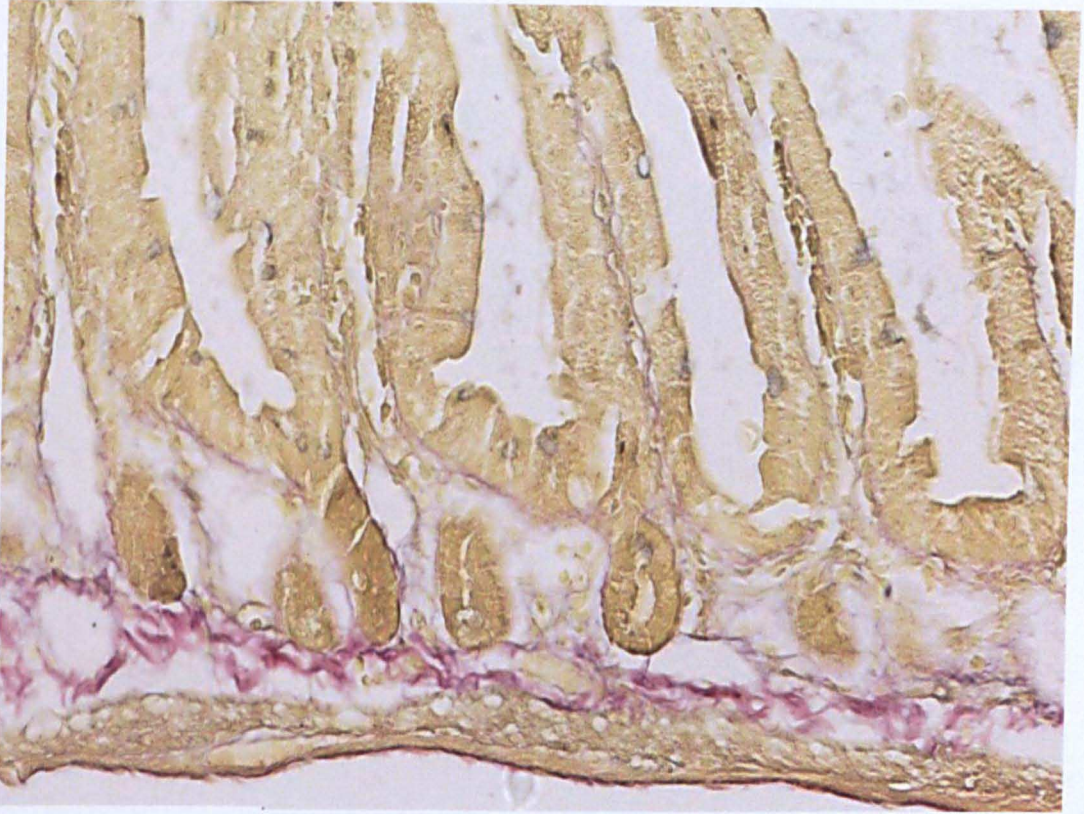


Figure 4: Background colonic mucosa stained with EVG stain with collagen stained in red and elastin in blue-black

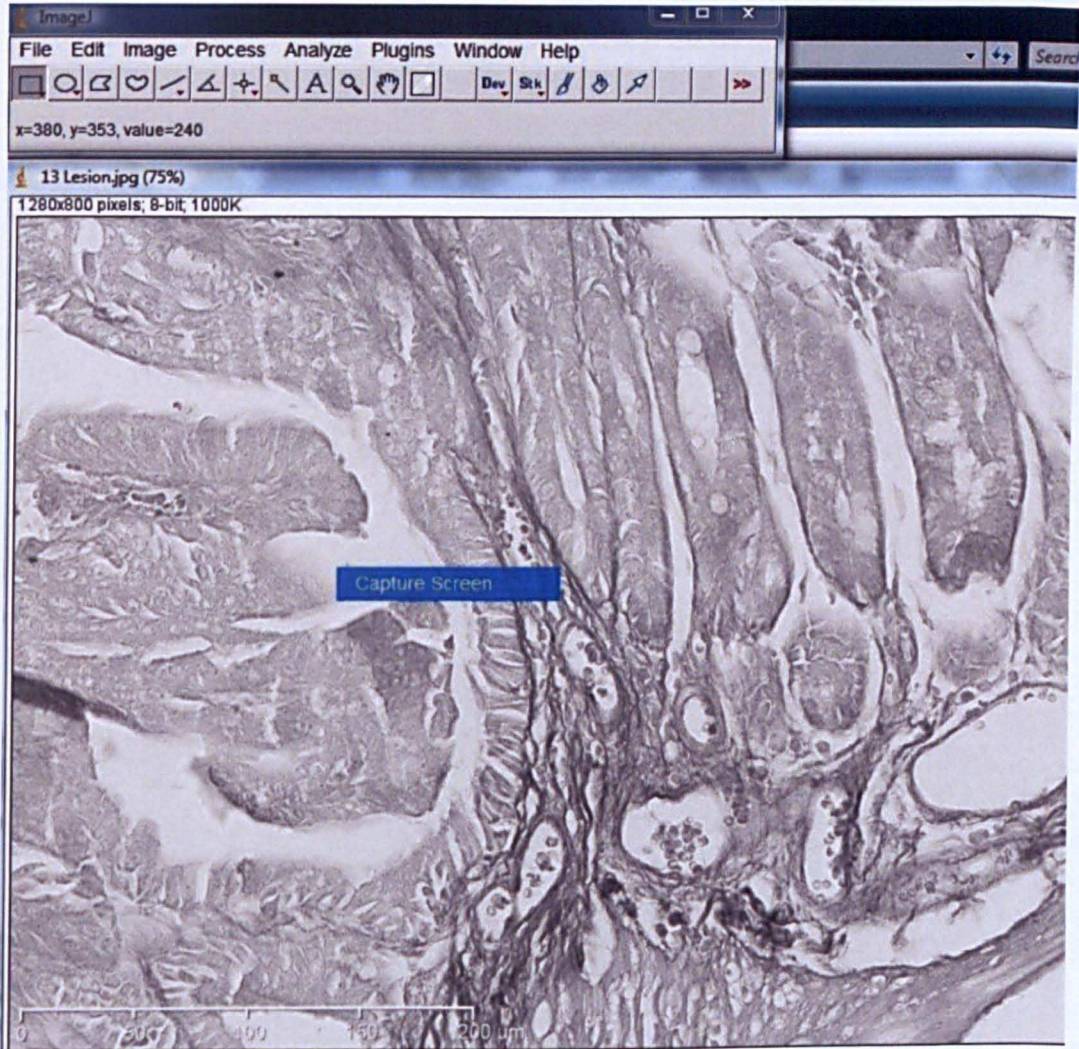


Figure 5: ImageJ software with RGB image converted to a 8-bit image before measuring the area fraction of collagen and elastin (screen shot)

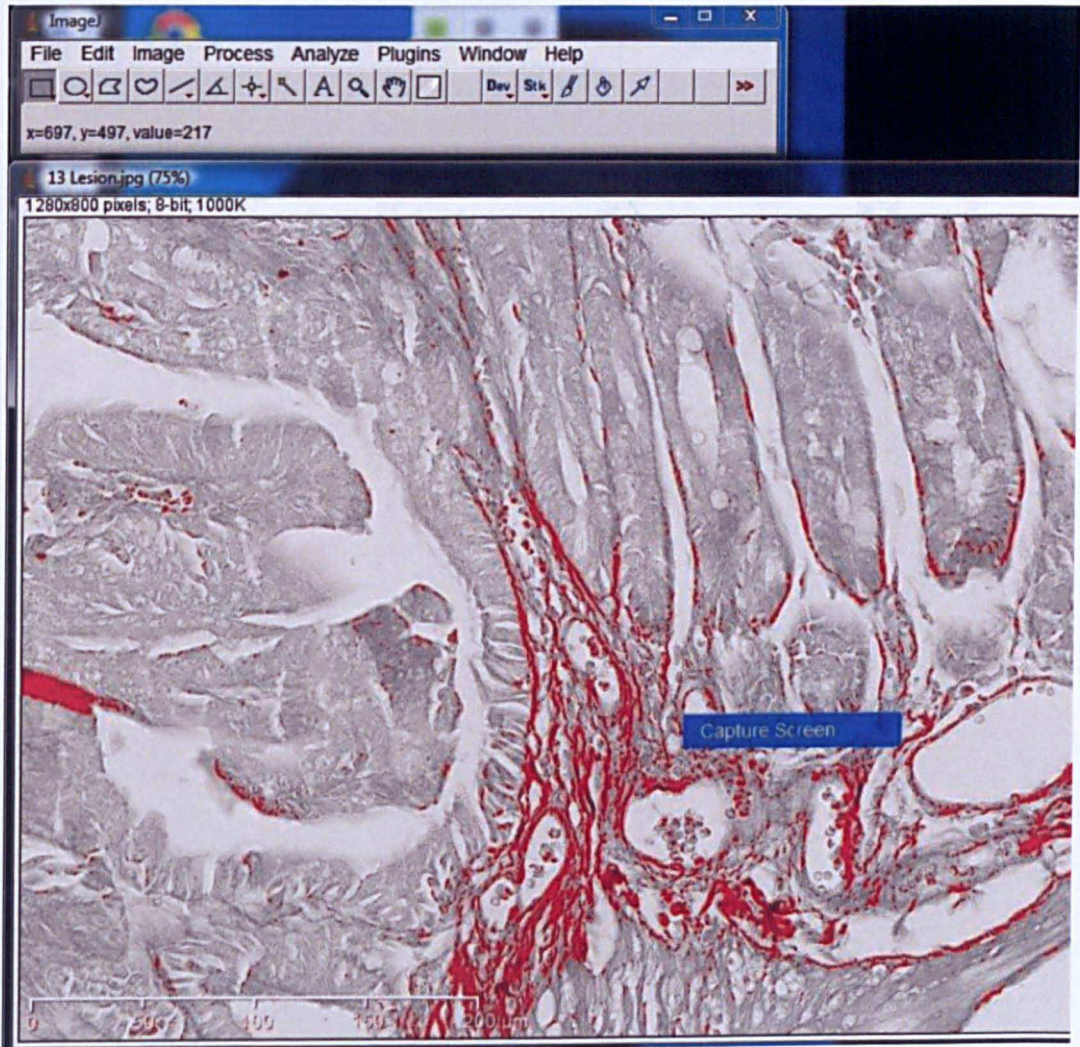


Figure 6: The 8 bit image is analysed with 'threshold colour' marking the areas of interest in red and analysing the area fraction (screen shot)

8.2.7 Statistical analysis

The descriptive statistics are expressed as mean and standard deviation. The comparison of means was done using non parametric tests of significance (Mann-Whitney U test) taking into account the relatively small number of cases. $P < 0.05$ was considered statistically significant

8.3 Results

A total of 30 formalinised mice colons from APC^{min} mice were included in the study. These colonic specimens were that of mice sacrificed at various ages, 10 each sacrificed at 12 weeks, 18 weeks and 24 weeks.

8.3.1 Quantifying autofluorescence in normal colon of APC^{min} mice sacrificed at different time points

The autofluorescence ratio as defined by the ratio of red to green colour tone of the normal colonic mucosa among the 12 weeks, 18 weeks and 24 weeks mice colons were compared (table 1). The mean (\pm standard deviation) AF ratio of macroscopically normal colonic mucosa from APC^{min} mice sacrificed at 12 weeks was 0.36 ± 0.06 , 18 weeks was 0.39 ± 0.05 and 24 weeks was 0.47 ± 0.07 . There was a statistically significant increase in the AF ratio between 12 and 24 weeks ($p=0.003$) and between 18 and 24 weeks ($p=0.005$) but no significant difference between 12 and 18 weeks ($p=0.18$).

Table 1: Autofluorescence ratio (red/green tone) of background mice colonic mucosa and mice colonic lesions of different ages

Age of mice colons	AF ratio of background colonic mucosa (mean \pm SD)	AF ratio of Colonic lesions (mean \pm SD)
12 weeks	0.36 \pm 0.06	0.35 \pm 0.05
18 weeks	0.39 \pm 0.05	0.38 \pm 0.05
24 weeks	0.47 \pm 0.07	0.45 \pm 0.05
P value	12 Vs 18= 0.18 18 Vs 24= 0.005* 12 Vs 24= 0.003*	12 Vs 18= 0.27 18 Vs 24= 0.015* 12 Vs 24= 0.001*

SD-Standard deviation

Table 2: Area fraction of collagen and elastin in background mice colonic mucosa and colonic lesions of different age groups

Age of mice colons	Area fraction of Collagen and Elastin in background colonic mucosa (mean \pm SD)	Area fraction of Collagen and Elastin in colonic lesions (mean \pm SD)
12 weeks	1.08 \pm 0.57	2.19 \pm 1.1
18 weeks	1.41 \pm 0.84	3.88 \pm 2.5
24 weeks	1.54 \pm 1.0	4.69 \pm 2.6
P value	12 Vs 18= 0.33 18 Vs 24= 0.97 12 Vs 24= 0.41	12 Vs 18= 0.23 18 Vs 24= 0.33 12 Vs 24= 0.01*

SD-Standard deviation

8.3.2 Autofluorescence in mice colonic lesions from different ages

The autofluorescence ratio of the colonic lesions among the 12 weeks, 18 weeks and 24 weeks mice colons were compared (table 1). The mean (\pm Standard deviation) autofluorescence ratio for the APC^{min} mice sacrificed at 12 weeks was 0.35 ± 0.05 . The mean AF ratio was 0.38 ± 0.05 for colonic lesion in APC^{min} mice sacrificed at 18 weeks. There was no statistical significance between these results ($P=0.27$). The mean AF ratio for colonic lesions in APC^{min} mice sacrificed at 24 weeks was 0.45 ± 0.05 , which was significantly higher than that at 12 weeks ($p=0.001$) and 18 weeks ($p=0.015$).

8.3.3 Elastin and collagen staining

The area fraction of collagen and elastin in mice colonic lesions and normal background areas were compared in the 12, 18 and 24 week old mice colons (table 2). The mean area fraction of elastin and collagen in macroscopically normal background mucosa from APC^{min} mice sacrificed at 12 weeks was (mean \pm SD) 1.08 ± 0.57 ; 18 weeks was 1.41 ± 0.84 , and 24 weeks was 1.54 ± 1.0 . There was no statistical difference between these groups ($p=0.33$ for 12 Vs 18 weeks, $p=0.41$ for 12 Vs 24 weeks and $p=0.97$ for 18 Vs 24 weeks), even though there was a trend towards increase in the amount of elastin and collagen as the mice colonic age increases.

The area fraction of elastin and collagen of colonic lesions in APC^{min} mice sacrificed at different time points was also compared. The mean area fraction for elastin and collagen from APC^{min} mice sacrificed at 12 weeks was 2.19 ± 1.1 , 18

weeks was 3.88 ± 2.5 , and for 24 weeks was 4.69 ± 2.6 . There was a significant increase in the area fraction of collagen and elastin between 12 weeks and 24 weeks ($p=0.01$). There was no statistically significant difference between 12 and 18 weeks ($p=0.23$) as well as 18 and 24 weeks ($p=0.33$). There was a trend towards an absolute increase in the amount of collagen and elastin as age of the colonic lesions increased

8.4 Discussion

This study used a well known mouse model for colon cancer (APC^{min}) for quantification of autofluorescence and to compare the ratio of AF to reflected light intensity with the amount of collagen and elastin in the submucosal tissue. The APC^{min} mice colons were chosen as they are well known and well characterised mouse model for intestinal neoplasia. The genetic and morphological changes in the normal as well as neoplastic mucosa have been reported before^{225, 227, 228}.

There are no similar animal models for Barrett's early neoplasia to perform such a study; hence the APC^{min} mouse colon model was used.

The difference in autofluorescence detected between normal and dysplastic lesions in the GI tract is not well established. Previous studies on colonic tissue have identified strong fluorescence in the submucosal layer, which could correspond to the amount of collagen and elastin. No difference in fluorescence was found at the mucosal layer between normal and abnormal tissue. Thus it was hypothesised that the decreased fluorescence found in dysplastic and neoplastic tissue could be due to the screening effect of mucosal thickening or due to replacement of submucosal

layer by cancer cells thus reducing the amount of collagen²²⁰. This study was performed on human colonic tissue obtained from resection of lesions. Another study performed on whole colonic crypts and short term primary cultures of epithelial cells attributed the difference in autofluorescence to the intrinsic numbers of mitochondria and lysosomes. This study did not examine the role of submucosal collagen as only epithelial tissue was isolated for the study²²⁹.

In our study, we used formalinised mice colons for imaging followed by assessment of the collagen and elastin in the submucosal layer. This study has clearly identified an increase in autofluorescence ratio (red/green tone) and a reduction in autofluorescence as the age of the mice colon increases. The background mucosa of these genetically modified mice showed a reduction of fluorescence between 12 and 24 weeks and 18 and 24 weeks which clearly implies that as the colon becomes genetically abnormal and with increasing age the autofluorescence decreases. This was true in case of colonic lesions in the mouse model as well and as age advanced the lesions became less fluorescent which was statistically significant between 12 weeks and 24 weeks as well as 18 weeks and 24 weeks. These findings show that the fluorescence decreases as the dysplasia progresses over the period of time and provides a biological basis for the quantification of autofluorescence from video autofluorescence endoscopy.

Following the AF imaging, the APC^{min} mice colons and the lesions were cut into sections and stained with EVG. This demonstrated the amount of collagen in red colour and the elastin in blue black. These stained sections from the lesion and the background was examined to quantify the amount of connective tissue. The

principal finding was that there is an absolute increase in the percentage of tissue area with collagen and elastin in colonic lesions of 12 and 24 week old APC^{min} mice. Interestingly, there was no significant difference in the amount of collagen and elastin in the background mucosa. These findings demonstrate the fact that the reduction in fluorescence and an increase in the autofluorescence ratio in colonic lesions is not due to a reduction in the collagen and elastin. On the contrary, the connective tissue area fraction is more in the colonic lesions as age advances. The difference in autofluorescence between macroscopically normal tissue and tumour is thought to be due to various reasons. This is believed to be either due to changes in the physical structure such as thickening of the epithelium or due to tumour tissue, secondary to changes in the blood volume or due to the changes in the content of various fluorescent substances in the tissue like flavins and NADH in the mucosa or collagen in the sub mucosa²³⁰⁻²³². However the study by Izuishi *et al* found that, in colonic specimens there was no difference between the amount of flavins in the normal and diseased tissue. There was strong fluorescence detected in the colonic sub mucosal layer using fluorescence microscopy and this was from the collagen content of the tissue. The reduction in fluorescence in neoplastic tissue was thought to be due to either a reduction in collagen due to tumour infiltration or due to changes in the physical structure such as thickening of the mucosal layer due to the neoplastic process²²⁰. In our study we have demonstrated that the actual amount of collagen and elastin increases with increasing age of the colonic lesions with a reduction in fluorescence. The most likely explanation for the reduction in autofluorescence in the colonic lesions would be due to the

mucosal thickening associated with the lesion which attenuates the autofluorescence as the light could not penetrate through the thickened mucosa to reach the collagen and elastin.

8.4.1 Limitations of the study

This study was performed on formalinised mice colons from 12, 18 and 24 weeks old APC^{min} mice. The autofluorescence of tissue depends on various factors including presence of blood flow and mucosal flavins and NADH. This study was intended to assess autofluorescence and its correlation with submucosal collagen and elastin. Because we used formalinised tissue we could not assess the effect of blood flow, haemoglobin content or assess the amount of other autofluorescent substances in the tissue.

8.4.2 Conclusions

The ratio of fluorescent to reflected light reduces with increasing age of the APC^{min} mice in both the macroscopically normal colonic mucosa and colonic lesions which supports the hypothesis that AF reduces with worsening dysplasia. The amount of sub mucosal collagen, which is known to be the strongest tissue fluorophores, increases in the colonic lesions of APC^{min} mouse as age advances. The reduction in AF is unlikely to be due to reduction in collagen but could very well be due to physical changes to the mucosal structure such as increased thickening due to the neoplastic process. Further studies are needed of AF imaging of pre-operative adenocarcinoma/dysplasia patients with Barrett's oesophagus and correlate this with the submucosal collagen in the resected specimens.

CHAPTER 9

CONCLUSIONS AND CLINICAL IMPLICATIONS

9.1 The role of multimodal imaging in Barrett's oesophagus

The challenge during Barrett's surveillance is to identify subtle and inconspicuous lesions at an early stage. This is often difficult as some of the dysplastic lesions are flat. An early intervention either endoscopically or surgically would prevent development of symptomatic cancers. There are various simple techniques which an endoscopist could adopt to improve visualisation such as cleaning thoroughly and using mucolytics to visualise the Barrett's segment well. However, it is argued that image enhanced endoscopy and high definition endoscopy could improve the yield of dysplasia during Barrett's surveillance.

This thesis examined the value of different modalities of imaging in Barrett's oesophagus. The endoscopy systems in the modern world have significantly improved in resolution and picture quality. By altering the light wavelengths and introducing filters, we are able to offer narrow band imaging and autofluorescence imaging to utilise the tissue characteristics and thus identify subtle changes in mucosal architecture.

The resolution of endoscopes has improved significantly over the past decade. The first study utilised a regular Barrett's surveillance population to investigate whether there is a difference in identifying dysplasia between high definition and standard definition endoscopy. This is a retrospective analysis of clinical data obtained from Nottingham University Hospitals NHS Trust. There was no significant difference between the HD and SD group in terms the age and gender of the patients. The HD endoscopy was found to be superior to SD endoscopy in targeted detection of all dysplasia and detection of dysplasia with random and

targeted biopsies combined. We have included indefinite for dysplasia in this group which could be the reason for the significant differences seen. However, there was no difference between HD and SD in detecting HGD/cancer. This could be due to the fact that the absolute number of cases with HGD/cancer was small in both groups. It is difficult to conclude whether HD endoscopy is superior to SD in Barrett's surveillance based on this small retrospective study; however HD system could be used wherever available as a preferred option for BO surveillance.

Narrow band imaging is a technique used to highlight the mucosal vascular patterns by increasing the contribution of blue light. The pit patterns are also distinctly seen and there are various studies which investigated the accuracy of various pit patterns and vascular patterns in predicting dysplasia in Barrett's oesophagus. NBI with magnification (NBI-Z) of the suspicious areas could provide significant details of the mucosal surface patterns. A meta-analysis showed that the accuracy of this technique is more than 95% when analysed both on a per-patient and per-lesion analysis for characterising HGD/cancer. The studies included are all from centres of excellence and performed on an enriched Barrett's population. However, NBI-Z could be a valuable tool to characterise a lesion prior to target biopsying and also to examine suspicious and subtle lesions. This study does not address whether detection of dysplasia is superior with NBI as there is a paucity of literature on this aspect.

Autofluorescence endoscopy is a relatively new technique which is proposed to be useful as a red flag technique to detect areas of dysplasia and these lesions could be closely observed with magnification endoscopy or NBI for further

characterisation. This would be an ideal technique for wide field imaging especially in long segment Barrett's to focus areas of abnormality. A meta-analysis was performed to identify the incremental yield of AFI over white light endoscopy in detecting dysplastic lesions. AFI showed a 49% increased yield of HGD/cancer and 46% incremental yield for detecting all dysplasia over WLE. This is at the expense of detecting significant number of false positive areas. Nonetheless, AFI is a valuable tool to improve the yield of dysplasia, particularly if it is possible to define what constitutes a true positive AFI signal.

A true positive AF signal was proposed to be magenta in colour with opaque intensity, away from gastric folds and that shows mucosal irregularities in white light endoscopy. These criteria were included in an inter-observer study including 74 sets of white light and AFI images of corresponding areas of Barrett's oesophagus. A training presentation was offered to both AFI experts and non-experts followed by scoring the images. Among experts, the inter-observer agreement was only fair to moderate when AF images were shown which improved when white light images were also displayed. The overall accuracy in identifying dysplasia was modest. This study clearly shows the need for improvement in this technique which could be achieved by improving technical aspects or by creating an objective measure of the autofluorescence intensity.

An objective way to assess the AF intensity of an area of interest is by measuring the ratio of the red to green colour tone (AF ratio) and when the AF ratio of the lesion to that of background is calculated, this is called AF index. A pilot study was performed using 82 AF images from patients with Barrett's oesophagus

which was correlated with histology. A cut off value of 1.32 for the AF index was selected arbitrarily, based on the receiver operating curve of several AF indices. This was validated using the same dataset which is the limitation of this study, but this has raised the potential of an objective index which could very well be incorporated to real time endoscopy. Real time prospective studies are necessary to assess the value of such an index.

The biological basis of the phenomenon of autofluorescence is debatable. Various fluorophores in the gastro-intestinal tract were implied. The strongest fluorophores are thought to be submucosal collagen and elastin. It is well known that the autofluorescence reduces when tissue becomes dysplastic. It is not clear whether this reduction in fluorescence is due to a reduction of collagen and elastin in the submucosal tissue or due to the mucosal thickness reducing the fluorescence. A genetically modified mouse colonic model was used as Barrett's animal models are not available. The colonic lesions were imaged with autofluorescence endoscopy and the AF ratio was calculated as described earlier. This was followed by staining for collagen and elastin. This study showed that the ratio of fluorescent to reflected light reduces with increasing age of the APC^{min} mice, both in the macroscopically normal colonic mucosa and in colonic lesions. This supports the hypothesis that AF reduces with worsening dysplasia. The amount of sub mucosal collagen, which is known to be one of the strongest tissue fluorophores, increases in the colonic lesions of APC^{min} mouse as age advances. The reduction in AF is unlikely to be due to reduction in collagen but could very well be due to physical

changes to the mucosal structure such as increased thickening due to the neoplastic process.

In conclusion, high definition and autofluorescence imaging improve targeted detection of dysplasia in Barrett's oesophagus. NBI with magnification has a high accuracy in characterising HGD/cancer in Barrett's oesophagus. However, none of these techniques could replace random biopsies. There is limited agreement regarding what constitutes a true positive autofluorescence signal. Methods to quantify autofluorescence intensity are likely to reduce the false positive rates of AFI. The intensity of AFI reduces with worsening dysplasia and is likely to be due to thickening of the mucosal layer.

CHAPTER 10

REFERENCES

1. Sivak MV. Gastrointestinal endoscopy: past and future. *Gut* 2006;55(8):1061-1064.
2. Hirschowitz BI, Curtiss LE, Peters CW, Pollard HM. Demonstration of a new gastroscope, the fiberscope. *Gastroenterology* 1958;35(1):50-53.
3. Marvik R, Lango T. High-definition television in medicine. *Surg Endosc* 2006;20(3):349-350.
4. Hurlstone DP, Fujii T. Practical uses of chromoendoscopy and magnification at colonoscopy. *Gastrointest Endosc Clin N Am* 2005;15(4):687-702.
5. Tanaka K, Toyoda H, Kadowaki S et al. Features of early gastric cancer and gastric adenoma by enhanced-magnification endoscopy. *J Gastroenterol* 2006;41(4):332-338.
6. Togashi K, Hewett DG, Whitaker DA, Hume GE, Francis L, Appleyard MN. The use of acetic acid in magnification chromocolonoscopy for pit pattern analysis of small polyps. *Endoscopy* 2006;38(6):613-616.
7. Yao K, Takaki Y, Ohara J et al. Magnification endoscopy outlines the microvascular architecture and extent of Barrett's intramucosal carcinoma prior to endoscopic resection. *Gastrointest Endosc* 2006;63(7):1064-1065.

8. Anagnostopoulos GK, Ragnath K, Shonde A, Hawkey CJ, Yao K. Diagnosis of autoimmune gastritis by high resolution magnification endoscopy. *World J Gastroenterol* 2006;12(28):4586-4587.
9. Gonen C, Simsek I, Sarioglu S, Akpinar H. Comparison of high resolution magnifying endoscopy and standard videoendoscopy for the diagnosis of *Helicobacter pylori* gastritis in routine clinical practice: a prospective study. *Helicobacter* 2009;14(1):12-21.
10. Anagnostopoulos GK, Yao K, Kaye P et al. High-resolution magnification endoscopy can reliably identify normal gastric mucosa, *Helicobacter pylori*-associated gastritis, and gastric atrophy. *Endoscopy* 2007;39(3):202-207.
11. Mannath J, Ragnath K. Narrow band imaging and high resolution endoscopy with magnification could be useful in identifying gastric atrophy. *Dig Dis Sci* 2010;55(6):1799-1800.
12. Badreldin R, Barrett P, Wooff DA, Mansfield J, Yiannakou Y. How good is zoom endoscopy for assessment of villous atrophy in coeliac disease? *Endoscopy* 2005;37(10):994-998.
13. Cammarota G, Martino A, Pirozzi GA et al. Direct visualization of intestinal villi by high-resolution magnifying upper endoscopy: a validation study. *Gastrointest Endosc* 2004;60(5):732-738.

14. Edebo A, Tam W, Bruno M et al. Magnification endoscopy for diagnosis of nonerosive reflux disease: a proposal of diagnostic criteria and critical analysis of observer variability. *Endoscopy* 2007;39(3):195-201.
15. Miyasaka M, Hirakawa M, Nakamura K et al. The endoscopic diagnosis of nonerosive reflux disease using flexible spectral imaging color enhancement image: a feasibility trial. *Dis Esophagus* 2011;24(6):395-400.
16. Kara MA, Peters FP, Rosmolen WD et al. High-resolution endoscopy plus chromoendoscopy or narrow-band imaging in Barrett's esophagus: a prospective randomized crossover study. *Endoscopy* 2005;37(10):929-936.
17. Endo T, Awakawa T, Takahashi H et al. Classification of Barrett's epithelium by magnifying endoscopy. *Gastrointest Endosc* 2002;55(6):641-647.
18. Stevens PD, Lightdale CJ, Green PH, Siegel LM, Garcia-Carrasquillo RJ, Rotterdam H. Combined magnification endoscopy with chromoendoscopy for the evaluation of Barrett's esophagus. *Gastrointest Endosc* 1994;40(6):747-749.
19. Fortun PJ, Anagnostopoulos GK, Kaye P et al. Acetic acid-enhanced magnification endoscopy in the diagnosis of specialized intestinal metaplasia, dysplasia and early cancer in Barrett's oesophagus. *Aliment Pharmacol Ther* 2006;23(6):735-742.

20. Hoffman A, Kiesslich R, Bender A et al. Acetic acid-guided biopsies after magnifying endoscopy compared with random biopsies in the detection of Barrett's esophagus: a prospective randomized trial with crossover design. *Gastrointest Endosc* 2006;64(1):1-8.
21. Curvers W, Baak L, Kiesslich R et al. Chromoendoscopy and narrow-band imaging compared with high-resolution magnification endoscopy in Barrett's esophagus. *Gastroenterology* 2008;134(3):670-679.
22. Rogart JN, Jain D, Siddiqui UD et al. Narrow-band imaging without high magnification to differentiate polyps during real-time colonoscopy: improvement with experience. *Gastrointest Endosc* 2008;68(6):1136-1145.
23. Zanoni EC, Cutait R, Averbach M et al. Magnifying colonoscopy: interobserver agreement in the assessment of colonic pit patterns and its correlation with histopathological findings. *Int J Colorectal Dis* 2007;22(11):1383-1388.
24. Pohl J, Nguyen-Tat M, Pech O, May A, Rabenstein T, Ell C. Computed virtual chromoendoscopy for classification of small colorectal lesions: a prospective comparative study. *Am J Gastroenterol* 2008;103(3):562-569.
25. Liu HH, Kudo SE, Juch JP. Pit pattern analysis by magnifying chromoendoscopy for the diagnosis of colorectal polyps. *J Formos Med Assoc* 2003;102(3):178-182.

26. East JE, Suzuki N, Saunders BP. Comparison of magnified pit pattern interpretation with narrow band imaging versus chromoendoscopy for diminutive colonic polyps: a pilot study. *Gastrointest Endosc* 2007;66(2):310-316.
27. Hurlstone DP, Cross SS, Adam I et al. Efficacy of high magnification chromoscopic colonoscopy for the diagnosis of neoplasia in flat and depressed lesions of the colorectum: a prospective analysis. *Gut* 2004;53(2):284-290.
28. Wong Kee Song LM, Adler DG, Chand B et al. Chromoendoscopy. *Gastrointest Endosc* 2007;66(4):639-649.
29. Singh R, Mei SC, Sethi S. Advanced endoscopic imaging in Barrett's oesophagus: a review on current practice. *World J Gastroenterol* 2011;17(38):4271-4276.
30. Olliver JR, Wild CP, Sahay P, Dexter S, Hardie LJ. Chromoendoscopy with methylene blue and associated DNA damage in Barrett's oesophagus. *Lancet* 2003;362(9381):373-374.
31. Sturmev RG, Wild CP, Hardie LJ. Removal of red light minimizes methylene blue-stimulated DNA damage in oesophageal cells: implications for chromoendoscopy. *Mutagenesis* 2009;24(3):253-258.

32. Canto MI, Setrakian S, Willis JE, Chak A, Petras RE, Sivak MV. Methylene blue staining of dysplastic and nondysplastic Barrett's esophagus: an in vivo and ex vivo study. *Endoscopy* 2001;33(5):391-400.
33. Canto MI, Setrakian S, Petras RE, Blades E, Chak A, Sivak MV, Jr. Methylene blue selectively stains intestinal metaplasia in Barrett's esophagus. *Gastrointest Endosc* 1996;44(1):1-7.
34. Kiesslich R, Hahn M, Herrmann G, Jung M. Screening for specialized columnar epithelium with methylene blue: chromoendoscopy in patients with Barrett's esophagus and a normal control group. *Gastrointest Endosc* 2001;53(1):47-52.
35. Gangarosa LM, Halter S, Mertz H. Methylene blue staining and endoscopic ultrasound evaluation of Barrett's esophagus with low-grade dysplasia. *Dig Dis Sci* 2000;45(2):225-229.
36. Sharma P, Topalovski M, Mayo MS, Weston AP. Methylene blue chromoendoscopy for detection of short-segment Barrett's esophagus. *Gastrointest Endosc* 2001;54(3):289-293.
37. Wo JM, Ray MB, Mayfield-Stokes S et al. Comparison of methylene blue-directed biopsies and conventional biopsies in the detection of intestinal metaplasia and dysplasia in Barrett's esophagus: a preliminary study. *Gastrointest Endosc* 2001;54(3):294-301.

38. Ngamruengphong S, Sharma VK, Das A. Diagnostic yield of methylene blue chromoendoscopy for detecting specialized intestinal metaplasia and dysplasia in Barrett's esophagus: a meta-analysis. *Gastrointest Endosc* 2009;69(6):1021-1028.
39. Marion JF, Waye JD, Present DH et al. Chromoendoscopy-targeted biopsies are superior to standard colonoscopic surveillance for detecting dysplasia in inflammatory bowel disease patients: a prospective endoscopic trial. *Am J Gastroenterol* 2008;103(9):2342-2349.
40. Davies J, Burke D, Olliver JR, Hardie LJ, Wild CP, Routledge MN. Methylene blue but not indigo carmine causes DNA damage to colonocytes in vitro and in vivo at concentrations used in clinical chromoendoscopy. *Gut* 2007;56(1):155-156.
41. Boller D, Spieler P, Schoenegg R et al. Lugol chromoendoscopy combined with brush cytology in patients at risk for esophageal squamous cell carcinoma. *Surg Endosc* 2009;23(12):2748-2754.
42. Lecleire S, Antonietti M, Iwanicki-Caron I et al. Lugol chromo-endoscopy versus narrow band imaging for endoscopic screening of esophageal squamous-cell carcinoma in patients with a history of cured esophageal cancer: a feasibility study. *Dis Esophagus* 2011;24(6):418-422.

43. Urabe Y, Hiyama T, Tanaka S et al. Metachronous multiple esophageal squamous cell carcinomas and Lugol-voiding lesions after endoscopic mucosal resection. *Endoscopy* 2009;41(4):304-309.
44. Dubuc J, Legoux JL, Winnock M et al. Endoscopic screening for esophageal squamous-cell carcinoma in high-risk patients: a prospective study conducted in 62 French endoscopy centers. *Endoscopy* 2006;38(7):690-695.
45. Woolf GM, Riddell RH, Irvine EJ, Hunt RH. A study to examine agreement between endoscopy and histology for the diagnosis of columnar lined (Barrett's) esophagus. *Gastrointest Endosc* 1989;35(6):541-544.
46. Hurlstone DP, Sanders DS, Cross SS et al. Colonoscopic resection of lateral spreading tumours: a prospective analysis of endoscopic mucosal resection. *Gut* 2004;53(9):1334-1339.
47. Hurlstone DP, Cross SS, Brown S, Sanders DS, Lobo AJ. A prospective evaluation of high-magnification chromoscopic colonoscopy in predicting completeness of EMR. *Gastrointest Endosc* 2004;59(6):642-650.
48. Fujii T, Hasegawa RT, Saitoh Y et al. Chromoscopy during colonoscopy. *Endoscopy* 2001;33(12):1036-1041.

49. Sharma P, Weston AP, Topalovski M, Cherian R, Bhattacharyya A, Sampliner RE. Magnification chromoendoscopy for the detection of intestinal metaplasia and dysplasia in Barrett's oesophagus. *Gut* 2003;52(1):24-27.
50. Brooker JC, Saunders BP, Shah SG et al. Total colonic dye-spray increases the detection of diminutive adenomas during routine colonoscopy: a randomized controlled trial. *Gastrointest Endosc* 2002;56(3):333-338.
51. Kiesslich R, von BM, Hahn M, Hermann G, Jung M. Chromoendoscopy with indigocarmine improves the detection of adenomatous and nonadenomatous lesions in the colon. *Endoscopy* 2001;33(12):1001-1006.
52. Hurlstone DP, Cross SS, Slater R, Sanders DS, Brown S. Detecting diminutive colorectal lesions at colonoscopy: a randomised controlled trial of pan-colonic versus targeted chromoscopy. *Gut* 2004;53(3):376-380.
53. Le RM, Coron E, Parlier D et al. High resolution colonoscopy with chromoscopy versus standard colonoscopy for the detection of colonic neoplasia: a randomized study. *Clin Gastroenterol Hepatol* 2006;4(3):349-354.
54. Axelrad AM, Fleischer DE, Geller AJ et al. High-resolution chromoendoscopy for the diagnosis of diminutive colon polyps: implications for colon cancer screening. *Gastroenterology* 1996;110(4):1253-1258.

55. Chiu HM, Chang CY, Chen CC et al. A prospective comparative study of narrow-band imaging, chromoendoscopy, and conventional colonoscopy in the diagnosis of colorectal neoplasia. *Gut* 2007;56(3):373-379.
56. Sonwalkar S, Rotimi O, Rembacken BJ. Characterization of colonic polyps at conventional (nonmagnifying) colonoscopy after spraying with 0.2 % indigo carmine dye. *Endoscopy* 2006;38(12):1218-1223.
57. Rutter MD, Saunders BP, Schofield G, Forbes A, Price AB, Talbot IC. Pancolonic indigo carmine dye spraying for the detection of dysplasia in ulcerative colitis. *Gut* 2004;53(2):256-260.
58. Hurlstone DP, Sanders DS, Lobo AJ, McAlindon ME, Cross SS. Indigo carmine-assisted high-magnification chromoscopic colonoscopy for the detection and characterisation of intraepithelial neoplasia in ulcerative colitis: a prospective evaluation. *Endoscopy* 2005;37(12):1186-1192.
59. Pohl J, Lotterer E, Balzer C et al. Computed virtual chromoendoscopy versus standard colonoscopy with targeted indigocarmine chromoscopy: a randomised multicentre trial. *Gut* 2009;58(1):73-78.
60. Camus M, Coriat R, Leblanc S et al. Helpfulness of the combination of acetic acid and FICE in the detection of Barrett's epithelium and Barrett's associated neoplasias. *World J Gastroenterol* 2012;18(16):1921-1925.

61. Osawa H, Yamamoto H, Yamada N et al. Diagnosis of endoscopic Barrett's esophagus by transnasal flexible spectral imaging color enhancement. *J Gastroenterol* 2009;44(11):1125-31.
62. Hoffman A, Kagel C, Goetz M et al. Recognition and characterization of small colonic neoplasia with high-definition colonoscopy using i-Scan is as precise as chromoendoscopy. *Dig Liver Dis* 2009;42(1):45-50.
63. Kang HS, Hong SN, Kim YS et al. The efficacy of i-SCAN for detecting reflux esophagitis: a prospective randomized controlled trial. *Dis Esophagus* 2013;26(2):204-211.
64. Kiesslich R, Goetz M, Burg J et al. Diagnosing *Helicobacter pylori* in vivo by confocal laser endoscopy. *Gastroenterology* 2005;128(7):2119-2123.
65. Kiesslich R, Gossner L, Goetz M et al. In vivo histology of Barrett's esophagus and associated neoplasia by confocal laser endomicroscopy. *Clin Gastroenterol Hepatol* 2006;4(8):979-987.
66. Dunbar KB, Okolo P, III, Montgomery E, Canto MI. Confocal laser endomicroscopy in Barrett's esophagus and endoscopically inapparent Barrett's neoplasia: a prospective, randomized, double-blind, controlled, crossover trial. *Gastrointest Endosc* 2009;70(4):645-54.

67. Hurlstone DP, Kiesslich R, Thomson M, Atkinson R, Cross SS. Confocal chromoscopic endomicroscopy is superior to chromoscopy alone for the detection and characterisation of intraepithelial neoplasia in chronic ulcerative colitis. *Gut* 2008;57(2):196-204.
68. Hurlstone DP, Baraza W, Brown S, Thomson M, Tiffin N, Cross SS. In vivo real-time confocal laser scanning endomicroscopic colonoscopy for the detection and characterization of colorectal neoplasia. *Br J Surg* 2008;95(5):636-645.
69. Kimura T, Muguruma N, Ito S et al. Infrared fluorescence endoscopy for the diagnosis of superficial gastric tumors. *Gastrointest Endosc* 2007;66(1):37-43.
70. Yoshida Y, Matsuda K, Tamai N et al. A pilot study using an infrared imaging system in prevention of post-endoscopic submucosal dissection ulcer bleeding. *Gastric Cancer* 2013 Feb 8 [Epub ahead of print].
71. Gono K, Obi T, Yamaguchi M et al. Appearance of enhanced tissue features in narrow-band endoscopic imaging. *J Biomed Opt* 2004;9(3):568-577.
72. Machida H, Sano Y, Hamamoto Y et al. Narrow-band imaging in the diagnosis of colorectal mucosal lesions: a pilot study. *Endoscopy* 2004;36(12):1094-1098.

73. Su MY, Hsu CM, Ho YP, Chen PC, Lin CJ, Chiu CT. Comparative study of conventional colonoscopy, chromoendoscopy, and narrow-band imaging systems in differential diagnosis of neoplastic and nonneoplastic colonic polyps. *Am J Gastroenterol* 2006;101(12):2711-2716.
74. Hirata M, Tanaka S, Oka S et al. Magnifying endoscopy with narrow band imaging for diagnosis of colorectal tumors. *Gastrointest Endosc* 2007;65(7):988-995.
75. Wolfsen HC, Crook JE, Krishna M et al. Prospective, controlled tandem endoscopy study of narrow band imaging for dysplasia detection in Barrett's Esophagus. *Gastroenterology* 2008;135(1):24-31.
76. Singh R, Anagnostopoulos GK, Yao K et al. Narrow-band imaging with magnification in Barrett's esophagus: validation of a simplified grading system of mucosal morphology patterns against histology. *Endoscopy* 2008;40(6):457-463.
77. Kara M, Dacosta RS, Wilson BC, Marcon NE, Bergman J. Autofluorescence-based detection of early neoplasia in patients with Barrett's esophagus. *Dig Dis* 2004;22(2):134-141.
78. Panjehpour M, Overholt BF, Vo-Dinh T, Haggitt RC, Edwards DH, Buckley FP, III. Endoscopic fluorescence detection of high-grade dysplasia in Barrett's esophagus. *Gastroenterology* 1996;111(1):93-101.

79. Brand S, Wang TD, Schomacker KT et al. Detection of high-grade dysplasia in Barrett's esophagus by spectroscopy measurement of 5-aminolevulinic acid-induced protoporphyrin IX fluorescence. *Gastrointest Endosc* 2002;56(4):479-487.
80. von Holstein CS, Nilsson AM, Andersson-Engels S, Willen R, Walther B, Svanberg K. Detection of adenocarcinoma in Barrett's oesophagus by means of laser induced fluorescence. *Gut* 1996;39(5):711-716.
81. Haringsma J, Tytgat GN, Yano H et al. Autofluorescence endoscopy: feasibility of detection of GI neoplasms unapparent to white light endoscopy with an evolving technology. *Gastrointest Endosc* 2001;53(6):642-650.
82. Kara MA, Smits ME, Rosmolen WD et al. A randomized crossover study comparing light-induced fluorescence endoscopy with standard videoendoscopy for the detection of early neoplasia in Barrett's esophagus. *Gastrointest Endosc* 2005;61(6):671-678.
83. Kara MA, Peters FP, ten Kate FJ, Van Deventer SJ, Fockens P, Bergman JJ. Endoscopic video autofluorescence imaging may improve the detection of early neoplasia in patients with Barrett's esophagus. *Gastrointest Endosc* 2005;61(6):679-685.

84. Kara MA, Peters FP, Fockens P, ten Kate FJ, Bergman JJ. Endoscopic video-autofluorescence imaging followed by narrow band imaging for detecting early neoplasia in Barrett's esophagus. *Gastrointest Endosc* 2006;64(2):176-185.
85. Borovicka J, Fischer J, Neuweiler J et al. Autofluorescence endoscopy in surveillance of Barrett's esophagus: a multicenter randomized trial on diagnostic efficacy. *Endoscopy* 2006;38(9):867-872.
86. Curvers WL, Singh R, Song LM et al. Endoscopic tri-modal imaging for detection of early neoplasia in Barrett's oesophagus: a multi-centre feasibility study using high-resolution endoscopy, autofluorescence imaging and narrow band imaging incorporated in one endoscopy system. *Gut* 2008;57(2):167-172.
87. Matsuda T, Saito Y, Fu KI et al. Does autofluorescence imaging videoendoscopy system improve the colonoscopic polyp detection rate?--a pilot study. *Am J Gastroenterol* 2008;103(8):1926-1932.
88. Matsumoto T, Esaki M, Fujisawa R, Nakamura S, Yao T, Iida M. Chromoendoscopy, narrow-band imaging colonoscopy, and autofluorescence colonoscopy for detection of diminutive colorectal neoplasia in familial adenomatous polyposis. *Dis Colon Rectum* 2009;52(6):1160-1165.

89. Barrett NR. Chronic peptic ulcer of the oesophagus and 'oesophagitis'. *Br J Surg* 1950;38(150):175-182.
90. Allison PR, Johnstone AS. The oesophagus lined with gastric mucous membrane. *Thorax* 1953;8(2):87-101.
91. Paull A, Trier JS, Dalton MD, Camp RC, Loeb P, Goyal RK. The histologic spectrum of Barrett's esophagus. *N Engl J Med* 1976;295(9):476-480.
92. Sharma P, Dent J, Armstrong D et al. The development and validation of an endoscopic grading system for Barrett's esophagus: the Prague C & M criteria. *Gastroenterology* 2006;131(5):1392-1399.
93. Balasubramanian G, Singh M, Gupta N et al. Prevalence and predictors of columnar lined esophagus in gastroesophageal reflux disease (GERD) patients undergoing upper endoscopy. *Am J Gastroenterol* 2012;107(11):1655-1661.
94. Falk GW, Jacobson BC, Riddell RH et al. Barrett's esophagus: prevalence-incidence and etiology-origins. *Ann N Y Acad Sci* 2011;1232:1-17.
95. Hardikar S, Onstad L, Blount PL, Odze RD, Reid BJ, Vaughan TL. The role of tobacco, alcohol, and obesity in neoplastic progression to esophageal adenocarcinoma: a prospective study of Barrett's esophagus. *PLoS One* 2013;8(1):e52192.

96. Coleman HG, Bhat S, Johnston BT, McManus D, Gavin AT, Murray LJ. Tobacco smoking increases the risk of high-grade dysplasia and cancer among patients with Barrett's esophagus. *Gastroenterology* 2012;142(2):233-240.
97. Hampel H, Abraham NS, El-Serag HB. Meta-analysis: obesity and the risk for gastroesophageal reflux disease and its complications. *Ann Intern Med* 2005;143(3):199-211.
98. Ronkainen J, Aro P, Storskrubb T et al. Prevalence of Barrett's esophagus in the general population: an endoscopic study. *Gastroenterology* 2005;129(6):1825-1831.
99. Chak A, Lee T, Kinnard MF et al. Familial aggregation of Barrett's oesophagus, oesophageal adenocarcinoma, and oesophagogastric junctional adenocarcinoma in Caucasian adults. *Gut* 2002;51(3):323-328.
100. Orloff M, Peterson C, He X et al. Germline mutations in *MSR1*, *ASCC1*, and *CTHRC1* in patients with Barrett esophagus and esophageal adenocarcinoma. *JAMA* 2011;306(4):410-419.
101. Dodds WJ, Dent J, Hogan WJ et al. Mechanisms of gastroesophageal reflux in patients with reflux esophagitis. *N Engl J Med* 1982;307(25):1547-1552.

102. Ter RB, Castell DO. Gastroesophageal reflux disease in patients with columnar-lined esophagus. *Gastroenterol Clin North Am* 1997;26(3):549-563.
103. Castell DO, Murray JA, Tutuian R, Orlando RC, Arnold R. Review article: the pathophysiology of gastro-oesophageal reflux disease - oesophageal manifestations. *Aliment Pharmacol Ther* 2004;20 Suppl 9:14-25.
104. Hershcovici T, Mashimo H, Fass R. The lower esophageal sphincter. *Neurogastroenterol Motil* 2011;23(9):819-830.
105. Kahrilas PJ, Dodds WJ, Hogan WJ, Kern M, Arndorfer RC, Reece A. Esophageal peristaltic dysfunction in peptic esophagitis. *Gastroenterology* 1986;91(4):897-904.
106. Fitzgerald RC, Omary MB, Triadafilopoulos G. Dynamic effects of acid on Barrett's esophagus. An ex vivo proliferation and differentiation model. *J Clin Invest* 1996;98(9):2120-2128.
107. Lagergren J, Bergstrom R, Lindgren A, Nyren O. Symptomatic gastroesophageal reflux as a risk factor for esophageal adenocarcinoma. *N Engl J Med* 1999;340(11):825-831.
108. Cameron AJ, Lomboy CT. Barrett's esophagus: age, prevalence, and extent of columnar epithelium. *Gastroenterology* 1992;103(4):1241-1245.

109. Kelty CJ, Gough MD, Van WQ, Stephenson TJ, Ackroyd R. Barrett's oesophagus: intestinal metaplasia is not essential for cancer risk. *Scand J Gastroenterol* 2007;42(11):1271-1274.
110. Sikkema M, Looman CW, Steyerberg EW et al. Predictors for neoplastic progression in patients with Barrett's Esophagus: a prospective cohort study. *Am J Gastroenterol* 2011;106(7):1231-1238.
111. Wani S. Management of low-grade dysplasia in Barrett's esophagus. *Curr Opin Gastroenterol* 2012;28(4):370-376.
112. Skacel M, Petras RE, Gramlich TL, Sigel JE, Richter JE, Goldblum JR. The diagnosis of low-grade dysplasia in Barrett's esophagus and its implications for disease progression. *Am J Gastroenterol* 2000;95(12):3383-3387.
113. Kerkhof M, van DH, Steyerberg EW et al. Grading of dysplasia in Barrett's oesophagus: substantial interobserver variation between general and gastrointestinal pathologists. *Histopathology* 2007;50(7):920-927.
114. Farrow DC, Vaughan TL, Hansten PD et al. Use of aspirin and other nonsteroidal anti-inflammatory drugs and risk of esophageal and gastric cancer. *Cancer Epidemiol Biomarkers Prev* 1998;7(2):97-102.
115. Funkhouser EM, Sharp GB. Aspirin and reduced risk of esophageal carcinoma. *Cancer* 1995;76(7):1116-1119.

116. Buttar NS, Wang KK, Leontovich O et al. Chemoprevention of esophageal adenocarcinoma by COX-2 inhibitors in an animal model of Barrett's esophagus. *Gastroenterology* 2002;122(4):1101-1112.
117. Heath EI, Canto MI, Piantadosi S et al. Secondary chemoprevention of Barrett's esophagus with celecoxib: results of a randomized trial. *J Natl Cancer Inst* 2007;99(7):545-557.
118. Leedham S, Jankowski J. The evidence base of proton pump inhibitor chemopreventative agents in Barrett's esophagus--the good, the bad, and the flawed! *Am J Gastroenterol* 2007;102(1):21-23.
119. El-Serag HB, Aguirre TV, Davis S, Kuebel M, Bhattacharyya A, Sampliner RE. Proton pump inhibitors are associated with reduced incidence of dysplasia in Barrett's esophagus. *Am J Gastroenterol* 2004;99(10):1877-1883.
120. Kastelein F, Spaander MC, Steyerberg EW et al. Proton Pump Inhibitors Reduce the Risk of Neoplastic Progression in Patients With Barrett's Esophagus. *Clin Gastroenterol Hepatol* 2013;11(4):382-388.
121. Hvid-Jensen F, Pedersen L, Drewes AM, Sorensen HT, Funch-Jensen P. Incidence of adenocarcinoma among patients with Barrett's esophagus. *N Engl J Med* 2011;365(15):1375-1383.

122. Jankowski JA, Provenzale D, Moayyedi P. Esophageal adenocarcinoma arising from Barrett's metaplasia has regional variations in the west. *Gastroenterology* 2002;122(2):588-590.
123. Urschel JD, Vasan H, Blewett CJ. A meta-analysis of randomized controlled trials that compared neoadjuvant chemotherapy and surgery to surgery alone for resectable esophageal cancer. *Am J Surg* 2002;183(3):274-279.
124. Fountoulakis A, Zafirellis KD, Dolan K, Dexter SP, Martin IG, Sue-Ling HM. Effect of surveillance of Barrett's oesophagus on the clinical outcome of oesophageal cancer. *Br J Surg* 2004;91(8):997-1003.
125. Barr H, Kendall C, Bazant-Hegemark F, Moayyedi P, Shetty G, Stone N. Endoscopic screening and surveillance for Barrett's esophagus--clinical implications. *MedGenMed* 2006;8(2):88.
126. Wang KK, Sampliner RE. Updated guidelines 2008 for the diagnosis, surveillance and therapy of Barrett's esophagus. *Am J Gastroenterol* 2008;103(3):788-797.
127. Sharma P. Clinical practice. Barrett's esophagus. *N Engl J Med* 2009;361(26):2548-2556.
128. Jankowski JA, Harrison RF, Perry I, Balkwill F, Tselepis C. Barrett's metaplasia. *Lancet* 2000;356(9247):2079-2085.

129. Almond LM, Barr H. Advanced endoscopic imaging in Barrett's oesophagus. *Int J Surg* 2012;10(5):236-241.
130. Kendall C, Stone N, Shepherd N et al. Raman spectroscopy, a potential tool for the objective identification and classification of neoplasia in Barrett's oesophagus. *J Pathol* 2003;200(5):602-609.
131. Kendall C, Day J, Hutchings J et al. Evaluation of Raman probe for oesophageal cancer diagnostics. *Analyst* 2010;135(12):3038-3041.
132. Sanz-Ortega J, Hernandez S, Saez MC et al. 3p21, 5q21, 9p21 and 17p13.1 allelic deletions are potential markers of individuals with a high risk of developing adenocarcinoma in Barrett's epithelium without dysplasia. *Hepatogastroenterology* 2003;50(50):404-407.
133. Chaves P, Crespo M, Ribeiro C et al. Chromosomal analysis of Barrett's cells: demonstration of instability and detection of the metaplastic lineage involved. *Mod Pathol* 2007;20(7):788-796.
134. Helm J, Enkemann SA, Coppola D, Barthel JS, Kelley ST, Yeatman TJ. Dedifferentiation precedes invasion in the progression from Barrett's metaplasia to esophageal adenocarcinoma. *Clin Cancer Res* 2005;11(7):2478-2485.

135. Reid BJ, Levine DS, Longton G, Blount PL, Rabinovitch PS. Predictors of progression to cancer in Barrett's esophagus: baseline histology and flow cytometry identify low- and high-risk patient subsets. *Am J Gastroenterol* 2000;95(7):1669-1676.
136. Wijnhoven BP, Tilanus HW, Dinjens WN. Molecular biology of Barrett's adenocarcinoma. *Ann Surg* 2001;233(3):322-337.
137. Kim NW, Piatyszek MA, Prowse KR et al. Specific association of human telomerase activity with immortal cells and cancer. *Science* 1994;266(5193):2011-2015.
138. Fitzgerald RC. Barrett's oesophagus and oesophageal adenocarcinoma: how does acid interfere with cell proliferation and differentiation? *Gut* 2005;54 Suppl 1:i21-i26.
139. Kerkhof M, Steyerberg EW, Kusters JG et al. Aneuploidy and high expression of p53 and Ki67 is associated with neoplastic progression in Barrett esophagus. *Cancer Biomark* 2008;4(1):1-10.
140. Casson AG, Evans SC, Gillis A et al. Clinical implications of p53 tumor suppressor gene mutation and protein expression in esophageal adenocarcinomas: results of a ten-year prospective study. *J Thorac Cardiovasc Surg* 2003;125(5):1121-1131.
141. Goldblum JR. Barrett's esophagus and Barrett's-related dysplasia. *Mod Pathol* 2003;16(4):316-324.

142. Ouatu-Lascar R, Fitzgerald RC, Triadafilopoulos G. Differentiation and proliferation in Barrett's esophagus and the effects of acid suppression. *Gastroenterology* 1999;117(2):327-335.
143. Ouatu-Lascar R, Triadafilopoulos G. Complete elimination of reflux symptoms does not guarantee normalization of intraesophageal acid reflux in patients with Barrett's esophagus. *Am J Gastroenterol* 1998;93(5):711-716.
144. Spechler SJ, Sharma P, Traxler B, Levine D, Falk GW. Gastric and esophageal pH in patients with Barrett's esophagus treated with three esomeprazole dosages: a randomized, double-blind, crossover trial. *Am J Gastroenterol* 2006;101(9):1964-1971.
145. Peters FT, Ganesh S, Kuipers EJ et al. Endoscopic regression of Barrett's oesophagus during omeprazole treatment; a randomised double blind study. *Gut* 1999;45(4):489-494.
146. Chang EY, Morris CD, Seltman AK et al. The effect of antireflux surgery on esophageal carcinogenesis in patients with barrett esophagus: a systematic review. *Ann Surg* 2007;246(1):11-21.
147. Manner H, May A, Pech O et al. Early Barrett's carcinoma with "low-risk" submucosal invasion: long-term results of endoscopic resection with a curative intent. *Am J Gastroenterol* 2008;103(10):2589-2597.

148. Pech O, Behrens A, May A et al. Long-term results and risk factor analysis for recurrence after curative endoscopic therapy in 349 patients with high-grade intraepithelial neoplasia and mucosal adenocarcinoma in Barrett's oesophagus. *Gut* 2008;57(9):1200-1206.
149. Pouw RE, Peters FP, Sempoux C, Piessevaux H, Deprez PH. Stepwise radical endoscopic resection for Barrett's esophagus with early neoplasia: report on a Brussels' cohort. *Endoscopy* 2008;40(11):892-898.
150. Peters FP, Kara MA, Curvers WL et al. Multiband mucosectomy for endoscopic resection of Barrett's esophagus: feasibility study with matched historical controls. *Eur J Gastroenterol Hepatol* 2007;19(4):311-315.
151. van Vilsteren FG, Pouw RE, Herrero LA et al. Learning to perform endoscopic resection of esophageal neoplasia is associated with significant complications even within a structured training program. *Endoscopy* 2012;44(1):4-12.
152. Montes CG, Brandalise NA, Deliza R, Novais de Magalhaes AF, Ferraz JG. Antireflux surgery followed by bipolar electrocoagulation in the treatment of Barrett's esophagus. *Gastrointest Endosc* 1999;50(2):173-177.
153. Sampliner RE, Faigel D, Fennerty MB et al. Effective and safe endoscopic reversal of nondysplastic Barrett's esophagus with thermal electrocoagulation combined with high-dose acid inhibition: a multicenter study. *Gastrointest Endosc* 2001;53(6):554-558.

154. Schulz H, Miehke S, Antos D et al. Ablation of Barrett's epithelium by endoscopic argon plasma coagulation in combination with high-dose omeprazole. *Gastrointest Endosc* 2000;51(6):659-663.
155. Madisch A, Miehke S, Bayerdorffer E et al. Long-term follow-up after complete ablation of Barrett's esophagus with argon plasma coagulation. *World J Gastroenterol* 2005;11(8):1182-1186.
156. Van Laethem JL, Jagodzinski R, Peny MO, Cremer M, Deviere J. Argon plasma coagulation in the treatment of Barrett's high-grade dysplasia and in situ adenocarcinoma. *Endoscopy* 2001;33(3):257-261.
157. Attwood SE, Lewis CJ, Caplin S, Hemming K, Armstrong G. Argon beam plasma coagulation as therapy for high-grade dysplasia in Barrett's esophagus. *Clin Gastroenterol Hepatol* 2003;1(4):258-263.
158. Pouw RE, Sharma VK, Bergman JJ, Fleischer DE. Radiofrequency ablation for total Barrett's eradication: a description of the endoscopic technique, its clinical results and future prospects. *Endoscopy* 2008;40(12):1033-1040.
159. Shaheen NJ, Sharma P, Overholt BF et al. Radiofrequency ablation in Barrett's esophagus with dysplasia. *N Engl J Med* 2009;360(22):2277-2288.

160. Fleischer DE, Overholt BF, Sharma VK et al. Endoscopic ablation of Barrett's esophagus: a multicenter study with 2.5-year follow-up. *Gastrointest Endosc* 2008;68(5):867-876.
161. Pouw RE, Gondrie JJ, Sondermeijer CM et al. Eradication of Barrett esophagus with early neoplasia by radiofrequency ablation, with or without endoscopic resection. *J Gastrointest Surg* 2008;12(10):1627-1636.
162. Semlitsch T, Jeitler K, Schoefl R et al. A systematic review of the evidence for radiofrequency ablation for Barrett's esophagus. *Surg Endosc* 2010;24(12):2935-2943.
163. Barr H, Kendall C, Stone N. Photodynamic therapy for esophageal cancer: a useful and realistic option. *Technol Cancer Res Treat* 2003;2(1):65-76.
164. Barr H, Dix AJ, Kendall C, Stone N. Review article: the potential role for photodynamic therapy in the management of upper gastrointestinal disease. *Aliment Pharmacol Ther* 2001;15(3):311-321.
165. Barr H, MacRobert AJ, Tralau CJ, Boulos PB, Bown SG. The significance of the nature of the photosensitizer for photodynamic therapy: quantitative and biological studies in the colon. *Br J Cancer* 1990;62(5):730-735.
166. Overholt BF, Panjehpour M. Photodynamic therapy in Barrett's esophagus. *J Clin Laser Med Surg* 1996;14(5):245-249.

167. Overholt BF, Panjehpour M. Photodynamic therapy for Barrett's esophagus: clinical update. *Am J Gastroenterol* 1996;91(9):1719-1723.
168. Overholt BF, Wang KK, Burdick JS et al. Five-year efficacy and safety of photodynamic therapy with Photofrin in Barrett's high-grade dysplasia. *Gastrointest Endosc* 2007;66(3):460-468.
169. van Lanschot JJ, Hulscher JB, Buskens CJ, Tilanus HW, ten Kate FJ, Obertop H. Hospital volume and hospital mortality for esophagectomy. *Cancer* 2001;91(8):1574-1578.
170. Karl RC, Schreiber R, Boulware D, Baker S, Coppola D. Factors affecting morbidity, mortality, and survival in patients undergoing Ivor Lewis esophagogastrectomy. *Ann Surg* 2000;231(5):635-643.
171. Curvers WL, Herrero LA, Wallace MB et al. Endoscopic tri-modal imaging is more effective than standard endoscopy in identifying early-stage neoplasia in Barrett's esophagus. *Gastroenterology* 2010;139(4):1106-1114.
172. Levine DS, Blount PL, Rudolph RE, Reid BJ. Safety of a systematic endoscopic biopsy protocol in patients with Barrett's esophagus. *Am J Gastroenterol* 2000;95(5):1152-1157.
173. Schlemper RJ, Riddell RH, Kato Y et al. The Vienna classification of gastrointestinal epithelial neoplasia. *Gut* 2000;47(2):251-255.

174. Chan YH. Biostatistics 202: logistic regression analysis. Singapore Med J 2004;45(4):149-153.
175. Bennett C, Vakil N, Bergman J et al. Consensus statements for management of Barrett's dysplasia and early-stage esophageal adenocarcinoma, based on a Delphi process. Gastroenterology 2012;143(2):336-346.
176. Peters FP, Curvers WL, Rosmolen WD et al. Surveillance history of endoscopically treated patients with early Barrett's neoplasia: nonadherence to the Seattle biopsy protocol leads to sampling error. Dis Esophagus 2008;21(6):475-479.
177. Kariv R, Plesec TP, Goldblum JR et al. The Seattle protocol does not more reliably predict the detection of cancer at the time of esophagectomy than a less intensive surveillance protocol. Clin Gastroenterol Hepatol 2009;7(6):653-658.
178. Pohl H, Wrobel K, Bojarski C et al. Risk factors in the development of esophageal adenocarcinoma. Am J Gastroenterol 2013;108(2):200-207.
179. van BM, Looman CW, Johnston BJ, Caygill CP. Age and sex distribution of the prevalence of Barrett's esophagus found in a primary referral endoscopy center. Am J Gastroenterol 2005;100(3):568-576.

180. Cook MB, Wild CP, Forman D. A systematic review and meta-analysis of the sex ratio for Barrett's esophagus, erosive reflux disease, and nonerosive reflux disease. *Am J Epidemiol* 2005;162(11):1050-1061.
181. Yousef F, Cardwell C, Cantwell MM, Galway K, Johnston BT, Murray L. The incidence of esophageal cancer and high-grade dysplasia in Barrett's esophagus: a systematic review and meta-analysis. *Am J Epidemiol* 2008;168(3):237-249.
182. Stein HJ, Siewert JR. Barrett's esophagus: pathogenesis, epidemiology, functional abnormalities, malignant degeneration, and surgical management. *Dysphagia* 1993;8(3):276-288.
183. Sampliner RE. Practice guidelines on the diagnosis, surveillance, and therapy of Barrett's esophagus. The Practice Parameters Committee of the American College of Gastroenterology. *Am J Gastroenterol* 1998;93(7):1028-1032.
184. Hameeteman W, Tytgat GN, Houthoff HJ, van den Tweel JG. Barrett's esophagus: development of dysplasia and adenocarcinoma. *Gastroenterology* 1989;96(5 Pt 1):1249-1256.
185. Falk GW, Rice TW, Goldblum JR, Richter JE. Jumbo biopsy forceps protocol still misses unsuspected cancer in Barrett's esophagus with high-grade dysplasia. *Gastrointest Endosc* 1999;49(2):170-176.

186. Kim SL, Waring JP, Spechler SJ et al. Diagnostic inconsistencies in Barrett's esophagus. Department of Veterans Affairs Gastroesophageal Reflux Study Group. *Gastroenterology* 1994;107(4):945-949.
187. East JE, Tan EK, Bergman JJ, Saunders BP, Tekkis PP. Meta-analysis: narrow band imaging for lesion characterization in the colon, oesophagus, duodenal ampulla and lung. *Aliment Pharmacol Ther* 2008;28(7):854-867.
188. Anagnostopoulos GK, Yao K, Kaye P, Hawkey CJ, Ragnath K. Novel endoscopic observation in Barrett's oesophagus using high resolution magnification endoscopy and narrow band imaging. *Aliment Pharmacol Ther* 2007;26(3):501-507.
189. Whiting P, Rutjes AW, Reitsma JB, Bossuyt PM, Kleijnen J. The development of QUADAS: a tool for the quality assessment of studies of diagnostic accuracy included in systematic reviews. *BMC Med Res Methodol* 2003;3:25.
190. Zamora J, Abraira V, Muriel A, Khan K, Coomarasamy A. Meta-DiSc: a software for meta-analysis of test accuracy data. *BMC Med Res Methodol* 2006;6:31.
191. Walter SD. Properties of the summary receiver operating characteristic (SROC) curve for diagnostic test data. *Stat Med* 2002;21(9):1237-1256.

192. Jaeschke R, Guyatt GH, Sackett DL. Users' guides to the medical literature. III. How to use an article about a diagnostic test. B. What are the results and will they help me in caring for my patients? The Evidence-Based Medicine Working Group. *JAMA* 1994;271(9):703-707.
193. Higgins JP, Thompson SG, Deeks JJ, Altman DG. Measuring inconsistency in meta-analyses. *BMJ* 2003;327(7414):557-560.
194. Kara MA, Ennahachi M, Fockens P, ten Kate FJ, Bergman JJ. Detection and classification of the mucosal and vascular patterns (mucosal morphology) in Barrett's esophagus by using narrow band imaging. *Gastrointest Endosc* 2006;64(2):155-166.
195. Sharma P, Bansal A, Mathur S et al. The utility of a novel narrow band imaging endoscopy system in patients with Barrett's esophagus. *Gastrointest Endosc* 2006;64(2):167-175.
196. Goda K, Tajiri H, Ikegami M, Urashima M, Nakayoshi T, Kaise M. Usefulness of magnifying endoscopy with narrow band imaging for the detection of specialized intestinal metaplasia in columnar-lined esophagus and Barrett's adenocarcinoma. *Gastrointest Endosc* 2007;65(1):36-46.
197. Hamamoto Y, Endo T, Noshō K, Arimura Y, Sato M, Imai K. Usefulness of narrow-band imaging endoscopy for diagnosis of Barrett's esophagus. *J Gastroenterol* 2004;39(1):14-20.

198. Curvers WL, Bohmer CJ, Mallant-Hent RC et al. Mucosal morphology in Barrett's esophagus: interobserver agreement and role of narrow band imaging. *Endoscopy* 2008;40(10):799-805.
199. Singh R, Karageorgiou H, Owen V et al. Comparison of high-resolution magnification narrow-band imaging and white-light endoscopy in the prediction of histology in Barrett's oesophagus. *Scand J Gastroenterol* 2009;44(1):85-92.
200. Kara MA, Peters FP, Rosmolen WD et al. High-resolution endoscopy plus chromoendoscopy or narrow-band imaging in Barrett's esophagus: a prospective randomized crossover study. *Endoscopy* 2005;37(10):929-936.
201. Song F, Khan KS, Dinnes J, Sutton AJ. Asymmetric funnel plots and publication bias in meta-analyses of diagnostic accuracy. *Int J Epidemiol* 2002;31(1):88-95.
202. Prasad GA, Bansal A, Sharma P, Wang KK. Predictors of progression in Barrett's esophagus: current knowledge and future directions. *Am J Gastroenterol* 2010;105(7):1490-1502.
203. Spechler SJ, Sharma P, Souza RF, Inadomi JM, Shaheen NJ. American Gastroenterological Association technical review on the management of Barrett's esophagus. *Gastroenterology* 2011;140(3):e18-e52.

204. Spechler SJ, Sharma P, Souza RF, Inadomi JM, Shaheen NJ. American Gastroenterological Association medical position statement on the management of Barrett's esophagus. *Gastroenterology* 2011;140(3):1084-1091.
205. DerSimonian R, Laird N. Meta-analysis in clinical trials. *Control Clin Trials* 1986;7(3):177-188.
206. Egger M, Davey SG, Schneider M, Minder C. Bias in meta-analysis detected by a simple, graphical test. *BMJ* 1997;315(7109):629-634.
207. Curvers WL, van Vilsteren FG, Baak LC et al. Endoscopic trimodal imaging versus standard video endoscopy for detection of early Barrett's neoplasia: a multicenter, randomized, crossover study in general practice. *Gastrointest Endosc* 2011;73(2):195-203.
208. Curvers WL, Singh R, Wallace MB et al. Identification of predictive factors for early neoplasia in Barrett's esophagus after autofluorescence imaging: a stepwise multicenter structured assessment. *Gastrointest Endosc* 2009;70(1):9-17.
209. Corley DA, Levin TR, Habel LA, Weiss NS, Buffler PA. Surveillance and survival in Barrett's adenocarcinomas: a population-based study. *Gastroenterology* 2002;122(3):633-640.

210. Borovicka J, Fischer J, Neuweiler J et al. Autofluorescence endoscopy in surveillance of Barrett's esophagus: a multicenter randomized trial on diagnostic efficacy. *Endoscopy* 2006;38(9):867-872.
211. Puri KS, Suresh KR, Gogtay NJ, Thatte UM. Declaration of Helsinki, 2008: implications for stakeholders in research. *J Postgrad Med* 2009;55(2):131-134.
212. Fleiss JL. Measuring nominal scale agreement among many raters. *Psychological Bulletin* 1971;76:378-382.
213. Landis JR, Koch GG. The measurement of observer agreement for categorical data. *Biometrics* 1977;33(1):159-174.
214. Lee J, Fung KP. Confidence interval of the kappa coefficient by bootstrap resampling. *Psychiatry Res* 1993;49(1):97-98.
215. Raghavendra M, Hewett DG, Rex DK. Differentiating adenomas from hyperplastic colorectal polyps: narrow-band imaging can be learned in 20 minutes. *Gastrointest Endosc* 2010;72(3):572-576.
216. Devesa SS, Blot WJ, Fraumeni JF, Jr. Changing patterns in the incidence of esophageal and gastric carcinoma in the United States. *Cancer* 1998;83(10):2049-2053.

217. Pohl H, Welch HG. The role of overdiagnosis and reclassification in the marked increase of esophageal adenocarcinoma incidence. *J Natl Cancer Inst* 2005;97(2):142-146.
218. Gillison EW, Powell J, McConkey CC, Spychal RT. Surgical workload and outcome after resection for carcinoma of the oesophagus and cardia. *Br J Surg* 2002;89(3):344-348.
219. Sampliner RE. Updated guidelines for the diagnosis, surveillance, and therapy of Barrett's esophagus. *Am J Gastroenterol* 2002;97(8):1888-1895.
220. Izuishi K, Tajiri H, Fujii T et al. The histological basis of detection of adenoma and cancer in the colon by autofluorescence endoscopic imaging. *Endoscopy* 1999;31(7):511-516.
221. McCallum AL, Jenkins JT, Gillen D, Molloy RG. Evaluation of autofluorescence colonoscopy for the detection and diagnosis of colonic polyps. *Gastrointest Endosc* 2008;68(2):283-290.
222. Dacosta RS, Wilson BC, Marcon NE. New optical technologies for earlier endoscopic diagnosis of premalignant gastrointestinal lesions. *J Gastroenterol Hepatol* 2002;17 Suppl:S85-104.
223. Kara MA, Dacosta RS, Streutker CJ, Marcon NE, Bergman JJ, Wilson BC. Characterization of tissue autofluorescence in Barrett's esophagus by confocal fluorescence microscopy. *Dis Esophagus* 2007;20(2):141-150.

224. Sieber OM, Howarth KM, Thirlwell C et al. Myh deficiency enhances intestinal tumorigenesis in multiple intestinal neoplasia (ApcMin/+) mice. *Cancer Res* 2004;64(24):8876-8881.
225. Moser AR, Luongo C, Gould KA, McNeley MK, Shoemaker AR, Dove WF. ApcMin: a mouse model for intestinal and mammary tumorigenesis. *Eur J Cancer* 1995;31A(7-8):1061-1064.
226. Moser AR, Pitot HC, Dove WF. A dominant mutation that predisposes to multiple intestinal neoplasia in the mouse. *Science* 1990;247(4940):322-324.
227. Fodde R, Edelmann W, Yang K et al. A targeted chain-termination mutation in the mouse Apc gene results in multiple intestinal tumors. *Proc Natl Acad Sci U S A* 1994;91(19):8969-8973.
228. Taketo MM. Mouse models of gastrointestinal tumors. *Cancer Sci* 2006;97(5):355-361.
229. Dacosta RS, Andersson H, Cirocco M, Marcon NE, Wilson BC. Autofluorescence characterisation of isolated whole crypts and primary cultured human epithelial cells from normal, hyperplastic, and adenomatous colonic mucosa. *J Clin Pathol* 2005;58(7):766-774.
230. Bohorfoush AG. Tissue spectroscopy for gastrointestinal diseases. *Endoscopy* 1996;28(4):372-380.

231. Schomacker KT, Frisoli JK, Compton CC et al. Ultraviolet laser-induced fluorescence of colonic polyps. *Gastroenterology* 1992;102(4 Pt 1):1155-1160.
232. Schomacker KT, Frisoli JK, Compton CC et al. Ultraviolet laser-induced fluorescence of colonic tissue: basic biology and diagnostic potential. *Lasers Surg Med* 1992;12(1):63-78.